A STUDY TO DETERMINE THE MECHANISMS OF CORROSION OF COPPER-NICKEL ALLOYS IN SULFIDE-POLLUTED SEAWATER

Annual Report Covering the Period
February 2, 1978 through February 1, 1979

February 1, 1979

By: B. C. Syrett, S. S. Wing, and D. D. Macdonald

Prepared for:

Office of Naval Research
800 North Quincy Street
Arlington, Virginia 22217

Attn: Dr. Philip A. Clarkin, Code 471
Director, Metallurgy Program
Materials Sciences Division

ONR Contract No. N00014-77-C-0046, NR 036-116
SRI Project PYU-6077

SRI International
333 Ravenswood Avenue
Menlo Park, California 94025
(415) 326-6200
Cable: SRI INTL MPK
TWX: 910-373-1246

A STUDY TO DETERMINE THE MECHANISMS OF CORROSION OF COPPER-NICKEL ALLOYS IN SULFIDE-POLLUTED SEAWATER.

Annual Report Covering the Period
February 2, 1978 through February 1, 1979

February 1979

By: B. C. Syrett, S. S. Wing, and D. D. Macdonald

Prepared for:

Office of Naval Research
800 North Quincy Street
Arlington, Virginia 22217

Attn: Dr. Philip A. Clarkin, Code 471
Director, Metallurgy Program
Materials Sciences Division

ONR Contract No. N00014-77-C-0046, NR 036-116
SRI Project PYU-6077

Approved:

R. W. Bartlett, Director
Materials Research Center

P. J. Jorgensen, Vice President
Physical and Life Sciences

Unclassified

SECURITY CLASSIFICATION OF THIS PAGE *(When Data Entered)*

REPORT DOCUMENTATION PAGE		READ INSTRUCTIONS BEFORE COMPLETING FORM
1. REPORT NUMBER	2. GOVT ACCESSION NO.	3. RECIPIENT'S CATALOG NUMBER
4. TITLE *(and Subtitle)* A STUDY TO DETERMINE THE MECHANISMS OF CORROSION OF COPPER-NICKEL ALLOYS IN SULFIDE-POLLUTED SEAWATER		5. TYPE OF REPORT & PERIOD COVERED ANNUAL REPORT Feb. 2, 1978 - Feb 1, 1979 6. PERFORMING ORG. REPORT NUMBER
7. AUTHOR(s) B. C. SYRETT, S. S. WING AND D. D. MACDONALD		8. CONTRACT OR GRANT NUMBER(s) N00014-77-C-0046, NR 036-116
9. PERFORMING ORGANIZATION NAME AND ADDRESS SRI INTERNATIONAL 333 RAVENSWOOD AVENUE, MENLO PARK, CALIFORNIA 94025		10. PROGRAM ELEMENT, PROJECT, TASK AREA & WORK UNIT NUMBERS
11. CONTROLLING OFFICE NAME AND ADDRESS OFFICE OF NAVAL RESEARCH MATERIALS SCIENCES DIVISION ARLINGTON, VIRGINIA 22217		12. REPORT DATE February 1, 1979 13. NUMBER OF PAGES 122
14. MONITORING AGENCY NAME & ADDRESS*(if different from Controlling Office)* DEFENSE CONTRACT ADMINISTRATION SERVICES 866 MALCOLM ROAD BURLINGAME, CALIFORNIA 94010		15. SECURITY CLASS. *(of this report)* 15a. DECLASSIFICATION/DOWNGRADING SCHEDULE UNCLASSIFIED
16. DISTRIBUTION STATEMENT *(of this Report)* APPROVED FOR PUBLIC RELEASE; DISTRIBUTION UNLIMITED		
17. DISTRIBUTION STATEMENT *(of the abstract entered in Block 20, if different from Report)*		
18. SUPPLEMENTARY NOTES CONTAINS THREE PAPERS SUBMITTED FOR PUBLICATION IN CORROSION JOURNAL.		
19. KEY WORDS *(Continue on reverse side if necessary and identify by block number)* EROSION-CORROSION, ELECTROCHEMICAL TECHNIQUES, SULFIDE CORROSION, SEAWATER, VELOCITY, COPPER ALLOYS, COPPER-NICKEL ALLOYS.		

20. ABSTRACT *(Continue on reverse side if necessary and identify by block number)*

The main objective of this research was to determine the role of dissolved sulfide pollutants on the seawater corrosion of two copper nickel alloys--90:10 Cu:Ni (CA 706) and 70:30 Cu:Ni (CA 715). Electrochemical techniques were used to monitor corrosion rates in rotating cylinder experiments and in flow loop experiments. The effects of flow (velocity) and the composition of the seawater environment were considered. The highlights of this work are as follows:

DD FORM 1 JAN 73 1473

Unclassified

SECURITY CLASSIFICATION OF THIS PAGE *(When Data Entered)*

(1) Electrochemical methods are suitable for monitoring the corrosion rate of copper-nickel alloys in seawater if certain precautions are taken.

(2) The presence of sulfide or one of several sulfide oxidation products turns noncorrosive deaerated seawater into a comparatively corrosive environment.

(3) Sulfide-polluted deaerated seawater is less corrosive than unpolluted aerated seawater at Reynolds numbers up to 74,000 (velocities up to 5 m/s).

(4) When the velocity of aerated seawater is increased from 2 m/s to 3 m/s (Reynolds number from 30,000 to 44,000), 70:30 Cu:Ni undergoes a transition from fairly uniform mild corrosion to accelerated localized corrosion. This breakaway corrosion phenomenon is interpreted in terms of a "breakaway potential."

CONTENTS

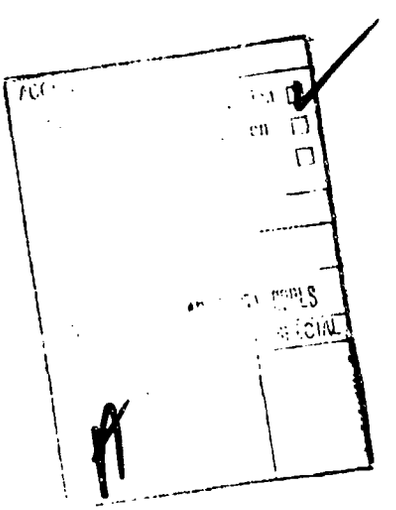

SUMMARY

The premature failure of copper-nickel seawater piping in naval ships being outfitted in a polluted estuary stimulated an ongoing research program at SRI International, funded by the Office of Naval Research (Contract N00014-77-C-0046). Specifically, the importance and role of dissolved sulfide pollutants on the seawater corrosion of two copper-nickel alloys--90:10 Cu:Ni (CA 706) and 70:30 Cu:Ni (CA 715)--are being investigated.

This report, which describes the progress we have made during the second year of the program, is split into three major sections. Each section is a paper that has been submitted for publication in CORROSION, and hence each section can stand alone, independent of the others. The titles and authors of the three papers are:

(1) "The Validity of Electrochemical Methods for Measuring Corrosion Rates of Copper-Nickel Alloys in Seawater," by B. C. Syrett and D. D. Macdonald.

(2) "Corrosion of Copper-Nickel Alloys in Seawater Polluted With Sulfide and Sulfide Oxidation Products," by B. C. Syrett, D. D. Macdonald, and S. S. Wing.

(3) "Effect of Flow on Corrosion of Cu-Ni Alloys in Aerated Seawater and In Sulfide-Polluted Seawater," by B. C. Syrett and S. S. Wing.

The first two papers have already been accepted for publication and should appear in CORROSION during 1979. In addition, the second paper will be presented at the Annual Conference of the National Association

of Corrosion Engineers (CORROSION/79) to be held in Atlanta, Georgia, in March 1979.

The highlights of this work may be summarized as follows:

(1) Electrochemical methods of monitoring the corrosion rate of copper-nickel alloys in seawater give results that correlate well with weight loss data as long as certain precautions are taken.

(2) The presence of sulilde, sulfur, polysulfides, or combinations of these species can turn essentially noncorrosive deaerated seawater into a comparatively corrosive enivironment. However, under the fairly mild flow conditions used, corrosion rates in seawater polluted with these sulfur species were not high enough to explain the accelerated attack of the copper-nickel piping in the naval ships.

(3) Both copper-nickel alloys investigated corrode less rapidly in sulfide-polluted ($\sim$ 0.2 mg [S]/dm^3) deaerated seawater than in aerated seawater at velocities up to 5 m/s. Thus even under comparatively adverse flow conditions, the mere presence of sulfide does not cause accelerated attack of copper-nickel alloys.

(4) When the velocity of the aerated seawater is increased from 2 m/s to 3 m/s (Reynolds number from 30,000 to 44,000), 70:30 Cu:Ni undergoes a transition from fairly uniform mild corrosion to accelerated localized corrosion. This pitting type of corrosion is intensified at velocities greater than 3 m/s. This breakaway corrosion phenomenon is interpreted in terms of the relationship between the corrosion potential and a "breakaway potential," defined as the potential at which a sudden increase in anodic current occurs on sweeping the potential in the active to noble direction.

THE VALIDITY OF ELECTROCHEMICAL METHODS FOR MEASURING CORROSION RATES OF COPPER-NICKEL ALLOYS IN SEAWATER

By

Barry C. Syrett and Digby D. Macdonald
Materials Research Center
SRI International
Menlo Park, California 94025

Key words: Corrosion rate, electrochemical techniques linear polarization, copper-nickel alloys, seawater, weight loss

Submitted for publication in Corrosion (1978).

ABSTRACT

This work was stimulated by reports that electrochemical methods for measuring the polarization resistance of copper, nickel, or copper-nickel alloys in aqueous systems may lead to appreciable errors in the estimates of the corrosion rate. In the present work, the polarization resistance (R_p) of two copper-nickel alloys (90:10 Cu:Ni and 70:30 Cu:Ni) was monitored as a function of time in flowing seawater that contained 0.045, 0.85, 6.6, or 26.3 mg/dm^3 dissolved oxygen. R_p values were obtained using the linear polarization, potential step, and ac impedance techniques. The total weight loss during the test period was calculated from the area under the $1/R_p$ versus time curve and compared with the measured weight loss. The experimental data support the validity of electrochemical methods for measuring corrosion rates of copper-nickel alloys in seawater, provided that a sufficient number of R_p measurements are made during the first 24 hours, and provided that proper consideration is given to the capacitive elements of the metal/solution interfacial impedance. Previous reports that electrochemical measurements may lead to underestimates of the corrosion rates are thought to have resulted primarily from undetected (and very high) corrosion rates at short exposure times. Reported overestimates of the corrosion rate are thought to have resulted

from the use of a potential sweep rate that was too high (linear polarization technique), a time for current decay that was too short (potential step technique), or excitation frequencies that were insufficiently low (ac impedance technique).

INTRODUCTION

The application of electrochemical techniques for measuring corrosion rates of metals in condensed media is now well established.[1,2] The most frequently used technique is linear polarization, which makes use of a linearized Butler-Volmer type of expression for the current within a few millivolts of the corrosion potential (E_{corr}). Experimentally, this technique requires estimation of the polarization resistance (R_p) equal to the slope ($\partial E/\partial i$) of the potential versus current curve at $E = E_{corr}$. The R_p value obtained is inversely proportional to the instantaneous corrosion current (i_{corr}), as defined by the Stern-Geary relationship.[3]

However, previous reports indicate that electrochemical methods for measuring the polarization resistances of copper, nickel, and copper-nickel alloys in aqueous systems may lead to values for the calculated weight losses that are substantially higher[4,5] or lower[4,6,7] than actual weight losses. Assuming that the normal corrections were made for the IR drop between the Luggin probe of the reference electrode and the specimen, there seems to be no valid theoretical foundation for <u>underestimates</u> of the corrosion rate. On the other hand, overestimates of the corrosion rate can be explained, for instance, in terms of the nonspecific

nature of R_p measurements. Any electrochemical reaction, irrespective of whether or not it leads to corrosion of the metal, will contribute to the current flowing across the interface and may lead to an overestimate of the corrosion rate (or underestimate of R_p). For example the oxidation of molecular hydrogen gives rise to an anodic current that, under some circumstances,[8] cannot be distinguished from a metal oxidation (i.e. corrosion) current on the basis of linear polarization measurements alone. As will be discussed later, there are also other satisfactory explanations for the reported overestimates of the corrosion rate calculated from R_p data.

The present work was initiated primarily to investigate the reports that electrochemical measurements underestimate (by as much as an order of magnitude, or more) the corrosion rate of copper,[7] nickel,[6] or copper-nickel alloys[4] in aqueous systems of near neutral pH. However, some consideration has also been given to the cause of corrosion rate overestimates. In this work, polarization resistance data for Copper Alloy 706 (90:10 Cu:Ni) and Alloy 715 (70:30 Cu:Ni) in flowing seawater are analyzed and are shown to be consistent with measured weight losses if certain precautions are taken.

EXPERIMENTAL

Five tubular specimens of each copper-nickel alloy were tested in tandem under well-defined hydrodynamic and mass transfer conditions at 26 ± 2C in a recirculating seawater flow loop. The specimens consisted of 2.54-cm lengths of condenser tubing (1.384 cm ID, 1.715 cm OD) separated from each other by thin Delrin[a] spacers. Each set of five specimens was preceded by a 67-cm long approach section of copper-nickel tubing of identical composition and internal diameter as the specimens; a 15-cm length of the same tubing was placed immediately downstream from the test section to serve as a counterelectrode. A saturated calomel reference electrode (SCE) was placed in a side-arm just upstream from each set of five specimens. Full details of the chemical compositions of the alloys, specimen preparation, seawater characteristics, flow loop design, and experimental procedures are given in previous publications.[9-11] In the present work, the seawater velocity was held constant at 1.62 m/s. Thus, the Reynolds number was about 25,000 (using the tube ID as the characteristic length), and turbulent conditions prevailed in all experiments. In addition, the long approach section ensured full development of the mass transfer and

---

[a] Delrin (polyformaldehyde) is a registered trademark of E. I. DuPont de Nemours and Co., Inc.

velocity boundary layers upstream from the specimens, so that all specimens were tested under essentially identical conditions.

The oxygen concentration in the seawater was held constant at one of four values in the range 0.045 to 26.3 mg/dm^3. The oxygen concentration was determined by Winkler titration.[12]

Corrosion Rate Measurements

The polarization resistance (R_p) at the metal/solution interface was determined using three different electrochemical techniques: linear polarization, ac impedance, and potential step. In each case, a potentiostat was used in the potential-control mode and, as described previously,[9-11] care was taken to ensure that the system response to a time-dependent excitation did not result from instrumental artifacts.

Linear polarization data were generated by imposing a small-amplitude (20 mV peak-to-peak) triangular potential excitation across the interface. Voltage sweep rates over the range 0.1 mV/s to 50 mV/s were employed, and the current/voltage curves were recorded with an X-Y recorder.

Surface impedance data were generated as a function of frequency (1×10^{-3} Hz to 4×10^{3} Hz) by imposing a 11 mV peak-to-peak sinusoidal signal across the interface. The components of the impedance were calculated from the dimensions of the steady-state Lissajous figures[2,9,11,13] generated by simultaneously imposing the sinusoidal response current

and voltage excitation across the Y and X axes, respectively, of an oscilloscope (1 Hz to 4 x 10^3 Hz) or fast response X-Y recorder (1 x 10^{-3} to 1 Hz).

The decay of current with time under potentiostatic conditions was investigated by imposing a small-amplitude potential step($\Delta E = \pm$ 10 mV) across the interface at zero time. The current was then recorded for approximately 5 minutes or until an apparently constant value was obtained.

The specimens were cleaned initially and were descaled after exposure to the seawater by immersion in HCl/H_2SO_4 (ASTM Recommended Practice G1-72 for copper alloys).

Each of the five specimens of a given alloy performed a single function. One was used solely for linear polarization, one for ac impedance, one for potential step, and the remaining two specimens were used solely for weight loss measurements. Because the mass transfer conditions were nominally identical for all five specimens, the results obtained for one specimen were expected to be entirely consistent with those for any other specimen.

RESULTS

Macdonald[14] analyzed the transient response of an equivalent circuit for an electrode/solution interface to the type of small-amplitude triangular potential excitation used in the linear polarization method. He demonstrated that the apparent polarization resistance value (R_{app}) obtained by the linear polarization technique can vary greatly with potential sweep rate, particularly when the interface has a large capacitive element, as in the present systems. Using some of the R_{app} data generated in the present work, Macdonald showed that the true polarization resistance, R_p, could be obtained by extrapolating the curve of $1/R_{app}$ versus potential sweep rate to zero sweep rate. In addition, his analysis showed that $R_{app} \approx R_p$ when the cyclic voltammogram recorded using the linear polarization technique showed minimal hysteresis. In the present work $R_{app} \approx R_p$ at the lowest potential sweep rate used (0.1 mV/s); therefore, only these polarization resistance values are reported below. For similar reasons,[2] care was taken to allow adequate time (up to 15 minutes) for current decay when the potential step technique was used, and to reach sufficiently low excitation frequencies (as low as 10^{-3} Hz) when the ac impedance technique was used. In this way, valid R_p data were obtained.

Much of the electrochemical data obtained in this study has been reported in previous publications,[11,14] but the data have been reevaluated and plotted in Figures 1 to 4 as $1/R_p$ versus time curves to facilitate a direct comparison of the electrochemical measurements with the weight loss data. It will be seen that there is generally good agreement between the $1/R_p$ values obtained by the linear polarization, potential step, and ac impedance techniques.

According to the Stern-Geary treatment of electrochemical corrosion,[3] the corrosion current (i_{corr}) is proportional to the reciprocal of the polarization resistance as shown in Eq. 1:

$$i_{corr} = \beta_a\beta_c/2.303\ R_p(\beta_a + \beta_c) \qquad (1)$$

where β_a and β_c are the Tafel coefficients for the anodic and cathodic reactions, respectively. Thus, if β_a and β_c are assumed to be constant, the data plotted in Figures 1, 2, 3, and 4 reflect the corrosion rates of the two alloys as a function of time in seawater containing 0.045, 0.85, 6.6, and 26.3 mg/dm^3 oxygen, respectively. Equation 1 may be integrated over time, t, to yield the charge, Q_{corr}, associated with metal loss,

$$Q_{corr} = [\beta_a\beta_c/2.303\ (\beta_a + \beta_c)] \int_0^t 1/R_p\ dt \qquad (2)$$

provided that no parasitic charge transfer reactions occur. For given values of β_a and β_c, Eq. 2 becomes

$$Q_{corr} = BA_t/2.303 \qquad (3)$$

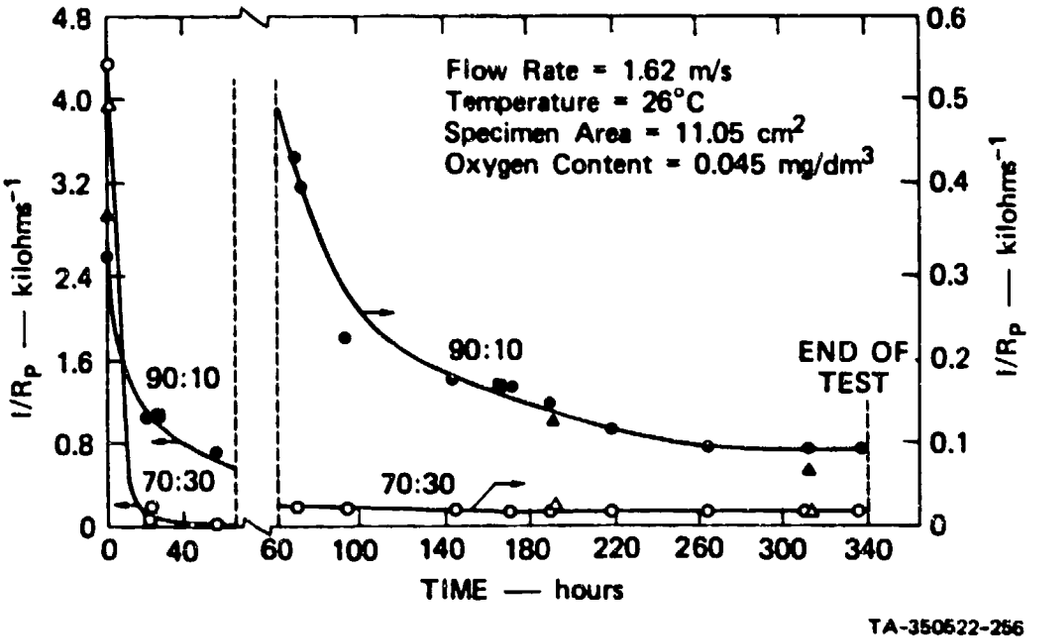

	90:10	70:30
Linear Polarization	●	○
Potential Step	▲	△
ac Impedance	■	□

FIGURE 1 CORROSION RATE (AS I/R_p) VERSUS TIME FOR 90:10 Cu:Ni AND 70:30 Cu:Ni IN FLOWING SEAWATER HAVING AN OXYGEN CONTENT OF 0.045 mg/dm^3

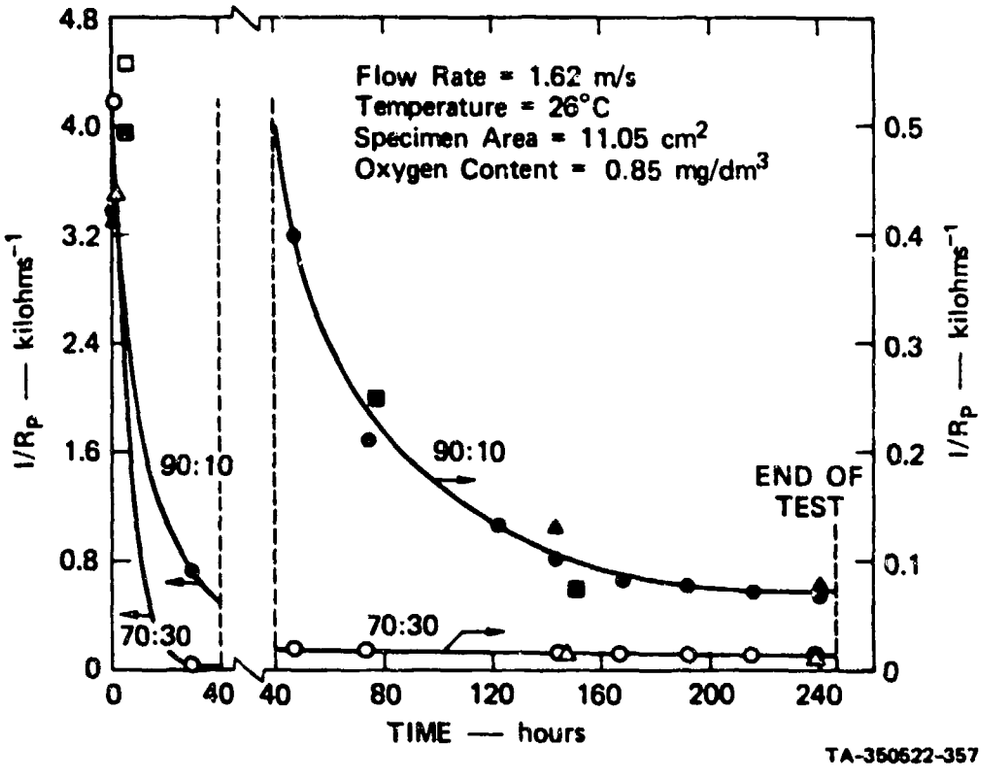

	90:10	70:30
Linear Polarization	●	○
Potential Step	▲	△
ac Impedance	■	□

FIGURE 2 CORROSION RATE (AS I/R_p) VERSUS TIME FOR 90:10 Cu:Ni AND 70:30 Cu:Ni IN FLOWING SEAWATER HAVING AN OXYGEN CONTENT OF 0.85 mg/dm³

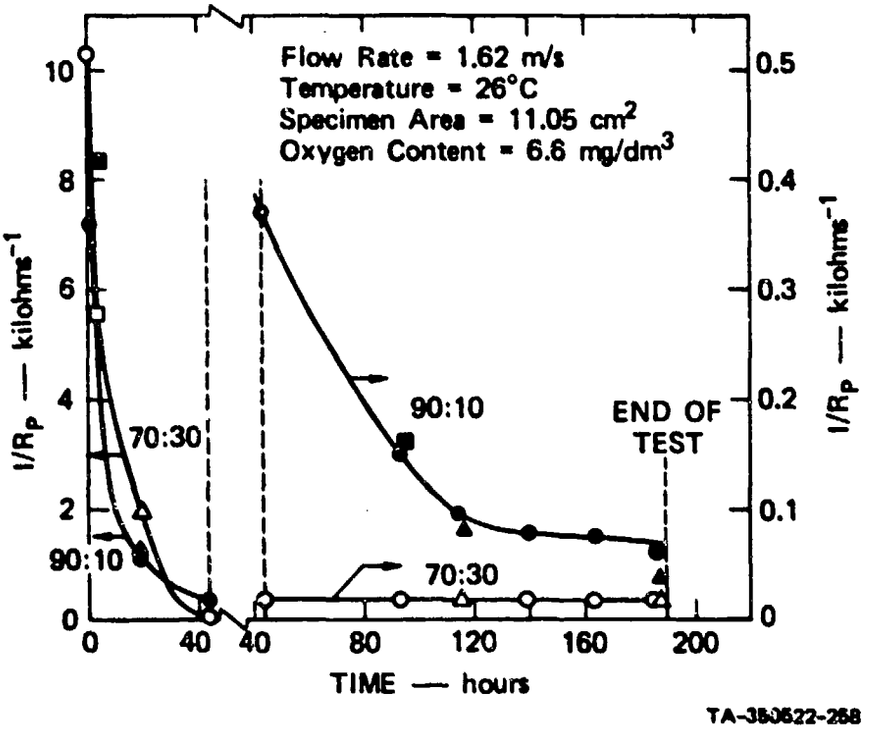

FIGURE 3 CORROSION RATE (AS I/R_p) VERSUS TIME FOR 90:10 Cu:Ni AND 70:30 Cu:Ni IN FLOWING SEAWATER HAVING AN OXYGEN CONTENT OF 6.6 mg/dm³

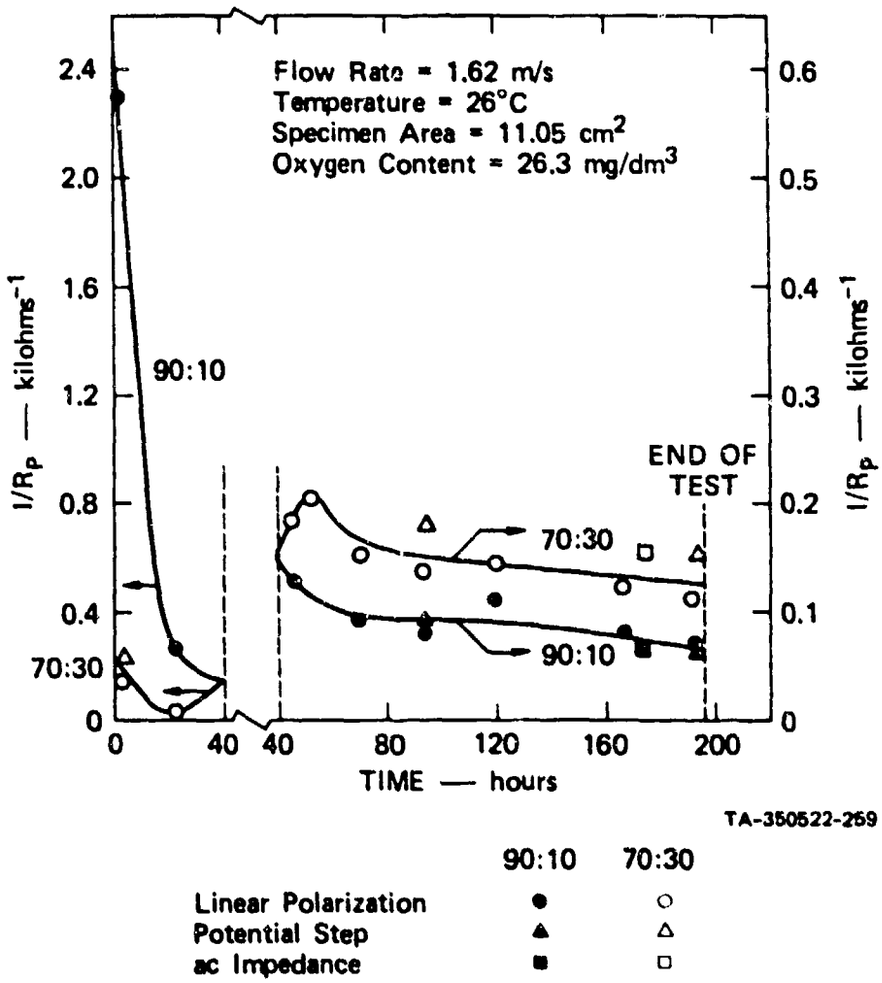

FIGURE 4 CORROSION RATE (AS I/R_p) VERSUS TIME FOR 90:10 Cu:Ni AND 70:30 Cu:Ni IN FLOWING SEAWATER HAVING AN OXYGEN CONTENT OF 26.3 mg/dm³

where B is a constant $[= \beta_a \beta_c / (\beta_a + \beta_c)]$ with units of volts, and A_t $[(= \int_0^t 1/R_p \, dt]$ is the area under the $1/R_p$ versus time curve in units of coulomb/volt. Application of Faraday's law then yields the weight loss, ΔW, in units of grams, as

$$\Delta W = \bar{M} Q_{corr} / \bar{n} F = \bar{M} B A_t / 2.303 \bar{n} F \quad (4)$$

where $\bar{M}$ and $\bar{n}$ are the composition averaged atomic weight and change in oxidation state, respectively. $\bar{M}$ and $\bar{n}$ are given by Eq. (5) and Eq. (6) in terms of the mole fractions of copper (X_{Cu}) and nickel (X_{Ni}), and the molecular weights of copper (M_{Cu}) and nickel (M_{Ni}):

$$\bar{M} = X_{Cu} M_{Cu} + X_{Ni} M_{Ni} \quad (5)$$

and

$$\bar{n} = X_{cu} + 2 X_{Ni} \quad (6)$$

It is assumed that the copper and nickel components are oxidized to the + 1 (cuprous) and + 2 (nickelous) states, respectively. For 90:10 Cu:Ni, $\bar{M}$ is 63.04 g and $\bar{n}$ is 1.107, whereas for 70:30 Cu:Ni, $\bar{M}$ is 62.03 g and $\bar{n}$ is 1.317. Substituting these values in Eq. 4 gives

$$\Delta W = 2.563 \times 10^{-4} B A_t \text{ for 90:10 Cu:Ni} \quad (7)$$

and

$$\Delta W = 2.120 \times 10^{-4} B A_t \text{ for 70:30 Cu:Ni} \quad (8)$$

The values of A_t, obtained by graphic integration of the curves shown in Figures 1 to 4, are listed in Table 1. The measurements of β_a and β_c, needed for the calculation of B, requires large deviations of the potential from E_{corr}, and hence significant changes in the morphology and nature of the specimen surface. Accordingly, direct evaluation of these coefficients was not considered practical in this work. Instead, the value of B needed to bring the calculated value of total weight loss in line with the measured value was determined (see Table 1). With one exception, these values of B lie in the range 0.058 to 0.083 volt, with an average of about 0.07 volt. Values of B quoted in the literature[15] for copper-nickel alloys in seawater are consistent with the present values, ranging from 0.041 to 0.124 volt. Consequently, all the calculated weight loss values shown in Table 1 have been obtained assuming B = 0.07 volt in Eq. 7 and Eq. 8. Because cathodic control of the corrosion reaction is likely for low oxygen concentrations and short exposure times, whereas anodic control is likely for high oxygen concentrations and longer exposure times,[11] a value of B = 0.07 volt can be interpreted in terms of the two limiting cases of $\beta_a = 0.07$ V, $\beta_c = \infty$ (pure cathodic control), and $\beta_a = \infty$, $\beta_c = 0.07$ V (pure anodic control). Other combinations of Tafel coefficients can be selected that yield a value of B = 0.07 volt, but the precise value of β_a and β_c are not critical to the interpretation of our results.

Table 1

COMPARISON BETWEEN MEASURED AND CALCULATED WEIGHT LOSS

$[O_2]$ (mg/dm^3)	Exposure Period (h)	A_t (coulomb/V)	Weight Loss (mg) Measured	Weight Loss (mg) Calculated[a]	B[b] (V)
		90:10 Cu:Ni			
0.045	336.5	380.23	5.92 ± 0.3	6.82	0.061
0.85	246.5	316.62	6.00 ± 0.1	5.68	0.074
6.60	189	364.90	7.78 ± 0.1	6.55	0.083
26.3	196	157.82	3.18 ± 0.1	2.83	0.079
		70:30 Cu:Ni			
0.045	336.5	118.12	1.65 ± 0.35	1.75	0.066
0.85	246.5	123.73	2.10 ± 0.1	1.84	0.080
6.60	189	360.18	4.45 ± 1.5	5.34	0.058
26.3	196	97.88[c]	9.33 ± 0.03	1.45[c]	0.450

[a] Weight loss calculated assuming B= 0.07 volt (Eq. 7 and Eq. 8)

[b] Value of B (Eq. 7 or Eq. 8) to give measured weight loss.

[c] This value is probably underestimated (see text)

Even though the Tafel coefficients were not measured directly and the true values of B could differ by ± 50% (possibly more) from those assumed, excellent agreement is obtained between the weight loss measured directly and that calculated using Eq. 7 or Eq. 8, with the exception of the 70:30 Cu:Ni alloy in the oxygen saturated system ($[O_2] = 26.3$ mg/dm^3). In the latter case, both the corrosion potential and the polarization resistance exhibited large fluctuations at short exposure times. Unobserved fluctuations of R_p to low values could have resulted in large, but undetected corrosion currents. Thus, the difference between the measured and calculated weight losses listed in Table 3 for this system is not considered a serious breakdown of the validity of electrochemical techniques.

DISCUSSION

The suggestion[4-6] that the linear polarization and related techniques tend to underestimate corrosion rates of copper, nickel, and their alloys does not seem justified on the basis of the present results. It is considered likely that the previous poor correlations between electrochemical measurements and weight loss data result primarily from undetected (and very high) corrosion rates at short exposure times. As shown in Figures 1 and 4, in many instances, the bulk of the weight loss (area under the curve) occurred during the first 24 hours.

A full discussion of the implications of the effect of oxygen is given elsewhere.[9,11] The primary intent of this paper is to demonstrate that linear polarization, potential step, ac impedance, and other methods of measuring R_p can give calculated weight losses that are entirely consistent with measured weight losses if R_p data are obtained at short exposure times. Without these short-term data, corrosion rates calculated from electrochemical measurements may be grossly underestimated.

It is also important to realize that the generally high capacitance of the metal/solution interface in these copper-nickel/seawater systems[9,11,14] can lead to overestimates of the corrosion rate unless proper precautions are taken. As mentioned in the results section and elsewhere,[14] such

overestimates would arise if too high a potential sweep rate were used for the linear polarization measurements. In these cases, the small amplitude cyclic voltammograms recorded would show significant hysteresis, and the apparent polarization resistances (R_{app}) would be lower than the true R_p values. In the present study, this source of error was circumvented by using a low enough sweep rate (0.1 mV/s) so that hysteresis was minimal and $R_{app} \approx R_p$. However, in other instances, the capacitance of the interface may be so high that the sweep rate needed to give minimal hysteresis is impractically low. Here, R_{app} should be determined at several potential sweep rates and the true R_p value determined by extrapolating the curve of $1/R_{app}$ versus sweep rate to zero sweep rate.[14]

Similarly, it is essential that sufficient time be given for the polarizing current to decay to a steady state value when the potential step technique is used. In the present study, decay times of at least 5 minutes and as much as 15 minutes were needed. Likewise, valid R_p values can be obtained using the ac impedance technique only if the low frequency semicircle in the complex plane impedance diagram is essentially complete.[11] In the present study, excitation frequencies down to 10^{-3} Hz were used, but in a few instances, even these low frequencies were not low enough to allow a reasonable estimate of the R_p value, and the data had to be discarded.

One of the major advantages of in situ electrochemical measurements is that the kinetics of the corrosion reactions are clearly defined no matter what the total test period. Thus, in the present work, exposure periods ranged from 189 hours to 336.5 hours. Average corrosion rates during these periods can be determined from weight loss data (Table 2), but because of the strong time dependence of the corrosion rate during the first few days, the corrosion rates so obtained do not reflect the true nature of the corrosion kinetics. In contrast, the corrosion rate can be calculated from the R_p data after any selected exposure period (see Figure 5 and Table 2), and these values accurately reflect the corrosion kinetics. For instance, it is clear from the $1/R_p$ data that the corrosion rate of 90:10 Cu:Ni after an 8-day exposure is inversely related to dissolved oxygen content (Table 2). The weight loss data suggest the opposite is true in the oxygen range 0.045 to 6.60 mg/dm^3. Similarly, the loss in the superiority of the high nickel alloy at the highest oxygen concentration is much more graphically demonstrated when the R_p data are used than when the weight loss data are used (see Table 2 and Figure 5).

Table 2

COMPARISON BETWEEN THE MEASURED AVERAGE CORROSION RATE AND THE CORROSION RATE CALCULATED FROM THE R_p VALUE OBTAINED AFTER AN 8 DAY EXPOSURE

$[O_2]$ (mg/dm^3)	Measured Average Corrosion Rate (mg/day)	Calculated[(a)] Corrosion Rate After 8 Days (mg/day)
	90:10 Cu:Ni	
0.045	0.42 ± 0.02	0.20
0.85	0.58 ± 0.01	0.12
6.60	0.99 ± 0.01	0.10
26.3	0.39 ± 0.01	0.10
	70:30 Cu:Ni	
0.045	0.12 ± 0.02	0.022
0.85	0.20 ± 0.01	0.019
6.60	0.57 ± 0.19	0.022
26.3	1.14 ± 0.00	0.160

(a) Calculated assuming B = 0.07 (Eq. 7 and Eq. 8)

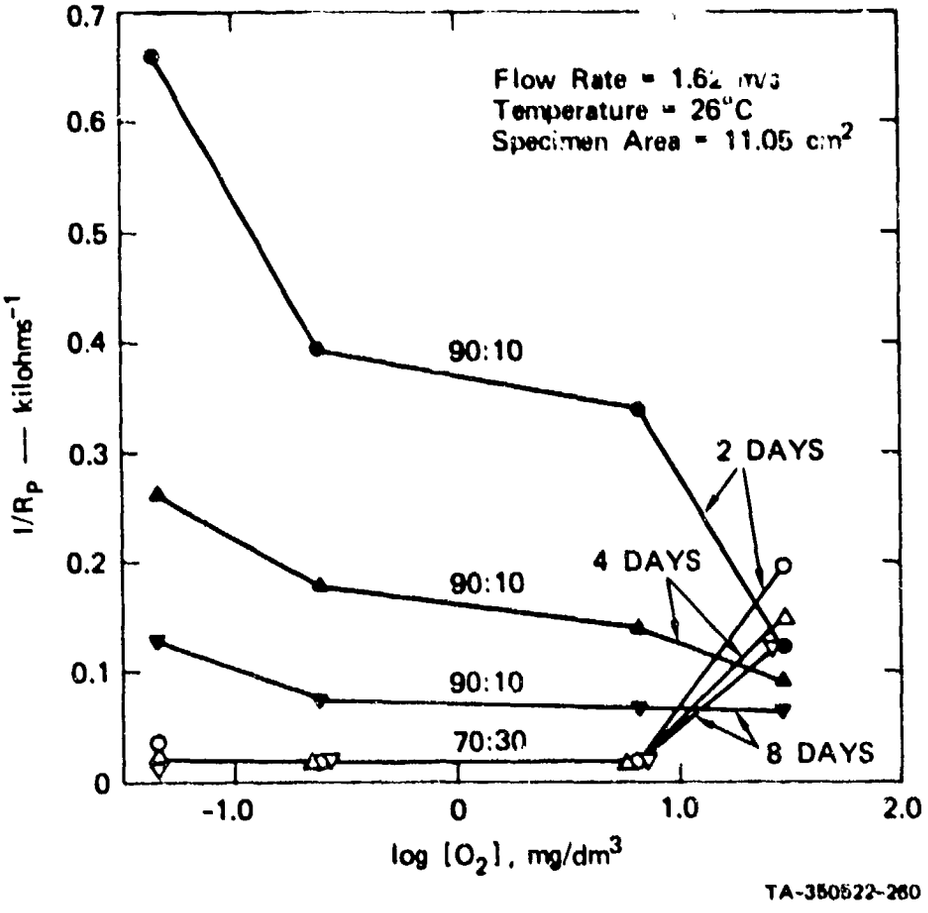

FIGURE 5 EFFECT OF OXYGEN CONCENTRATION ON CORROSION RATE (I/R_p) OF 90:10 Cu:Ni (CLOSED POINTS) AND 70:30 Cu:Ni (OPEN POINTS) AFTER 2, 4, AND 8 DAYS EXPOSURE

CONCLUSIONS

The experimental data support the validity of electrochemical methods for measuring corrosion rates of copper-nickel alloys in seawater. Furthermore, electrochemical measurements made over a 1- to 2-week period facilitate a more accurate and much more detailed examination of corrosion kinetics than is possible from a single weight loss measurement made over the same period.

ACKNOWLEDGMENTS

The financial support of the Office of Naval Research (Contract N00014-77-C-0046) is gratefully acknowledged. The authors also appreciate the assistance of Ms. Sharon Wing in performing much of the experimental work described in this paper.

REFERENCES

1. H. H. Uhlig, Corrosion and Corrosion Control, 2nd Edit., John Wiley and Sons, New York, 1971.

2. D. D. Macdonald, Transient Techniques in Electrochemistry, Plenum Publishing Co., New York, 1977.

3. M. Stern and A. L. Geary, J. Electrochem. Soc., Vol. 104, p. 56 (1957).

4. F. P. IJesseling, Corrosion Science, Vol. 14, p. 97 (1974).

5. J. R. Meyers, 23rd ISE Conference Abstracts, Stockholm, 1972.

6. K. G. Compton, H. L. Craig, and C. A. Smith, Determining Corrosion Rates of Metals in Seawater Using Linear Polarization Resistance Measurements," Paper No. 120 presented at N.A.C.E. CORROSION/74, Chicago, Illinois (1974).

7. B. C. Syrett, Corrosion, Vol. 33, p. 257 (1977).

8. M. E. Indig and C. Groot, Corrosion, Vol. 25, p. 455 (1969).

9. D. D. Macdonald, B. C. Syrett, and S. S. Wing, "A Study to Determine the Mechanisms of Corrosion of Copper-Nickel Alloys in Sulfide Polluted Seawater," Annual Report to Office of Naval Research, Contract No. N00014-77-C-0046 (February 1978).

10. D. D. Macdonald, B. C. Syrett, and S. S. Wing, "Methods for Measuring Corrosion Rates of Copper-Nickel Alloys in Flowing Seawater," Paper No. 25 presented at N.A.C.E. CORROSION/78, Houston, Texas (March 1978).

11. D. D. Macdonald, B. C. Syrett, and S. S. Wing, Corrosion, Vol. 34, p. 289 (1978).

12. Standard Methods for the Examination of Water and Wastewater Including Bottom Sediments and Sludges, 12th Edit. American Public Health Assoc., New York.

13. J. Czech, Oscilloscope Measuring Technique, Spring-Verlag, New York, 1965.

14. D. D. Macdonald, J. Electrochem. Soc., Vol. 125, p. 1443 (1978).

15. L. M. Callow, J. A. Richardson, and J. L. Dawson, Br. Corros. J., Vol. 11, p. 123 (1976).

CORROSION OF COPPER-NICKEL ALLOYS IN SEAWATER POLLUTED WITH SULFIDE AND SULFIDE OXIDATION PRODUCTS

by

B. C. Syrett, D. D. Macdonald, and S. S. Wing

To be presented at NACE CORROSION/79 in Atlanta, Ga. (March 1979). Also submitted for publication in Corrosion (1978).

CORROSION OF COPPER-NICKEL ALLOYS IN SEAWATER POLLUTED WITH SULFIDE AND SULFIDE OXIDATION PRODUCTS

by

B. C. Syrett, D. D. Macdonald, and S. S. Wing

SRI INTERNATIONAL
Materials Research Center
333 Ravenswood Avenue
Menlo Park, California 94025

ABSTRACT

The corrosion rates of Copper Alloys 706 (90:10 Cu:Ni) and 715 (70:30 Cu:Ni) were measured, using rotating cylinder specimens in seawater that contained oxygen, sulfide, sulfur, and polysulfide, either singly or in combination. In addition, a control test was performed using unpolluted deaerated seawater. Corrosion rates were monitored for over 24 hours, using linear polarization and potential step techniques. The work has shown that copper-nickel alloys can corrode quite rapidly in deaerated seawater if these normally "passive" alloys are made active by the presence of sulfide, or if sulfur is available as an oxidant.

CORROSION OF COPPER-NICKEL ALLOYS IN SEAWATER POLLUTED WITH SULFIDE AND SULFIDE OXIDATION PRODUCTS

by

B. C. Syrett, D. D. Macdonald, and S. S. Wing

SRI International
Materials Research Center
333 Ravenswood Avenue
Menlo Park, California 94025

Accelerated corrosion and premature failure of copper-nickel seawater piping has recently become a problem in naval ships operating in polluted seawater. From the outset, sulfide pollution was suspected as the cause of the unusually high corrosion rates. Sulfide levels as high as 0.27 mg/dm^3 were reported in the vicinity of the naval ships,[1] and it is well known[2-11] that sulfide can be aggressive toward copper alloys.

Macdonald, Syrett and Wing[2] demonstrated that the presence of sulfide in seawater induces a loss in the passivity of both 90:10 Cu:Ni (CA 706) and 70:30 Cu:Ni (CA 715). Furthermore, the accelerated corrosion in sulfide-polluted seawater appeared to arise from a shift in the corrosion potential to values active enough so that hydrogen evolution became a viable cathodic process. In "deaerated" seawater (dissolved oxygen content ~ 0.045 mg/dm^3), the corrosion potential was always more noble than -0.3 V (SCE), oxygen reduction was the only possible cathodic reaction, and therefore, the corrosion rates were low.[2,12] On the other hand, in deaerated water containing as little as 0.85 mg/dm^3 sulfide, the corrosion potential dropped to values in the range -0.45 to -0.72 V versus saturated calomel electrode (SCE), hydrogen ion reduction became possible, and the corrosion rates increased by about an order of magnitude. The overall anodic reaction changed from cuprous oxide formation in the sulfide-free system to cuprous sulfide formation in the sulfide-polluted system. In effect, therefore, sulfide ion converts the two copper-nickel alloys from an essentially passive state (protective corrosion product) into an active state (nonprotective corrosion product) that also involves an additional cathodic process (hydrogen evolution).

While sulfide is responsible for a significant increase in the corrosion rate in deaerated seawater, the polarization resistance (R_p) values given by Macdonald, Syrett, and Wing[2] indicate that, even in sulfide-polluted seawater, the corrosion rate is only of the order of 10 mg/dm^2/day at a seawater velocity of 1.62 m/s. It is possible, of course, that corrosion rates are much increased at somewhat higher seawater velocities, or in regions of high turbulence, or if localized corrosion processes (such as erosion-corrosion or pitting) are initiated. Such possibilities are currently being investigated in our laboratory, but another explanation of the premature failures of the shipboard piping system is now advanced. The sulfide-polluted seawater causing the problem is almost certainly not oxygen free. Thus, the dissolved oxygen can homogeneously oxidize the sulfide, possibly producing a species more aggressive towards copper alloys than sulfide.

Available data indicate that dissolved sulfide is oxidized fairly rapidly in seawater. Ostlund and Alexander[13] showed that for air-saturated seawater with a sulfide concentration of 3.3 mg/dm^3, the half-life of hydrogen sulfide is about 20 minutes. Avrahami and Golding,[14] in a detailed mechanistic study of this reaction, showed that elemental sulfur, sulfite (SO_3^{2-}), sulfate SO_4^{2-}), and thiosulfate ($S_2O_3^{2-}$) are reaction products and that the oxidation of sulfur to the oxyanions is slow. Kemp, Hyne, and Rennie[15] confirmed the latter finding and also showed that the oxidation of sulfur to sulfurous and sulfuric acid is catalyzed by ultraviolet radiation. Aerobic oxidation of sulfur by thiobacillus thiooxidans is also possible in aqueous systems,[16] producing sulfate concentrations as high as 1 mol/dm^3. Finally, sulfides may be oxidized by dissolved oxygen to a variety of polysulfides (S_{1+x}^{2-}, x = 1 to 4),[17] which are well known to be particularly active forms of sulfur.[18]

The primary objective of the present work was to investigate the possibility that seawater containing one or more of these sulfide oxidation products is more aggressive than either sulfide-free aerated seawater or sulfide-polluted deaerated seawater. To this end, rotating cylinder experiments were performed on 90:10 Cu:Ni and 70:30 Cu:Ni in seawater containing oxygen, sulfide, sulfur, and polysulfide, either singly or in combination. In addition, a control test was performed using unpolluted oxygen-free seawater.

EXPERIMENTAL

Rotating Cylinder Assembly

Tubular specimens of 90:10 Cu:Ni and 70:30 Cu:Ni alloys were cut from annealed copper-nickel alloy tubing with internal and external diameter of 1.35 cm and 1.71 cm, respectively. The chemical compositions and mechanical properties of the two alloys are given in Table 1. The specimens 1.27 cm in

length, were abraded with 600 grit SiC paper, degreased in acetone, rinsed with methyl alcohol then deionized water, and dried in warm air. One specimen of each alloy was then flushed-mounted into the rotating cylinder assembly shown in Figure 1. The tapered central section of the assembly fitted snugly into the central ground-glass opening of a conventional polarization cell, equipped with a platinum counterelectrode and a Luggin probe/electrolytic bridge to an external SCE. Sufficient seawater (~ 2 liters) was introduced into the test chamber to ensure that both specimens were well covered even when rotating, and to ensure that there was minimal buildup of soluble corrosion products during the 1- to 2-day test period. Well-defined turbulent flow conditions were obtained by controlling the rotational speed to 800 rpm in all experiments (peripheral velocity = 0.716 m/s; Reynolds Number $\approx$ 10,200 using the tube OD as the characteristic length).

Test Environments

The seawater used in all experiments was filtered Pacific Ocean water supplied by Steinhart Aquarium, San Francisco, California. Details of pH, salinity, and turbidity are given elsewhere.[12]

Each test environment was prepared in one or more preconditioning chambers, linked to the main test chamber by appropriate gravity-feed tubes fitted with shut-off valves. Any gases used to sparge the seawater in the preconditioning chambers flowed on into the initially empty test chamber, before finally being vented to a fume hood. In this way when the seawater was allowed to flow into the test chamber at the start of a test, the liquid and gaseous phases were relatively compatible.

Seawater containing sulfide (primarily as HS^-) was prepared by sparging first with high purity nitrogen to remove dissolved oxygen, then with a nitrogen/hydrogen sulfide gas mixture; the partial pressure of the hydrogen sulfide was chosen to be in equilibrium with the dissolved sulfide content required, in accordance with Henry's Law.

Colloidal sulfur was formed by adding sulfuric acid to a seawater solution of sodium thiosulfate until a pH of about 2.0 was reached. This solution, containing a suspension of colloidal sulfur, was flushed with air for 30 minutes to oxidize the sulfite that was also produced. The pH was adjusted to normal seawater values (8.2 ± 0.1) by making additions of sodium hydroxide, and the solution was then diluted with fresh seawater to give the desired sulfur level. Finally, this seawater was introduced into a preconditioning chamber for deaeration by sparging with high purity nitrogen.

Polysulfides, added to deaerated seawater as Na_2S_{x+1} (x = 1 to 4), were prepared from sodium sulfide and sulfur. Anhydrous sodium sulfide was made by heating $Na_2S \cdot 9H_2O$ crystals in a vacuum at 300 °C for about 16 hours. After cooling and backfilling the vacuum system with argon, elemental sulfur was added to give a weight ratio of Na_2S:S of 78:64 (that is, a gram molecular ratio of 1:2). By melting this sulfur-sulfide mixture and subsequently cooling, a mixture of polysulfides was formed centered on Na_2S_3.

This polysulfide mixture was dissolved in a small volume of deaerated seawater, filtered, and diluted to the required concentration with deaerated, nitrogen-sparged seawater. When any solid polysulfide is dissolved in an aqueous solution, it disproportionates to give free sulfide (H_2S, HS^-, or S^{2-}) and a mix of polysulfides. Several authors[17,19-21] have shown that, in aqueous solutions of pH ~ 8.2, the polysulfides SS^{2-}, S_2S^{2-}, S_3S^{2-}, and S_4S^{2-} may exist, but that only S_3S^{2-} and S_4S^{2-} are present in significant quantities. Polymerization is thought not to exceed the S_4S^{2-} stage.[20] At equilibrium, data provided by Chen and Gupta[17] indicate that the molar ratio at pH 8.2 is $[HS^-]:[S_3S^{2-}]:[S_4S^{2-}] = 1:0.0263:0.126$; or, in terms of the weight ratio of divalent to zero-valent sulfur, $S(-2):S(0) = 1:0.506$. However, in view of the difficulties inherent in any study of polysulfide chemistry, this weight ratio should be regarded as approximate. In addition, the present experiment was probably performed under nonequilibrium conditions with regard to the disproportionation reaction.

Before aerated seawater (6.60 mg/dm^3 oxygen) was introduced into the test chamber, it was held in a preconditioning chamber in contact with laboratory air but was not sparged with air.

In most tests, the total initial concentration of active species (oxygen or sulfur species) was in the range 6.5 to 6.8 mg/dm^3. However, a control test was also performed in which deaerated seawater containing no sulfur species was used. The initial compositions of the various test environments are given in Table 2.

Since gas flow was halted when the seawater was introduced into the test chamber, and since the active species were replenished during only one of the tests, the level of each species in seawater dropped as it reacted with the copper alloys. In addition, in seawater doped with colloidal sulfur, surface charge effects caused a significant fraction of the sulfur to cling to glass and plastic components of the apparatus and to the electrode surfaces. In Test No. 4, an attempt was made to counter this fairly rapid "loss" of sulfur by making intermittent additions of colloidal sulfur throughout the test, but the sulfur suspended in the seawater was never allowed to exceed a level of 6.8 mg/dm^3.

In Test No. 6, the initial oxygen and sulfide contents were controlled by delivering, from separate preconditioning chambers, equal volumes of air-saturated seawater containing 6.60 mg/dm^3 of oxygen and of deaerated seawater containing 6.84 mg/dm^3 sulfide. Mutual dilution resulted in initial oxygen and sulfide contents of 3.30 mg/dm^3 and 3.42 mg/dm^3, respectively (see Table 2). A similar procedure was adopted in Test No. 7, where sulfide and sulfur coexisted.

In all rotating cylinder experiments, the initial pH was adjusted to 8.2 ± 0.1 (when necessary) with hydrochloric acid or sodium hydroxide,

Chemical Analysis

Seawater samples could be drawn from the preconditioning or test chambers chambers for chemical analysis. Intermittent measurement of the level of active species dissolved in the seawater often provided information on the rates of reactions at the copper alloy surfaces.

Oxygen content was measured by Winkler titration[22] only at the beginning and end of Test 1 and 6 (see Table 2).

Sulfide level was measured by delivering a 75 cm^3 seawater sample into 25 cm^3 of a sulfide antioxidant buffer (SAOB) solution of high pH. This mixture was then titrated against lead perchlorate [$Pb(ClO_4)_2$] solution, using a S^{2-} ion electrode to determine the end point. The high pH of the SAOB solution (20 g/dm^3 sodium hydroxide, 80 g/dm^3 sodium salicylate, 18 g/dm^3 ascorbic acid) ensured that the sulfide was present as S^{2-}, and the presence of the ascorbic acid ensured that air oxidation of the sulfide was minimal.

To determine the concentration of colloidal sulfur suspended in the seawater, it was first necessary to extract the sulfur in n-hexane by vigorously agitating a two-phase hexane/seawater mixture. The sulfur level in the n-hexane was determined using UV-visible light spectrometry. The height of the absorbance peak at a wavelength of 260 nm was measured and compared with a calibration curve of peak height versus sulfur content.

The polysulfide content of the seawater was estimated using two methods. In each case, the polysulfides in solution as S_xS^{2-} were broken down into zero-valent sulfur [S(0)] and free sulfide [S(-2)]. The solution was then analyzed for sulfur and total free sulfide (existing sulfide plus polysulfide-derived sulfide).

In the first method, 50 cm^3 of the seawater were delivered into a closed chamber containing 10 cm^3 of concentrated hydrochloric acid that had previously been flushed with argon. The resulting low pH of the acidified seawater caused decomposition of the polysulfides:

$$S_xS^{2-} + 2H^+ \rightarrow H_2S + xS \qquad (1)$$

In addition, any HS^- ions that had coexisted with the polysulfides were converted to H_2S.

$$HS^- + H^+ \rightarrow H_2S \qquad (2)$$

The total free sulfide content (H_2S from Eq. 1 and Eq. 2) was determined by flushing the acidified seawater with argon. The resultant H_2S/argon gas

mixture was passed through a column of diluted SAOB solution (1 part SAOB: 3 parts water) to strip the H_2S, then this solution was titrated against lead perchlorate solution as described above. The colloidal sulfur that remained suspended in the acidified sulfide-free seawater was extracted with n-hexane and the concentration of sulfur was determined, as before, by UV-visible light spectrometry.

The second method was somewhat more convenient and gave almost identical results. Here, a 50 cm^3 sample of seawater was delivered into a separatory funnel that had previously been flushed with argon and into which 15 cm^3 of n-hexane had been placed. During the subsequent vigorous agitation of the two phase hexane/seawater mixture, the n-hexane caused decomposition of the labile polysulfides by providing a sink for the zero-valent sulfur.

$$S_x S^{2-} + H^+ \rightarrow HS^-(aq) + xS \text{ (hexane)} \qquad (3)$$

The total free sulfide content (HS^- from Eq. 3 plus preexisting HS^-) was determined by drawing a 37.5 cm^3 seawater sample from the separatory funnel, mixing this with 12.5 cm^3 of the SAOB solution, then performing the usual lead perchlorate titration. The sulfur content was determined by performing UV-visible light spectrometry on the n-hexane.

Some insight into the distribution of polysulfides in solution in the seawater was obtained by examining the complete UV-visible light spectrum in the wavelength range of 250 to 500 nm.[21]

Corrosion Rate Measurements

Previous work[12,23] has shown that in situ electrochemical techniques are eminently suitable for monitoring corrosion rates of copper-nickel alloys in seawater environments, provided that certain precautions are taken. Two techniques (linear polarization, and potential step) were used in the present study. Linear polarization measurements were made by potentiodynamically sweeping the specimen potential between the limits E_{corr} + 3 mV and E_{corr} - 3 mV and recording potential versus polarizing current. These small amplitude cyclic voltammograms were obtained at potential sweep rates in the range 0.01 to 0.5 mV/s so as to define the sweep rate dependence of the apparent polarization resistance, R_{app}. The true polarization resistance, R_p, was then obtained by plotting $1/R_{app}$ versus potential sweep rate and extrapolating the curve to zero sweep rate, as described in detail by Macdonald.[24] The corrosion rate is inversely proportional to the polarization resistance, as defined by the Stern-Geary relationship.[25]

The potential step technique involves recording the decay of the polarizing current after potentiostatically imposing a small step change in the specimen potential (ΔE). The steady state current (Δi) is then used to

determine the polarization resistance ($R_p = \Delta E/\Delta i$). In the present study, ΔE values of both + 2 mV and - 2 mV were used, and R_p was calculated as the average of the resulting $\Delta E/\Delta i$ values. Decay times of at least 5 minutes, and up to 15 minutes, were found to be necessary to establish the values of the steady-state polarizing current.

RESULTS

Rotating Cylinder Experiments

The corrosion rates of the two copper-nickel alloys in the various composeawater environments are shown as a function of time in Figures 2 to 9. The rates of removal of the active species dissolved in the seawater are also indicated in these figures. It is important to note that the sulfur levels given in Figures 4, 5, and 8 refer to the colloidal sulfur actually in suspension and that no allowance has been made for the sulfur clinging to glass, plastic, and metal surfaces within the test chamber. Because sulfur clung to the copper-nickel alloy surfaces during each of these tests (Nos. 3, 4, and 7), the local concentrations of sulfur were very much higher than those indicated in Figures 4, 5, and 8. It is very unlikely that the local concentration of sulfur ever reached zero at every location on the surface of a copper-nickel alloy specimen.

In Figure 6, the polysulfide content is expressed in terms of the components, sulfide [S(-2)] and sulfur [S(0)] (Eq. (1) to (3)) and also in terms of the total sulfur [S(-2) + S(0)]. The UV-visible light spectra for the seawater present 230 minutes and 1331 minutes after starting the test are shown in Figure 10, together with the spectrum for the stock seawater solution. This stock solution [S(-2) = 5.61 mg/dm^3, S(0) = 3.78 mg/dm^3] was diluted with fresh deaerated seawater just before starting the test to give an initial total sulfur [S(-2) + S(0)] content of 6.57 mg/dm^3. The presence of any polysulfide in the seawater gives rise to a set of peaks or shoulders in the spectrum at the wavelength ranges indicated at the top of Figure 10.[20] It can be seen that the spectra are consistent with the earlier suggestion that S_3S^{2-} and S_4S^{2-} are the only polysulfides present in significant quantity, but the spectra do not prove the absence of other polysulfides. The spectra have been plotted in terms of log I_0/I, where I_0 is the incident light intensity and I is the transmitted light intensity at a particular wavelength. It has been shown[17,19] that log I_0/I at 290 nm is proportional to the S(0) content. The present data are in good agreement with the previous studies, in that a plot of log I_0/I at 290 nm versus S(0) content yields a straight line passing through the origin (Beer's law).

The corrosion potentials for 90:10 Cu:Ni and 70:30 Cu:Ni have been plotted in Figures 11 and 12, respectively, as a function of time and environment. Bearing in mind that the levels of the active species changed

with time, it can be seen that sulfide plus sulfur environments gave rise to the most active potentials [< -0.70 volt (SCE)], aerated seawater gavo the most noble potentials (> -0.23 volt), and deaerated seawater and environments containing sulfur or polysulfides gave intermediate potentials (-0.40 to -0.60 volt). Seawater containing sulfide resulted in active potentials for the 90:10 Cu:Ni alloy but gave rise to intermediate potentials for the 70:30 Cu:Ni alloy.

Surface Examination

After each test, the surfaces of the copper nickel alloy specimens were examined by scanning electron microscopy (SEM). Surface topography was found to be dependent on the environmental conditions experienced during the test (see Figures 13 to 26). In seawater containing no sulfur species, the specimen surfaces showed little obvious sign of corrosion products (Figures 13, 14, 25, and 26) and the initial polishing scratches were plainly visible. In contrast, specimens that had been exposed to environments containing sulfide, sulfur, or polysulfides showed clear signs of corrosion and the surfaces were covered, at least in part, with a porous layer of small particles or crystallites. These particles appear light colored in Figure 15 to 24, but the corrosion products are black when viewed optically. Such crystallite layers would be expected when the corrosion product has precipitated from solution.

Energy dispersive X-ray (EDX) analyses of the surface corrosion products are also included in Figures 13 to 26. These analyses show that the corrosion products on specimens exposed to aerated or deaerated seawater may contain traces of sulfur (Figures 13, 25 and 26). The source of the sulfur is unknown, but it is possible that, under anaerobic conditions, sulfate reducing bacteria were sometimes present in the seawater and that the traces of sulfide produced were scavenged by the copper alloys. An EDX analysis does not detect oxygen, so the spectra shown in Figures 13, 14, 25, and 26 are not inconsistent with our expectation that the primary corrosion product is Cu_2O on specimens exposed to seawater free of sulfur species. The corrosion products on all specimens exposed to seawater containing sulfur, sulfide or polysulfide (Figures 15 to 24) contained a substantial amount of sulfur, probably as stoichiometric and substoichiometric cuprous sulfide.[2] In addition to sulfur, there was often evidence of significant quantities of silicon in these corrosion products, the silicon probably originating from the Pyrex test chamber. In previous work[2] in which the same copper-nickel alloys were exposed to flowing seawater contaminated with sulfide, the flow loop was fabricated almost completely from plastic, and silicon was not detected in the corrosion products. It is considered unlikely that the presence of silica or silicates had a significant effect on the corrosion mechanisms or corrosion rates, but this possibility cannot be entirely precluded.

In some instances, chlorine was also detected (Figures 13 and 17), presumably as copper hydroxychloride.

DISCUSSION

Mechanisms

This study has investigated a variety of seawater environments, ranging from those that are plainly oxidizing to those that are reducing in nature. Pertinent to the study are the thermodynamically possible mechanisms of corrosion in the various environments. In discussing these, reference will be made to the potential-pH diagrams derived by Verink[26] for copper in sulfide-polluted seawater and in sulfide-free seawater at 25°C. Figure 27 presents modified versions[2] of these diagrams.

In seawater containing no sulfur species, E_{corr} for both alloys lies on the noble side of the equilibrium line for hydrogen evolution [about -0.54 volt (SCE) at pH 8.2 and a partial pressure of hydrogen of 10^{-5} atm.]. Thus, H^+ ion (or water) reduction is not a viable cathodic reaction, and corrosion is possible only in the presence of dissolved oxygen;

$$Cu \rightarrow Cu^+ + e^- \qquad \text{(Anodic)} \qquad (4)$$

$$O_2 + 2H_2O + 4e^- \rightarrow 4OH^- \qquad \text{(Cathodic)} \qquad (5)$$

The Cu^+ ions hydrolyze at the surface to form a fairly protective Cu_2O film. Thus, in the absence of sulfur species and oxygen, corrosion will not occur to any significant extent because there is no viable cathodic reaction. This is illustrated in Test No. 8 where the small amount of corrosion that did occur can be attributed to traces of residual oxygen in the seawater.

In the presence of sulfide, however, the corrosion potentials generally shift to more active values (see Figure 11), and hydrogen evolution then becomes a possible cathodic partial process.

$$2H^+ + 2e^- \rightarrow H_2\uparrow \qquad (6)$$

$$2HS^- + 2e^- \rightarrow H_2\uparrow + 2S^{2-} \qquad (7)$$

$$2H_2O + 2e^- \rightarrow H_2\uparrow + 2OH^- \qquad (8)$$

The Cu^+ ions formed at anodic sites react, in this instance, with the HS^- ions in solution to form a cuprous sulfide film, as described previously by Macdonald, Syrett, and Wing.[2] It is interesting to note that in Test No. 2, in which the alloys were exposed to seawater containing sulfide, the potential of the 90:10 Cu:Ni alloy remained well below the -0.54 volt (SCE) level necessary for significant hydrogen evolution, whereas the potential of the

70:30 Cu:Ni alloy was more active than -0.54 volt (SCE) for the first three hours and more noble thereafter (see Figures 11 and 12). Predictably, the corrosion rate of the 90:10 Cu:Ni alloy was relatively high throughout the test, whereas the rate of the 70:30 Cu:Ni alloy was high only for the first 3 hours and then dropped sharply. These observations are entirely consistent with our previous suggestion[2] that hydrogen evolution is a possible cathodic reaction because the presence of sulfide causes a shift in the potential of the dominant anodic process (formation of Cu_2S versus Cu_2O) to more active values. It is important to note that the HS^- ions themselves cannot be reduced and hence are not directly involved in the electron exchange reactions that occur at the metal-solution interface.

In contrast, elemental sulfur can be reduced to sulfide. Thus, in deaerated seawater environments containing colloidal sulfur or dissolved sulfur (as polysulfides), cathodic reaction involving the reduction of sulfur becomes feasible:

$$S + H_2O + 2e^- \rightarrow HS^- + OH^- \qquad (9)$$

or

$$S_xS^{2-} + H_2O + 2e^- \rightarrow HS^- + S_{x-1}S^{2-} + OH^- \qquad (10)$$

Again, the HS^- ions may then react with the Cu^+ ions to produce a cuprous sulfide surface film at active potentials (Figure 27).

Thus, in Test No. 7, the presence of sulfide resulted in active potentials [< -0.7 volt (SCE)] for both copper-nickel alloys, and the cathodic evolution of hydrogen was a viable cathodic partial reaction. Since colloidal sulfur was also present in this system, a second partial process, sulfur reduction, was also possible. At least two cathodic reactions were also possible in Test No. 6, in which oxygen and sulfide coexisted initially. Under these conditions, some of the sulfide is probably homogeneously oxidized to sulfur[14] or polysulfides.[17] Thus, in addition to oxygen reduction, reduction of sulfur is also a viable cathodic partial reaction. The catastrophic attack by elemental sulfur on carbon steel in aqueous systems has been previously demonstrated by Macdonald, Roberts and Hyne.[27,28] It is interesting to note that the HS^- ions produced during the reduction of S or S_xS^{2-} may be homogeneously reoxidized to sulfur or polysulfide ions by the dissolved oxygen. Thus, the $HS^- \rightleftarrows S$ reaction can be regarded, in this instance, as an indirect oxygen reduction process.

Other reactions are undoubtedly possible. For example, Syrett[10] found that during the corrosion of copper in aqueous solutions containing oxygen and dissolved sulfide, Cu_2S formed at low oxygen/sulfide ratios, but CuS predominated when the oxygen/sulfide ratio was high. In addition, Mor and Beccaria[8] report the formation of $Cu_{1.8}$ and Cu_7S_4, as well as Cu_2S and CuS,

on copper exposed to artificial seawater containing sulfides.

Irrespective of the exact roles of the sulfide oxidation products in the corrosion process, the various reactions outlined above appear to explain why normally noncorrosive deaerated seawater may become highly corrosive when sulfur-containing species are present. Furthermore, these mechanisms offer an explanation for accelerated corrosion in aerated polluted seawater, because alternative cathodic reactions become possible that could increase the rate of charge transfer across the interface.

Corrosion Rate Data

The corrosion rate data in Figures 2 to 9 are given in terms of $1/R_p$ values. Stern and Geary[25] have shown that $1/R_p$ is directly proportional to the corrosion current (i_{corr})

$$i_{corr} = 1/R_p \left[\beta_a \beta_c / 2.303(\beta_a + \beta_c)\right] \quad (11)$$

or

$$i_{corr} = B/R_p \quad (12)$$

$$B = \beta_a \beta_c / 2.303(\beta_a + \beta_c) \quad (13)$$

where β_a and β_c are the anodic and cathodic Tafel coefficients, respectively. The weight loss per unit time (dW/dt) is determined by Faraday's Law

$$dW/dt = \bar{M}\, i_{corr}/96{,}500\, \bar{n} \quad (14)$$

where $\bar{M}$ and $\bar{n}$ are the atomic weight and change in oxidation state, respectively, suitably averaged for alloy composition.[23] Combining Eq. 11 and Eq. 13 yields

$$dW/dt = (\bar{M}\, B/96500\, \bar{n})\ 1/R_p \quad (15)$$

Thus, the corrosion rate is related to the $1/R_p$ value through a "constant" that is dependent on both alloy composition and the values of the Tafel coefficients; these coefficients are in turn, dependent on the environmental conditions. Nevertheless, the range of likely values of $\bar{M}\, B/96500\, \bar{n}$ is limited and, for many purposes, it is convenient to compare $1/R_p$ values directly for different alloys in different environments. In the copper-nickel alloy/seawater systems considered in the present work, it is most unlikely that the highest value of $\bar{M}\, B/96500\, \bar{n}$ differed from the lowest value by more than a factor of five. Since the main objective of these experiments was to

define environmental conditions that resulted in corrosion rates considerably higher than those obtained in unpolluted seawater, a direct comparison of the $1/R_p$ values seems justifiable.

On this basis, the corrosion rates in all but the deaerated seawater environment (Test 8) were quite similar: the $1/R_p$ values for 70:30 Cu:Ni were generally in the range 0.3 to 3.0 kilohms^{-1}, whereas the $1/R_p$ values for 90:10 Cu:Ni were generally in the range 0.5 to 5.0 kilohms^{-1}. The corrosion rate for the 90:10 Cu:Ni alloy was unusually high during the first two hours in the polysulfide environment, but thereafter the $1/R_p$ values dropped to the "normal" range. Similarly, the 70:30 Cu:Ni alloy experienced above average corrosion rates when first exposed to aerated water. However, it is emphasized that only semiquantitative comparisons of these $1/R_p$ values can be made because of the uncertainty in the values of B (Equation 14).

As expected, the $1/R_p$ values in deaerated seawater were more than an order-of-magnitude lower than in any other test environment. This finding supports previous studies by Macdonald, Syrett and Wing,[2] in which the corrosion rate of copper-nickel alloy tubing in flowing deaerated seawater was very low in the absence of dissolved sulfide, but increased dramatically when 0.85 mg/dm^3 of sulfide was added to the system.

The present experiments clearly confirm that the presence of sulfide, colloidal sulfur, polysulfides, or combinations of these species can turn essentially noncorrosive deaerated seawater into a comparatively corrosive environment. However, these corrosion rate data (Figures 2 to 9) do not explain the accelerated corrosion of the copper nickel seawater piping systems in naval ships, because the $1/R_p$ values in aerated seawater are approximately the same as those obtained in the environments containing sulfur species. However, these results can be compared with those obtained in previous experiments[2,12] that were performed for substantially longer periods. In these experiments, seawater flowed through 90:10 Cu:Ni and 70:30 Cu:Ni alloy tube specimens at 1.62 m/s, and R_p values were monitored intermittently for more than a week in both unpolluted aerated seawater and sulfide-polluted deaerated seawater. Although the hydrodynamic conditions were significantly different from those in the present test system, $1/R_p$ values for the two alloys were of the same order as those shown in Figure 2 to 9 during the first 24 hour period. However, after several days under test, it became clear that corrosion rates in the sulfide-polluted seawater were either constant or increasing with time, while corrosion rates in the aerated seawater were decreasing. We believe that the apparent lack of accelerated corrosion in the present system may reflect the short time over which the experiments were performed, and that the deleterious nature of sulfide (and other sulfur species) would have become increasingly apparent with time of immersion.

Although the corrosion rates measured in polluted and in aerated seawater did not differ significantly during the 1-day test period, examination of the specimen surfaces by scanning electron microscopy indicated, as described earlier, that the presence of the sulfur species has a marked effect on the

physical and chemical characteristics of the surface corrosion products. The cuprous oxide films formed in unpolluted seawater were generally smooth, nonporous, and adherent (Figures 13, 14, 25 and 26), while the sulfur-containing films were relatively thick, porous, and appeared to be composed of small crystallites (Figures 15 to 24). (The precipitation of cuprous sulfide would be expected as the anodically produced Cu^+ ions reacted with the HS^- ions.) These crystallites could be scraped off the specimen surfaces fairly easily, and therefore it seems reasonable to suggest that, under somewhat more adverse flow conditions than those in the present work, the surface film may break down and rapid attack of the underlying metal may result. Film breakdown may be electrochemical or mechanical in nature[29] and will occur preferentially, as observed,[1] in regions where the hydrodynamic and mass transfer boundary layers are thinnest--for instance, in elbows, tees, and near small surface projections.

If the removal of poorly adherent corrosion-product films is indeed the primary cause of the accelerated attack, it can be speculated that the presence of polysulfides will accentuate this attack, since the highest $1/R_p$ values recorded were obtained in the presence of polysulfides (see Figure 6). Under the hydrodynamic conditions of the present work, the copper sulfide film was observed to form rapidly on the specimen surface, and corrosion rates after the first two or three hours were comparatively low. However, under more adverse hydrodynamic conditions, the high corrosion rates might will have been maintained for long periods. There seems little doubt that polysulfides exist for at least short periods in polluted seawater, because sulfide has been detected[1] and homogeneous oxidation of sulfide by dissolved oxygen to polysulfides is likely.[17,19-21] The role of polysulfides in the accelerated attack of seawater piping should perhaps be studied in more detail in the future.

CONCLUSIONS

A study of the corrosion of 90:10 Cu:Ni and 70:30 Cu:Ni alloys in various seawater environments indicates that the presence of sulfide, sulfur, or polysulfides can turn essentially noncorrosive deaerated seawater into a comparatively corrosive environment. It is speculated that pollution of the seawater with sulfur species can cause accelerated attack if the formation of the loosely adherent copper sulfide corrosion product is coupled with adverse hydrodynamic conditions.

ACKNOWLEDGMENT

Financial support of this work by the Office of Naval Research (Contract No. N00014-88-C-0046), is gratefully acknowledged.

Table 1

CHEMICAL COMPOSITION AND MECHANICAL PROPERTIES
OF 90:10 Cu:Ni (Alloy 706) and 70:30 Cu:Ni (Alloy 715)

Element	Composition, wt% Alloy 706[a]	Alloy 715[b]
Cu	87.9	68.7
Ni	10.2	29.7
Mn	0.24	0.61
Fe	1.34	0.53
P	≤0.02	0.001
Pb	0.01	0.007
S	≤0.02	0.016
Zn	0.28	0.45

Mechanical Property	Alloy 706[a]	Alloy 715[b]
Yield Stress, MPa (ksi)	148 (21.4)	152 (22.0)
Tensile Stress, MPa (ksi)	312 (46.2)	420 (60.9)
Elongation, % (in 5.08 cm)	45.6	45.3

(a) Chemical composition and mechanical properties of Alloy 706 were supplied by The Anaconda Co., Brass Division, Los Angeles Plant, Paramount, California.

(b) Chemical composition and mechanical properties of Alloy 715 were supplied by Phelps Dodge Brass Co., Los Angeles Tube Division, Los Angeles, California.

Table 2

INITIAL CONCENTRATIONS OF THE ACTIVE SPECIES IN THE VARIOUS SEAWATER TEST ENVIRONMENTS

Test Number	Oxygen mg/dm^3	Sulfide mg/dm^3(a)	Sulfur mg/dm^3(a)	Polysulfide mg/dm^3(a)
1	6.60	0	0	0
2	0	6.67	0	0
3	0	0	6.80	0
4(b)	0	0	6.50	0
5	0	0	0	6.57
6	3.30	3.42	0	0
7	0	3.39	3.35	0
8	0	0	0	0

(a) Calculated as [S]

(b) Intermittent additions of sulfur (see text).

REFERENCES

1. R. B. Niederberger, J. P. Gudas, and G. J. Danek, "Accelerated Corrosion of Coppor-Nickel Alloys in Polluted Waters," Paper No. 76 presented at NACE CORROSION/76, Houston, Texas (1976).

2. D. D. Macdonald, B. C. Syrett, and S. S. Wing, "The Corrosion of Cu-Ni Alloys 706 and 715 in Flowing Seawater. II Effect of Dissolved Sulfide," accepted for publication in Corrosion (1978).

3. P. A. Akolzin and A. F. Bogachev, Protection of Metals, Vol. 5, p. 262 (1969).

4. H. Yamada and T. Nakamura, J. Japan Foundrymen's Soc., Vol. 36, p. 470 (1964).

5. J. C. Rowlands, J. Appl. Chem., Vol. 15, p. 57 (1965).

6. E. D. Mor and A. M. Beccaria, Corrosion, Vol. 30, p. 354 (1974).

7. J. F. Bates and J. M. Popplewell, Corrosion, Vol. 31, p. 269 (1975).

8. E. D. Mor and A. M. Beccaria, Br. Corr. J., Vol. 10, p. 33 (1975).

9. J. P. Gudas and H. P. Hack, "Sulfide Induced Corrosion of Copper-Nickel Alloys," Paper No. 93 presented at NACE CORROSION/77, San Francisco, California (1977).

10. B. C. Syrett, Corrosion, Vol. 33, p. 257 (1977).

11. L. Giuliani and G. Bombara, Br. Corr. J., Vol. 8, p. 20 (1973).

12. D. D. Macdonald, B. C. Syrett, and S. S. Wing, Corrosion, Vol. 34, p. 289 (1978).

13. H. G. Ostlund and J. Alexander, J. Geophys. Res., Vol. 68, p. 3995 (1963).

14. M. Avrahami and R. M. Golding, J. Chem. Soc. (A), p. 647 (1968).

15. E. Kemp, J. B. Hyne, and W. J. Rennie, Int. J. Sulfur Chem., (A) Vol. 1, p. 69 (1971).

16. R. L. Starkey, Soil Sci., Vol. 101, p. 297 (1966).

17. K. Y. Chen and S. K. Gupta, Environmental Letters, Vol. 4, p. 187 (1973).

18. R. G. Caldwell, "Kinetics and Mechanism of Active Sulfur Formation and Corrosion of Copper by Active Sulfur," Amer. Gas. Assoc. Report, Cat. No. 12/SR (1963).

19. G. Schwarzenbach and A. Fischer, Helv. Chem. Acta, Vol. 43, p. 1365 (1960).

20. D. Peschanski and G. Valensi, J. Chim. Phys., Vol. 46, p. 602 (1949).

21. W. Giggenbach, Inorg. Chem., Vol. 11, p. 1201 (1972).

22. Standard Methods for the Examination of Water and Wastewater Including Bottom Sediments and Sludges, 12th ed., Amer. Public Health Assoc., New York, (1965).

23. B. C. Syrett and D. D. Macdonald, "The Validity of Electrochemical Methods for Measuring Corrosion Rates of Copper-Nickel Alloys in Seawater," submitted for publication in Corrosion (1978).

24. D. D. Macdonald, J. Electrochem. Soc Vol. 125, p. 1443 (1978).

25. M. Stern and A. L. Geary, J. Electrochem. Soc., Vol. 104, p. 56 (1957).

26. E. D. Verink, in Electrochemical Techniques for Corrosion R. Baboian, ed., p. 43, NACE, Houston, Texas (1977).

27. D. D. Macdonald, B. Roberts, and J. B. Hyne, Corr. Sci., Vol. 18, p. 411 (1977).

28. D. D. Macdonald, B. Roberts, and J. B. Hyne, Corr. Sci., Vol. 18, p. 499 (1977).

29. B. C. Syrett, Corrosion, Vol. 32, p. 242 (1976).

FIGURES

Figure 27 Potential-pH Diagrams for Copper in Seawater at 25°C
The equilibrium lines for hydrogen evolution [line ⓐ] and oxygen evolution [line ⓑ] have been drawn for gas partial pressures of 10^{-5} atm.

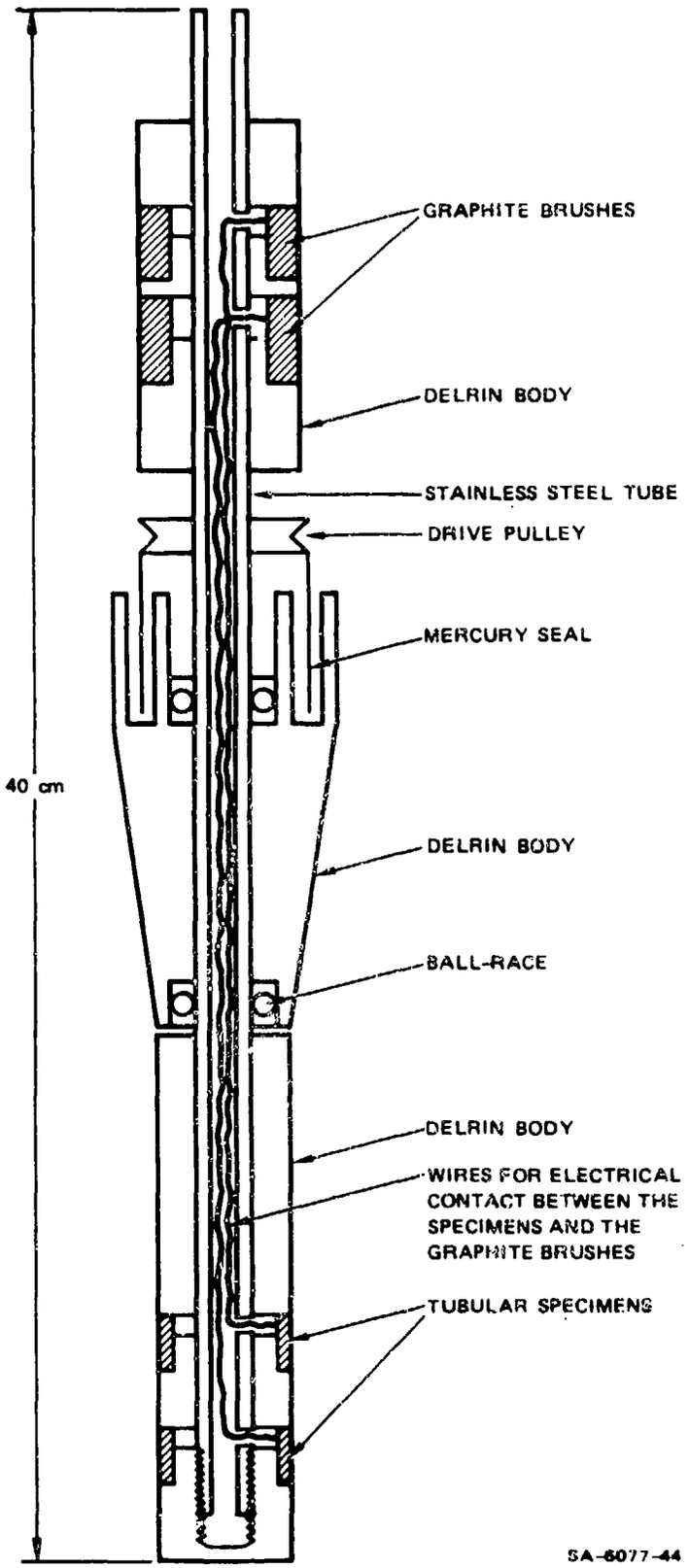

FIGURE 1 ROTATING CYLINDER ASSEMBLY

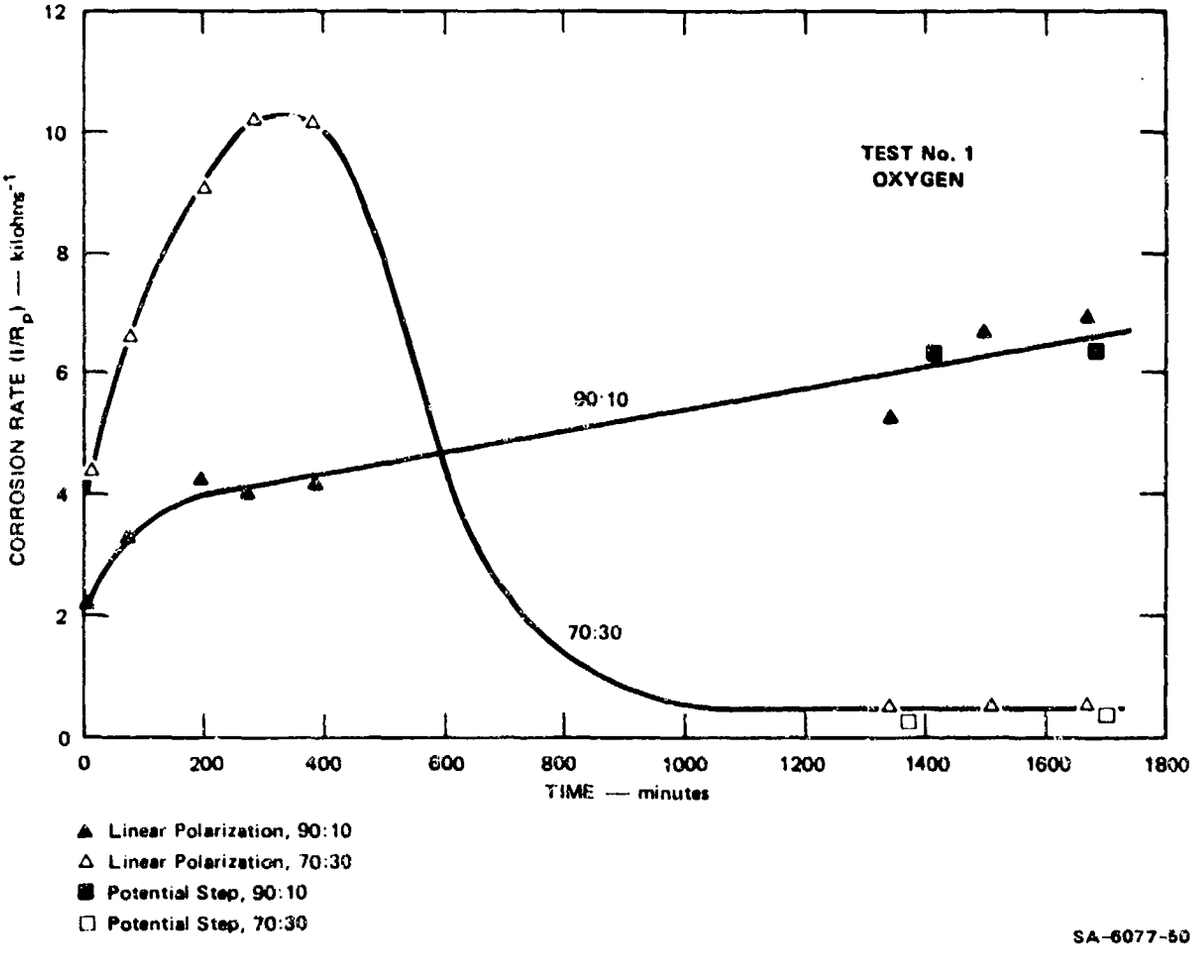

FIGURE 2 CORROSION RATE VERSUS TIME FOR 90:10 Cu:Ni AND 70:30 Cu:Ni ALLOYS IN AERATED SEAWATER

(Initial oxygen content = 6.60 mg/dm^3; final oxygen content = 5.99 mg/dm^3).

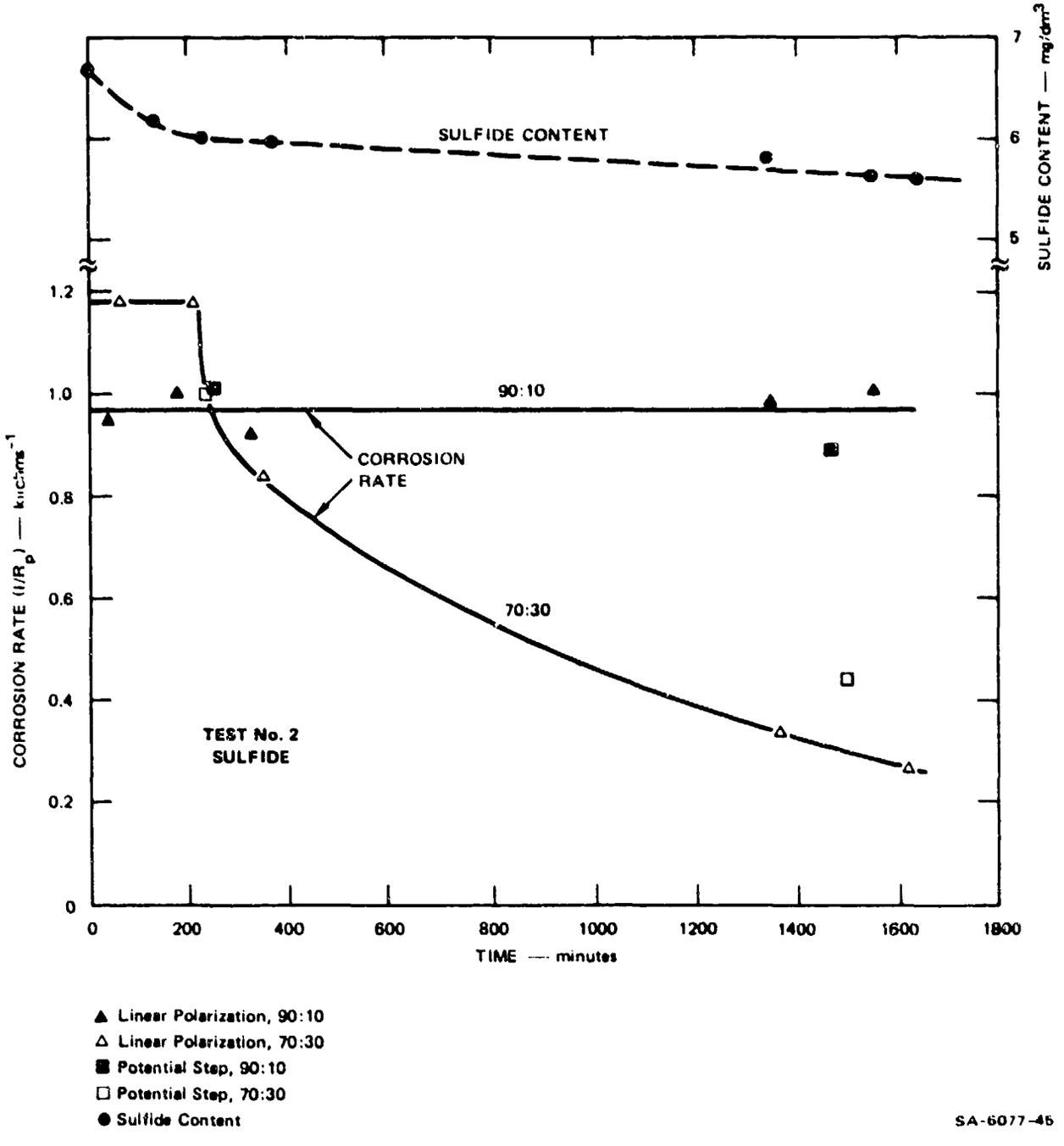

FIGURE 3 CORROSION RATE AND DISSOLVED SULFIDE CONTENT VERSUS TIME FOR 90:10 Cu:Ni AND 70:30 Cu:Ni ALLOYS IN SEAWATER.

Initial sulfide content = 6.67 mg/dm^3

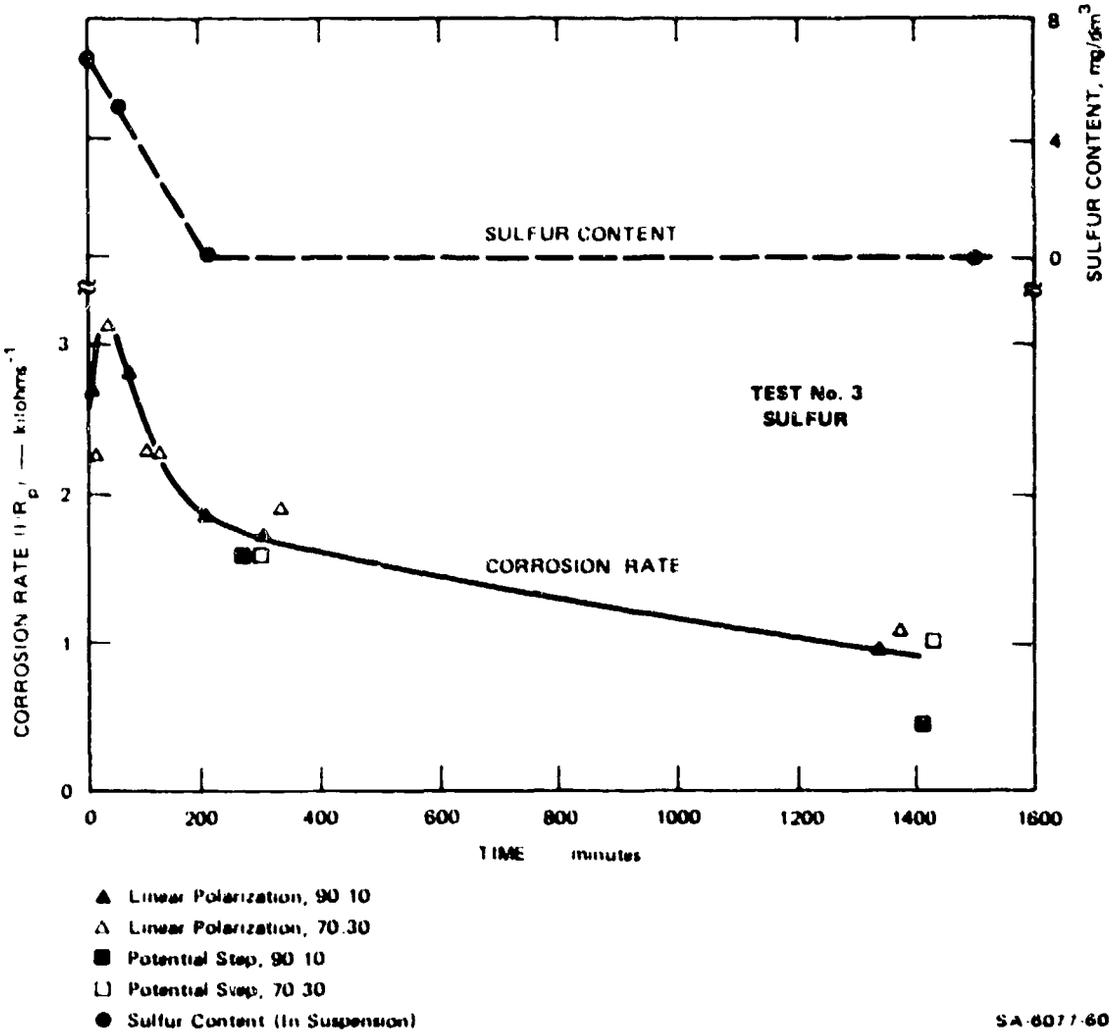

FIGURE 4 CORROSION RATE AND COLLOIDAL SULFUR CONTENT VERSUS TIME FOR 90:10 Cu:Ni AND 70:30 Cu:Ni ALLOYS IN SEAWATER.

Initial sulfur content 6.80 mg.dm^{3}

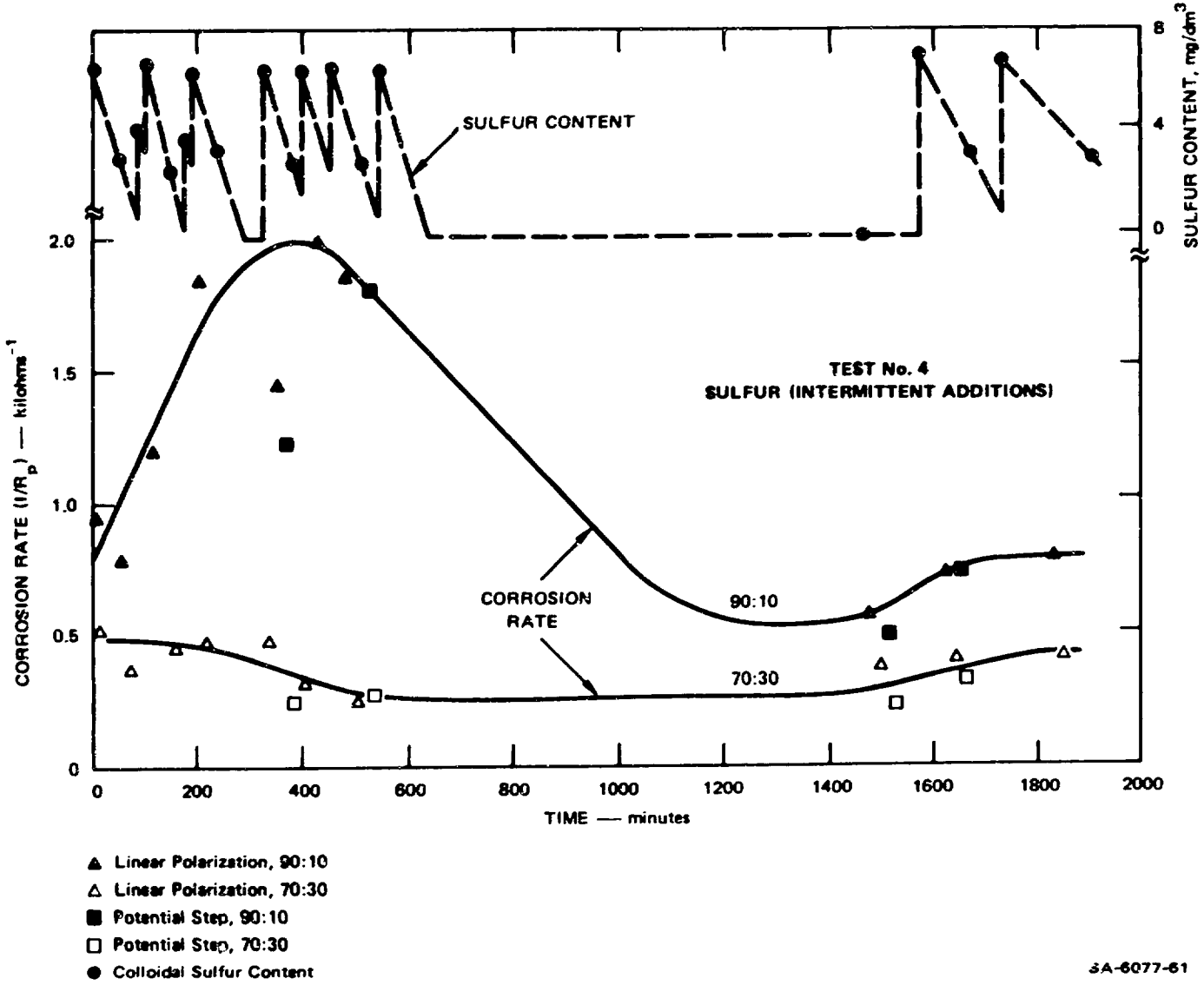

FIGURE 5 CORROSION RATE AND COLLOIDAL SULFUR CONTENT VERSUS TIME FOR 90:10 Cu:Ni AND 70:30 Cu:Ni ALLOYS IN SEAWATER.

Initial sulfur content = 6.50 mg/dm^3 and sulfur added intermittently throughout test

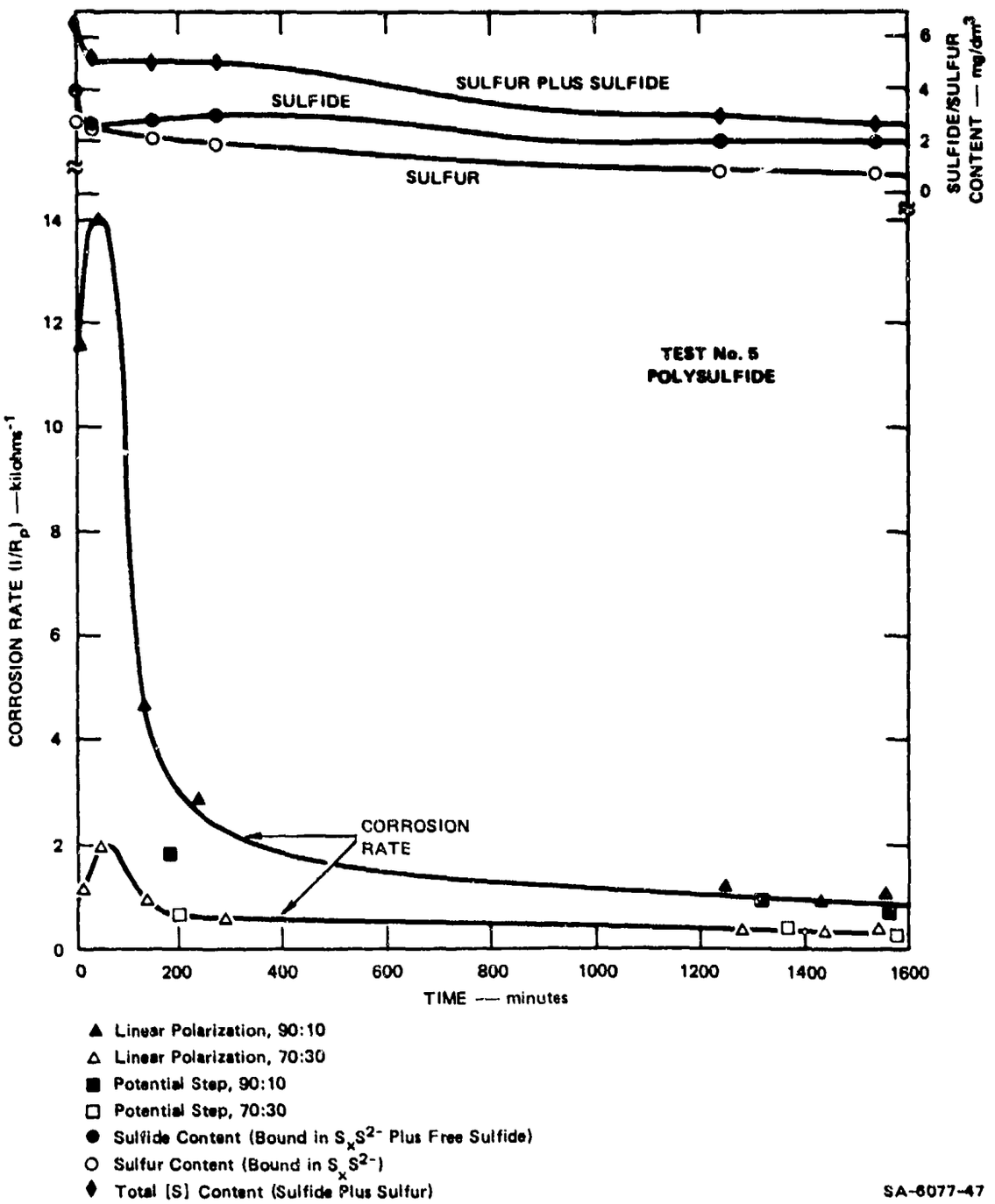

FIGURE 6 CORROSION RATE AND POLYSULFIDE CONTENT (EXPRESSED AS SULFIDE AND SULFUR COMPONENTS) VERSUS TIME FOR 90:10 Cu:Ni AND 70:30 Cu:Ni ALLOYS IN SEAWATER

Initial sulfide content = 3.93 mg/dm^3; initial sulfur content = 2.65 mg/dm^3.

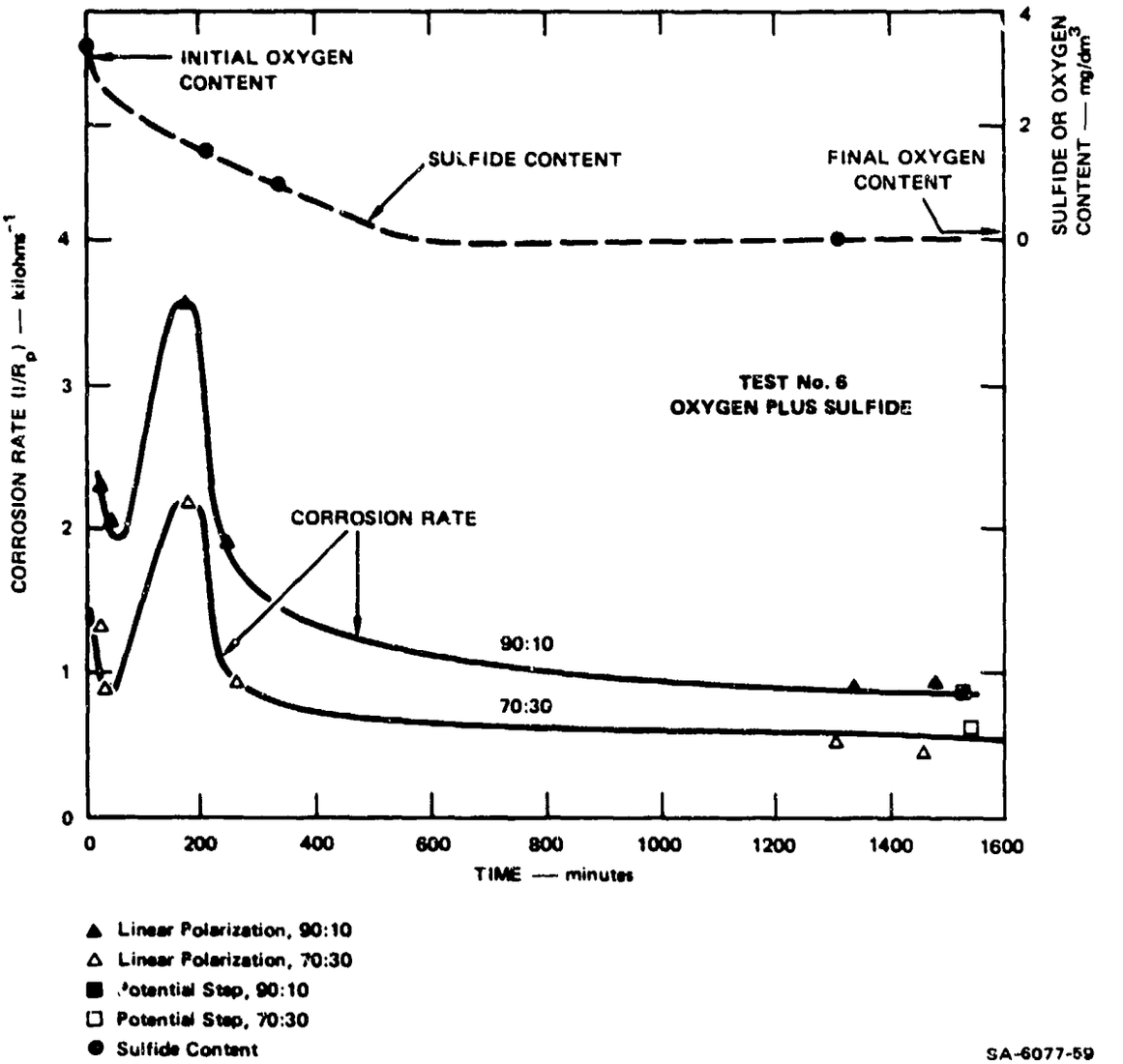

FIGURE 7 CORROSION RATE, SULFIDE CONTENT, AND OXYGEN CONTENT VERSUS TIME FOR 90:10 Cu:Ni AND 70:30 Cu:Ni ALLOYS IN SEAWATER.

Initial sulfide content = 3.42 mg/dm^3; initial oxygen content = 3.30 mg/dm^3

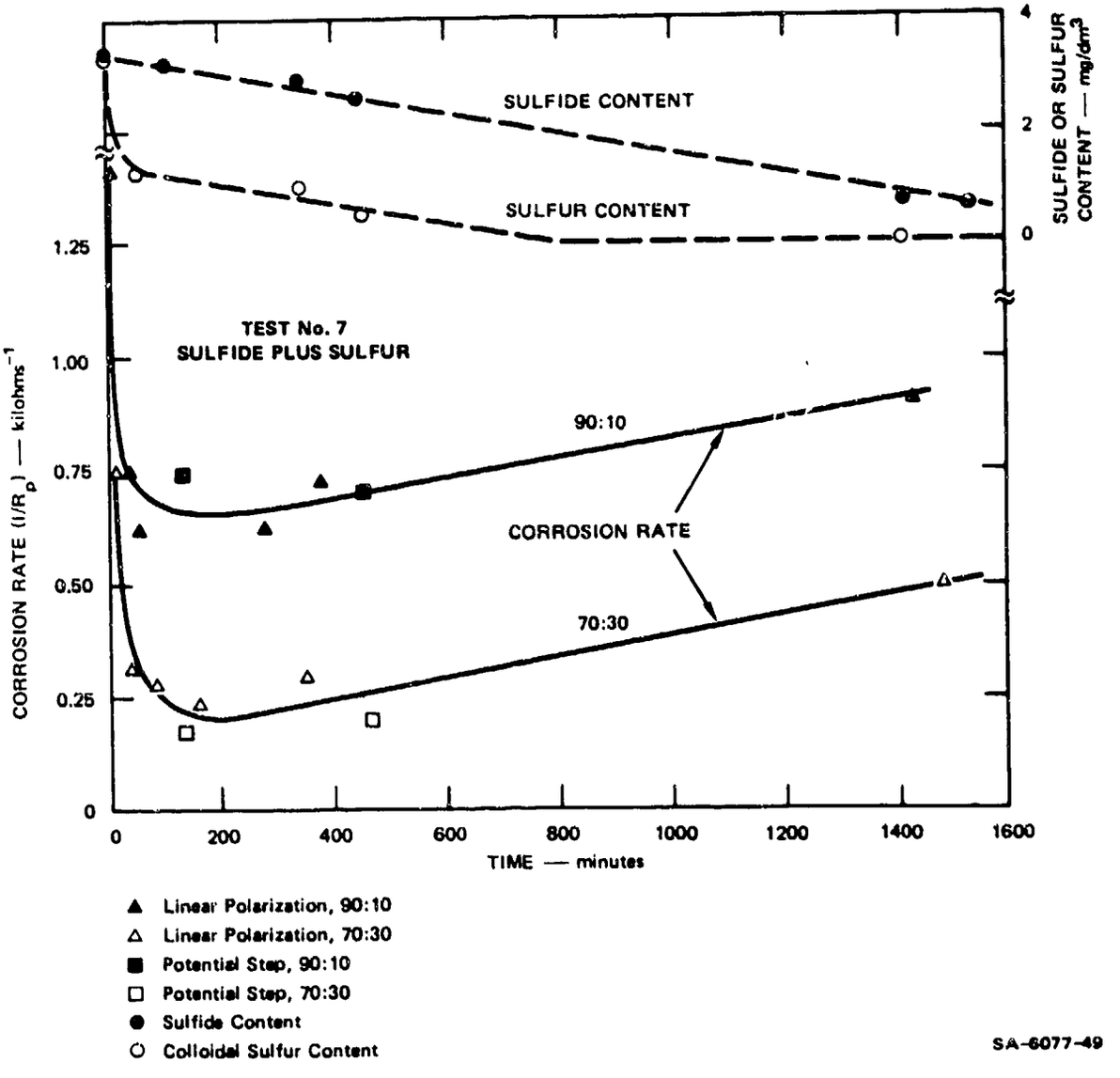

FIGURE 8 CORROSION RATE, DISSOLVED SULFIDE CONTENT, AND COLLOIDAL SULFUR CONTENT VERSUS TIME FOR 90:10 Cu:Ni AND 70:30 Cu:Ni ALLOYS IN SEAWATER

Initial sulfide content = 3.39 mg/dm^3; initial sulfur content = 3.35 mg/dm^3.

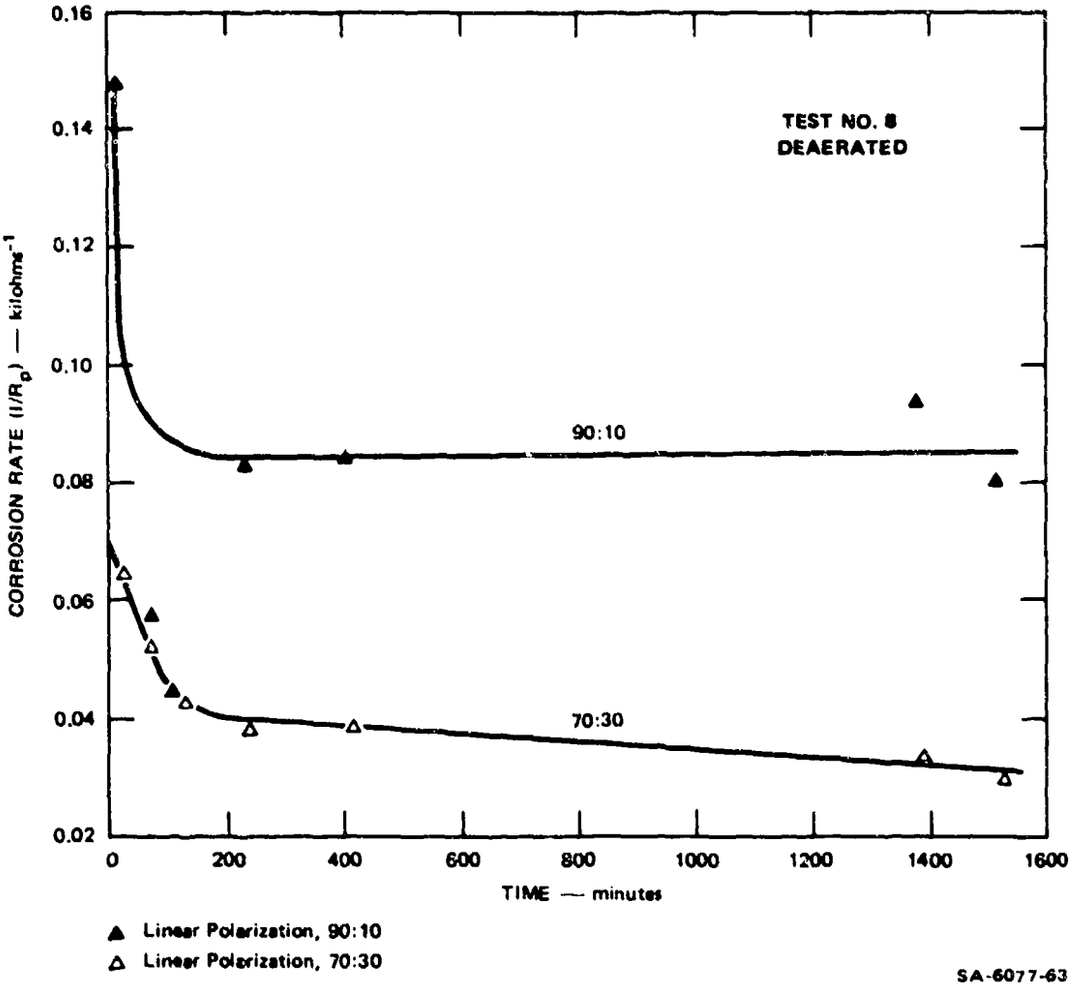

FIGURE 9 CORROSION RATE VERSUS TIME FOR 90:10 Cu:Ni AND 70:30 Cu:Ni ALLOYS IN DEAERATED SEAWATER.

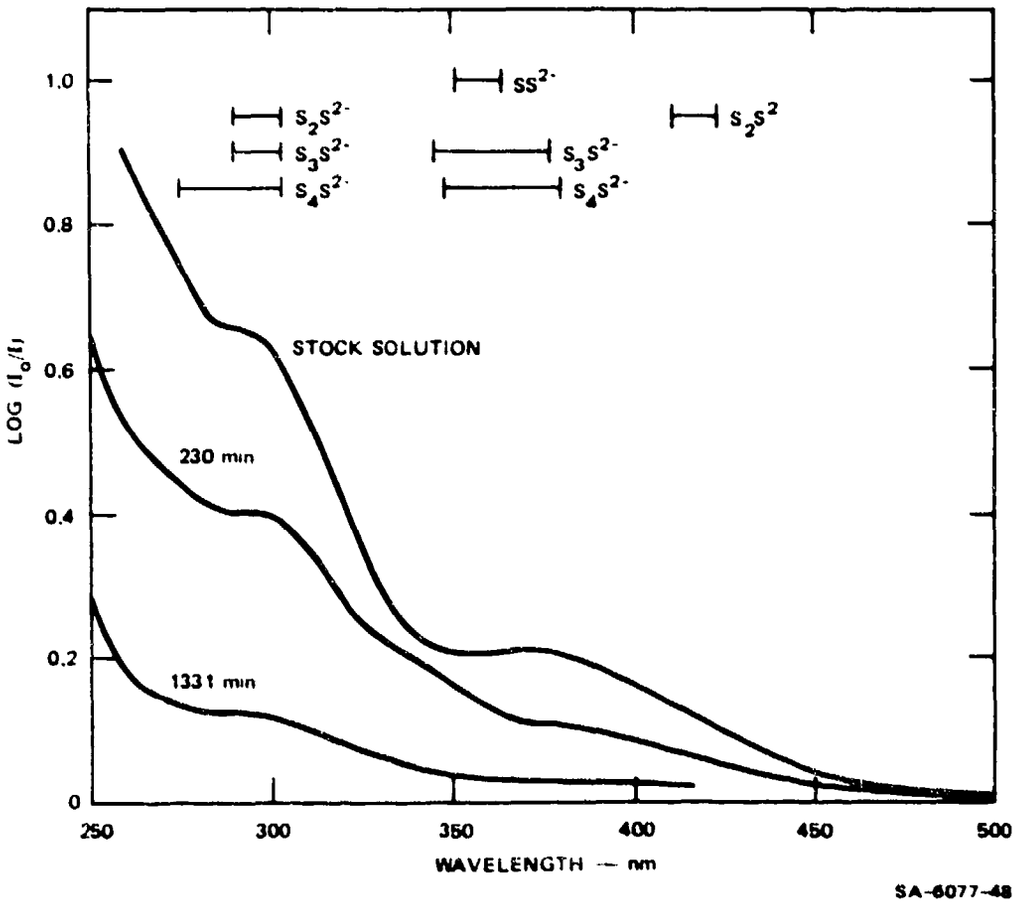

FIGURE 10 UV — VISIBLE LIGHT SPECTRA FOR STOCK SEAWATER SOLUTION AND FOR THE TEST SOLUTION 230 MINUTES AND 1331 MINUTES AFTER INITIATION OF THE EXPERIMENT

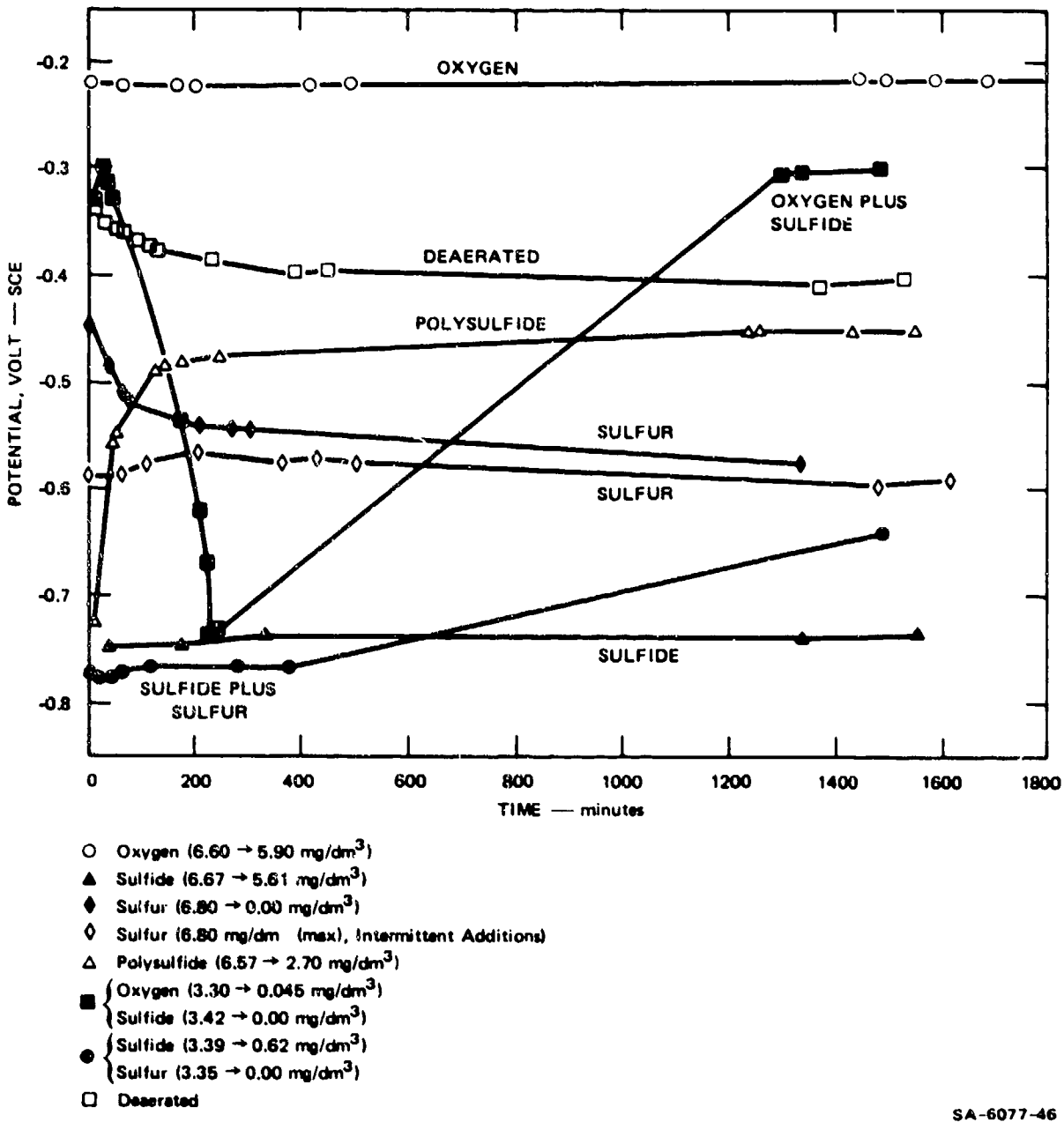

FIGURE 11 CORROSION POTENTIALS FOR 90:10 Cu:Ni IN SEAWATER CONTAINING VARIOUS SPECIES

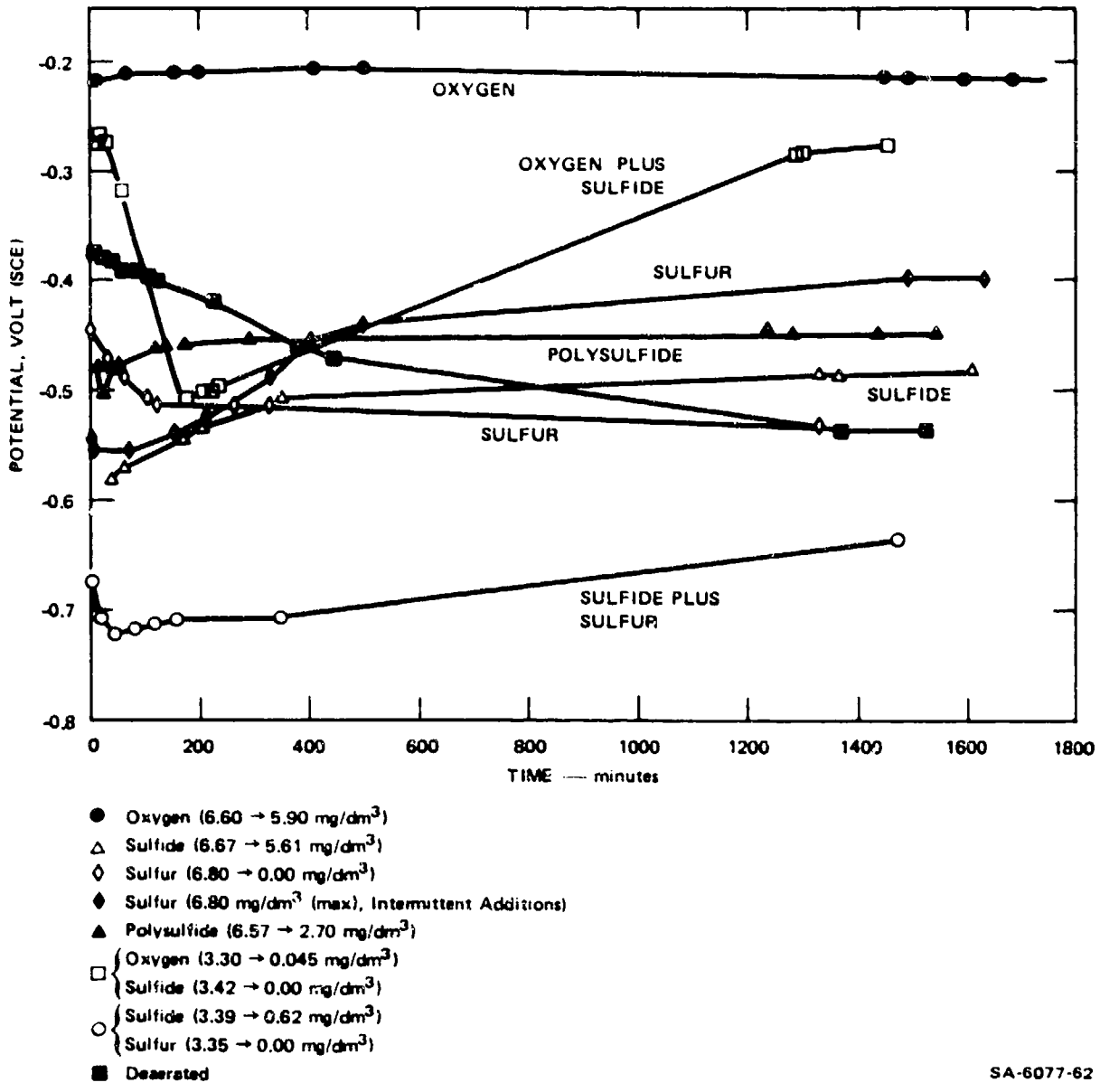

FIGURE 12 CORROSION POTENTIALS FOR 70:30 Cu:Ni IN SEAWATER CONTAINING VARIOUS SPECIES

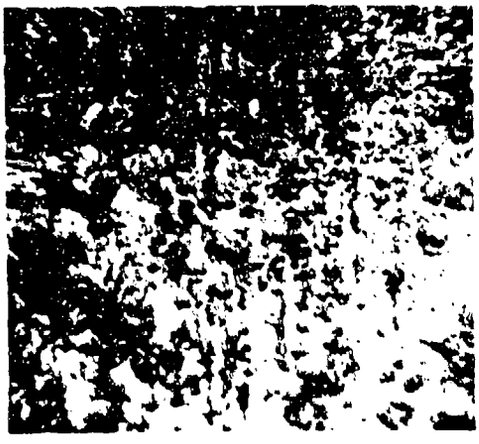

(a) WIDTH OF PHOTOGRAPH = 45 μm

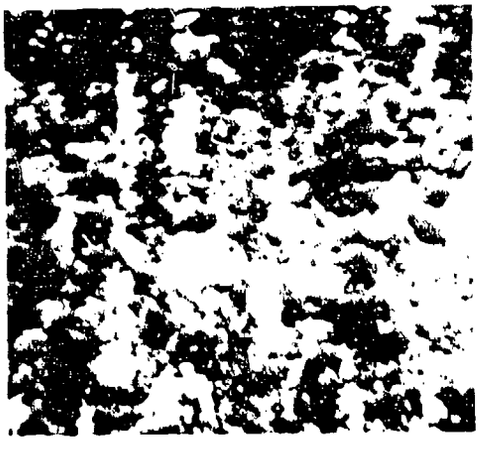

(b) WIDTH OF PHOTOGRAPH = 18 μm

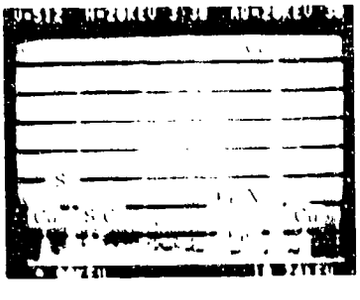

(c) BASE SCALE

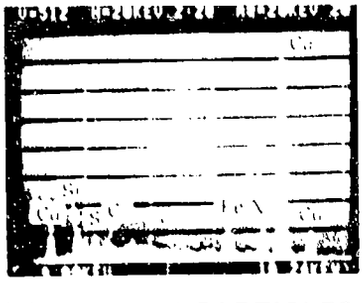

(d) SURFACE PARTICLES

SA 6077-64

FIGURE 13 SEM MICROGRAPHS AND EDX ANALYSES OF SURFACE OF 90:10 Cu:Ni AFTER EXPOSURE TO AERATED SEAWATER

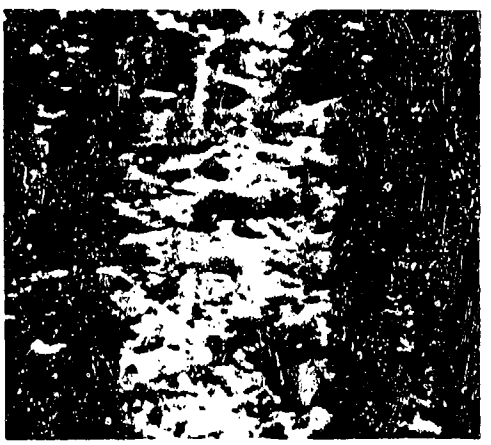

(a) WIDTH OF PHOTOGRAPH = 45 μm

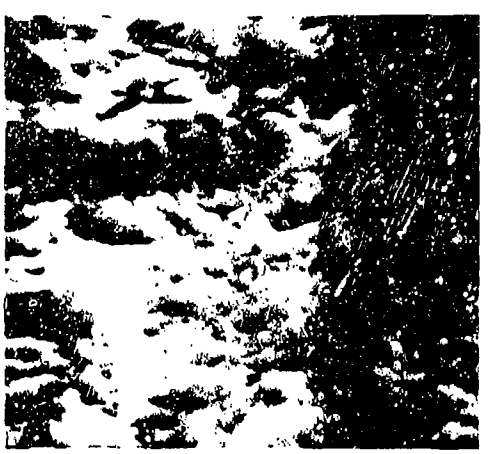

(b) WIDTH OF PHOTOGRAPH = 18 μm

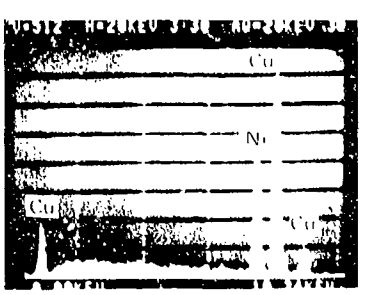

(c) SURFACE TARNISH

SA-6077-65

FIGURE 14 SEM MICROGRAPHS AND EDX ANALYSIS OF SURFACE OF 70:30 Cu-Ni AFTER EXPOSURE TO AERATED SEAWATER

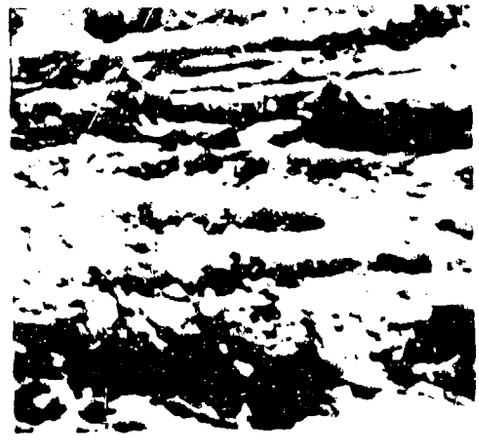

(a) WIDTH OF PHOTOGRAPH 45 μm

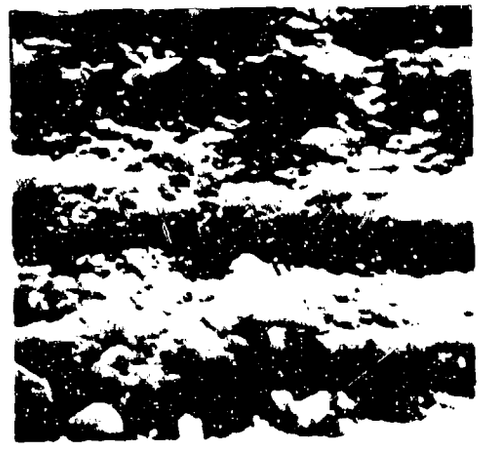

(b) WIDTH OF PHOTOGRAPH 18 μm

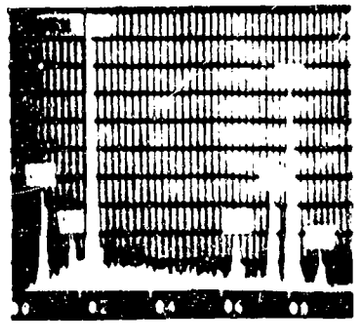

(c) BASE SCALE

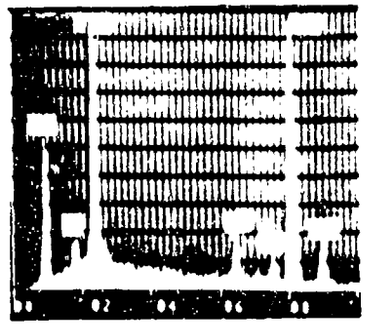

(d) SURFACE PARTICLES

FIGURE 15 SEM MICROGRAPHS AND EDX ANALYSES OF SURFACE OF 90/10 Cu-Ni AFTER EXPOSURE TO THE SUBSEA ENVIRONMENT (TEST NO. 3)

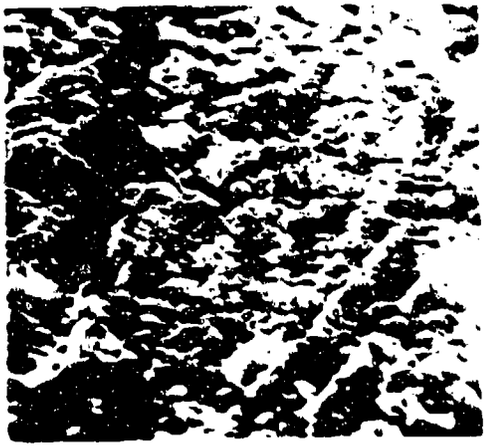

(a) WIDTH OF PHOTOGRAPH = 45 μm

(b) WIDTH OF PHOTOGRAPH 18 μm

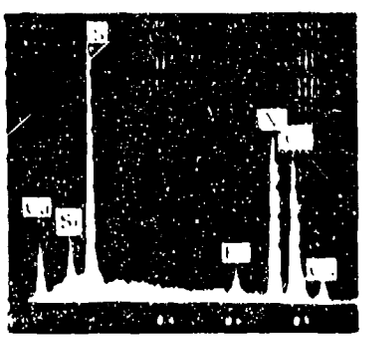

(c) BASE SCALE

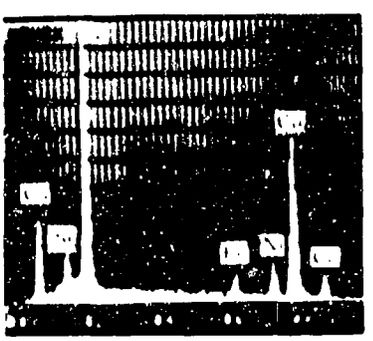

(d) SURFACE PARTICLES

FIGURE 16 SEM MICROGRAPHS AND EDX ANALYSES OF SURFACE OF 20/30 CG-N AFTER EXPOSURE TO THE SOLVENT ENVIRONMENT (TEST NO.)

(a) WIDTH OF PHOTOGRAPH = 45 μm

(b) WIDTH OF PHOTOGRAPH = 18 μm

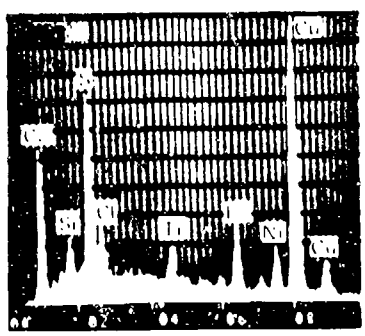

(c) BASE SCALE

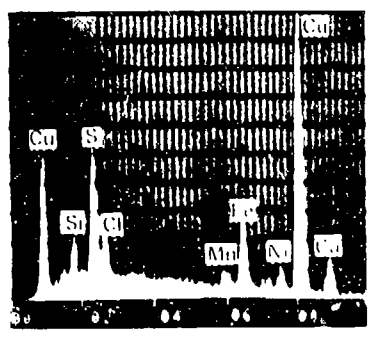

(d) SURFACE PARTICLES

SA 6077 53

FIGURE 17 SEM MICROGRAPHS AND EDX ANALYSES OF SURFACE OF 90 10 Cu Ni AFTER EXPOSURE TO THE SULFUR ENVIRONMENT (TEST NO 3)

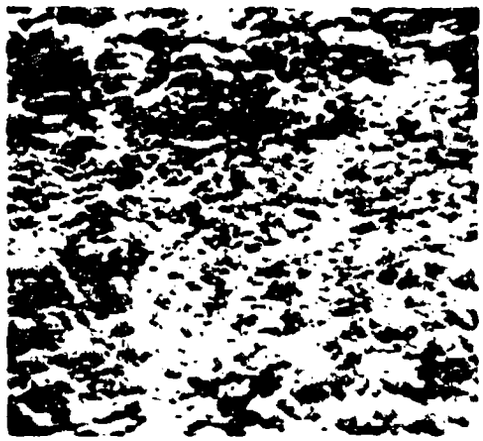

(a) WIDTH OF PHOTOGRAPH = 45 μm

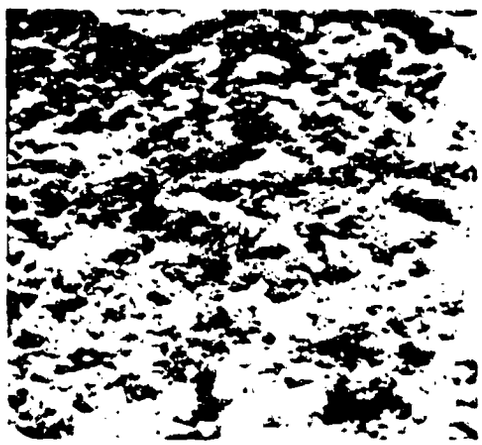

(b) WIDTH OF PHOTOGRAPH = 18 μm

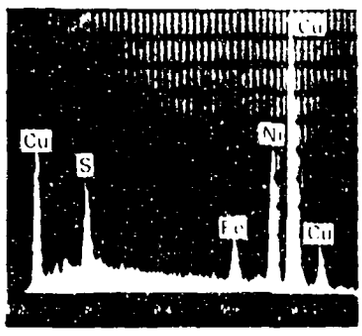

(c) BASE SCALE

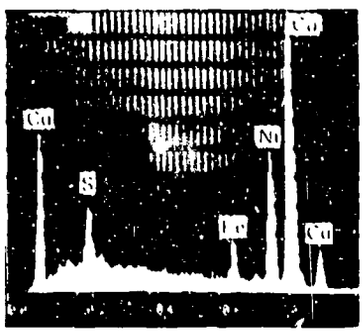

(d) SURFACE PARTICLES

SA-6077-54

FIGURE 18 SEM MICROGRAPHS AND EDX ANALYSES OF SURFACE OF 70:30 Cu:Ni AFTER EXPOSURE TO THE SULFUR ENVIRONMENT (TEST NO. 3)

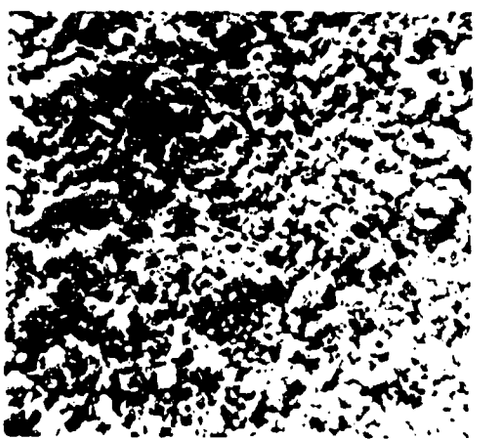

(a) WIDTH OF PHOTOGRAPH = 90 μm

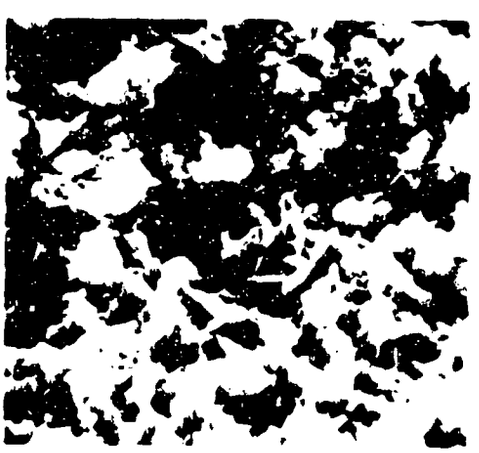

(b) WIDTH OF PHOTOGRAPH = 18 μm

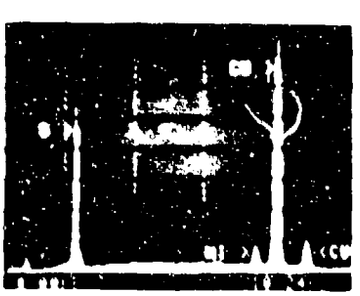

(c) BASE SCALE

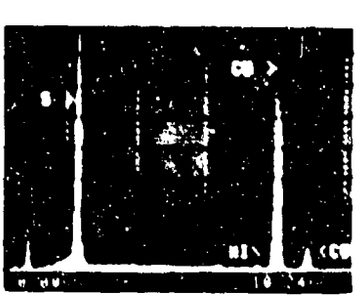

(d) SURFACE PARTICLES

SA 6077 66

FIGURE 19 SEM MICROGRAPHS AND EDX ANALYSES OF SURFACE OF 90 10 Cu Ni AFTER EXPOSURE TO THE POLYSULFIDE ENVIRONMENT (TEST NO. 5)

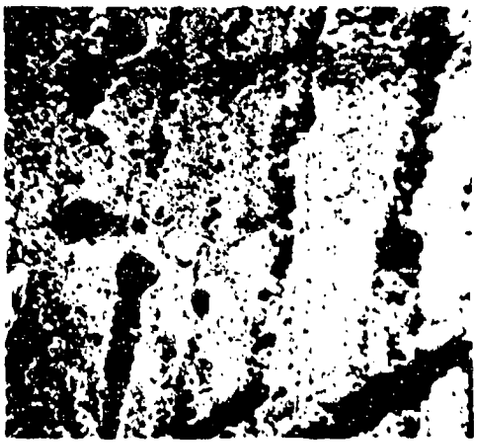

(a) WIDTH OF PHOTOGRAPH = 90 μm

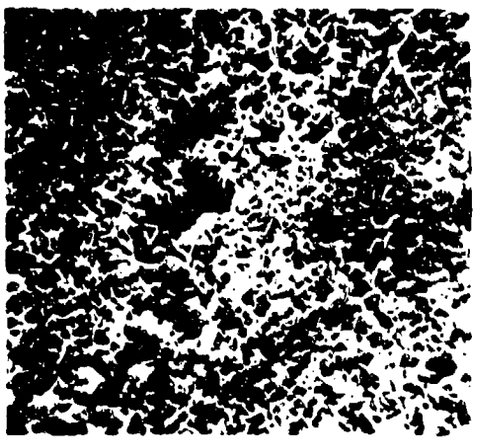

(b) WIDTH OF PHOTOGRAPH = 18 μm

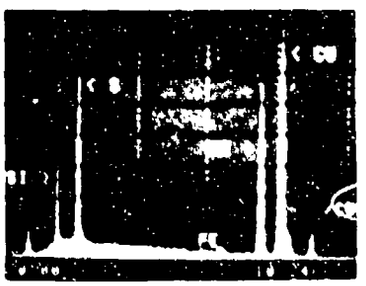

(c) BASE SCALE

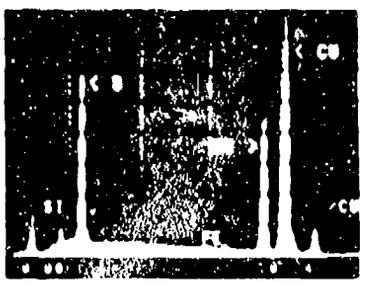

(d) SURFACE PARTICLES

SA 6077 67

FIGURE 20 SEM MICROGRAPHS AND EDX ANALYSES OF SURFACE OF 70 30 Cu Ni AFTER EXPOSURE TO THE POLYSULFIDE ENVIRONMENT (TEST NO. 5)

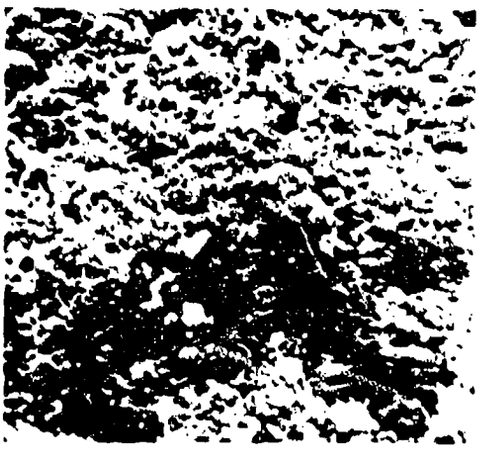

(a) WIDTH OF PHOTOGRAPH = 45 μm

(b) WIDTH OF PHOTOGRAPH = 18 μm

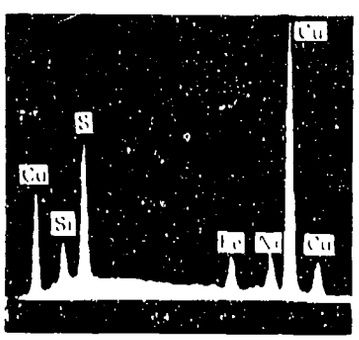

(c) BASE SCALE

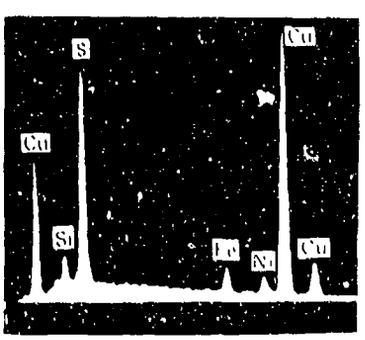

(d) SURFACE PARTICLES

SA 6077 55

FIGURE 21 SEM MICROGRAPHS AND EDX ANALYSES OF SURFACE OF 90:10 Cu:Ni AFTER EXPOSURE TO THE OXYGEN PLUS SULFIDE ENVIRONMENT (TEST NO. 6)

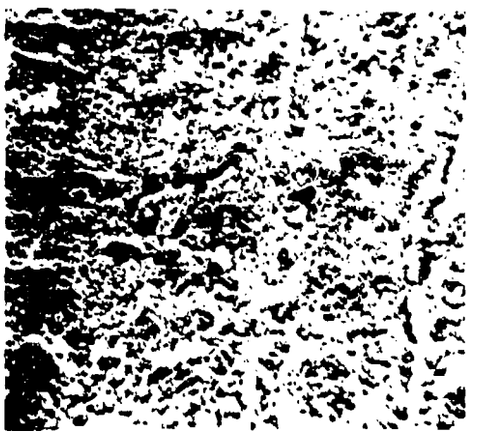

(a) WIDTH OF PHOTOGRAPH = 45 μm

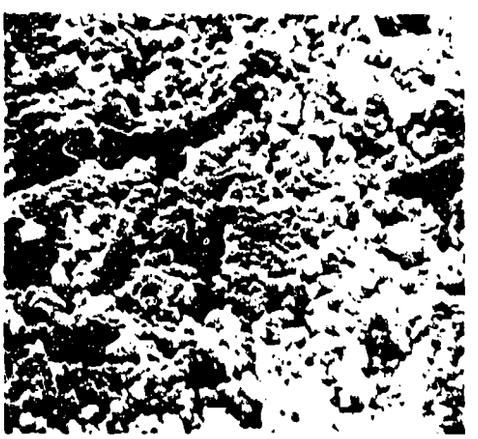

(b) WIDTH OF PHOTOGRAPH = 18 μm

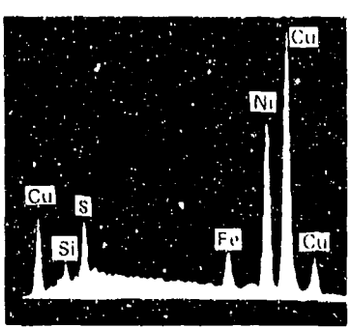

(c) BASE SCALE

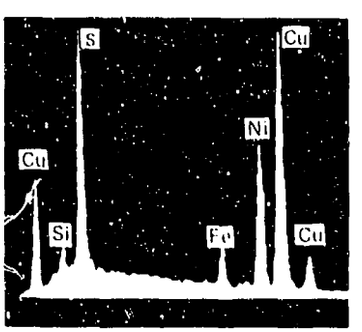

(d) SURFACE PARTICLES

SA-6077-56

FIGURE 22 SEM MICROGRAPHS AND EDX ANALYSES OF SURFACE OF 70:30 Cu:Ni AFTER EXPOSURE TO THE OXYGEN PLUS SULFIDE ENVIRONMENT (TEST NO. 6)

(a) WIDTH OF PHOTOGRAPH = 45 μm

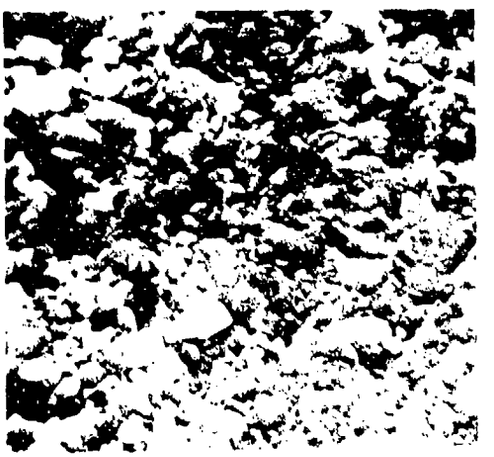

(b) WIDTH OF PHOTOGRAPH = 18 μm

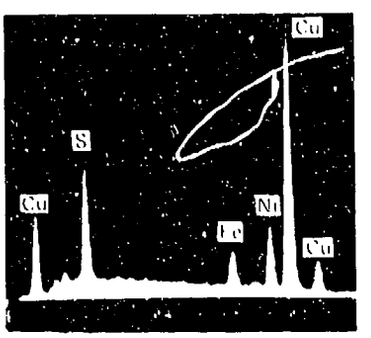

(c) BASE SCALE

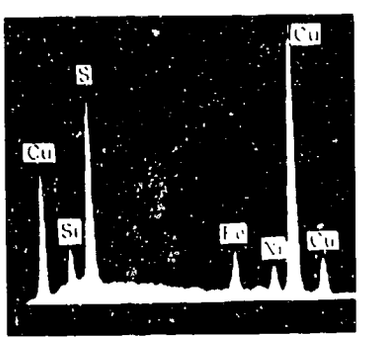

(d) SURFACE PARTICLES

SA 6077-57

FIGURE 23 SEM MICROGRAPHS AND EDX ANALYSES OF SURFACE OF 90-10 Cu-Ni AFTER EXPOSURE TO THE SULFIDE PLUS SULFUR ENVIRONMENT (TEST NO. 7)

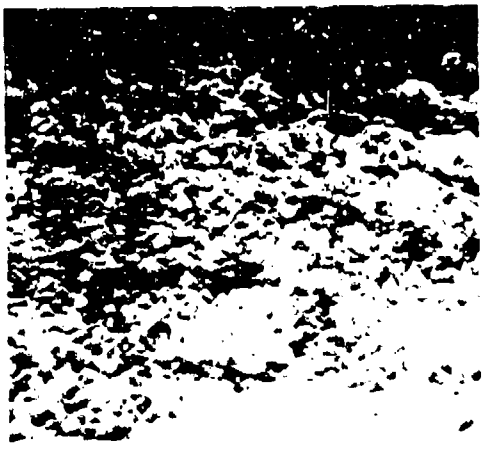

(a) WIDTH OF PHOTOGRAPH = 45 μm

(b) WIDTH OF PHOTOGRAPH = 18 μm

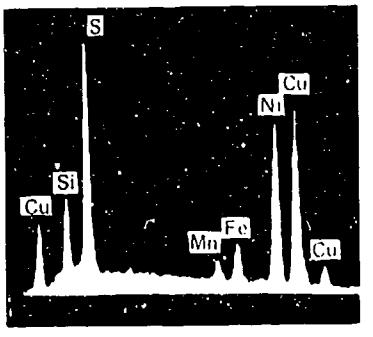

(c) BASE SCALE

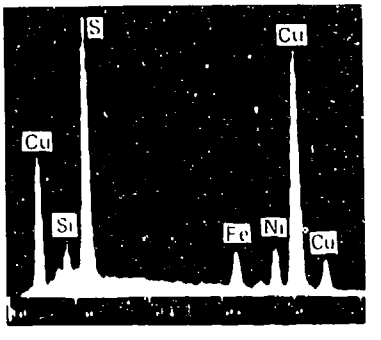

(d) SURFACE PARTICLES

SA-6077-58

FIGURE 24 SEM MICROGRAPHS AND EDX ANALYSES OF SURFACE OF 70:30 Cu:Ni AFTER EXPOSURE TO THE SULFIDE PLUS SULFUR ENVIRONMENT (TEST NO. 7)

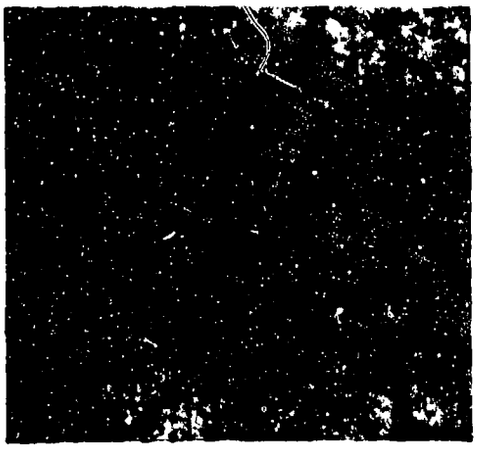

(a) WIDTH OF PHOTOGRAPH = 45 μm

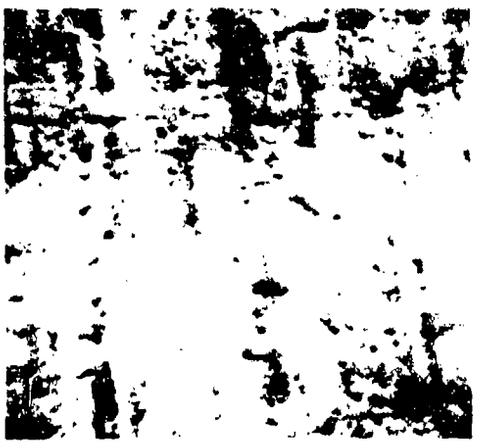

(b) WIDTH OF PHOTOGRAPH = 18 μm

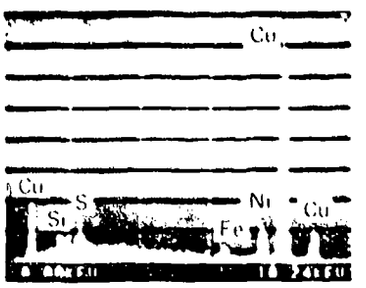

(c) SURFACE TARNISH

SA-6077-68

FIGURE 25 SEM MICROGRAPHS AND EDX ANALYSIS OF SURFACE OF 90:10 Cu:Ni AFTER EXPOSURE TO DEAERATED SEAWATER

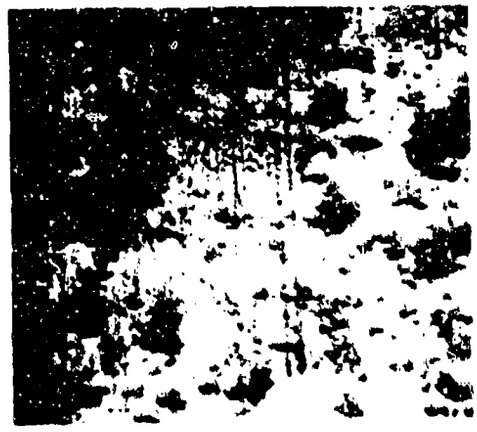

(a) WIDTH OF PHOTOGRAPH = 45 μm

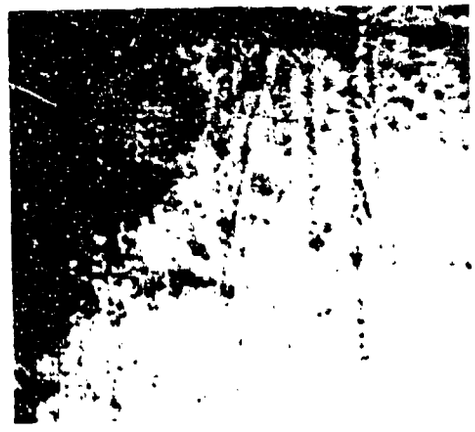

(b) WIDTH OF PHOTOGRAPH = 18 μm

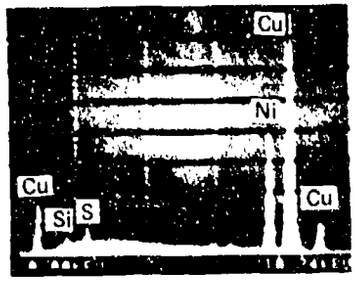

(c) SURFACE TARNISH

SA-6077-69

FIGURE 26 SEM MICROGRAPHS AND EDX ANALYSIS OF SURFACE OF 70.30 Cu:Ni AFTER EXPOSURE TO DEAERATED SEAWATER

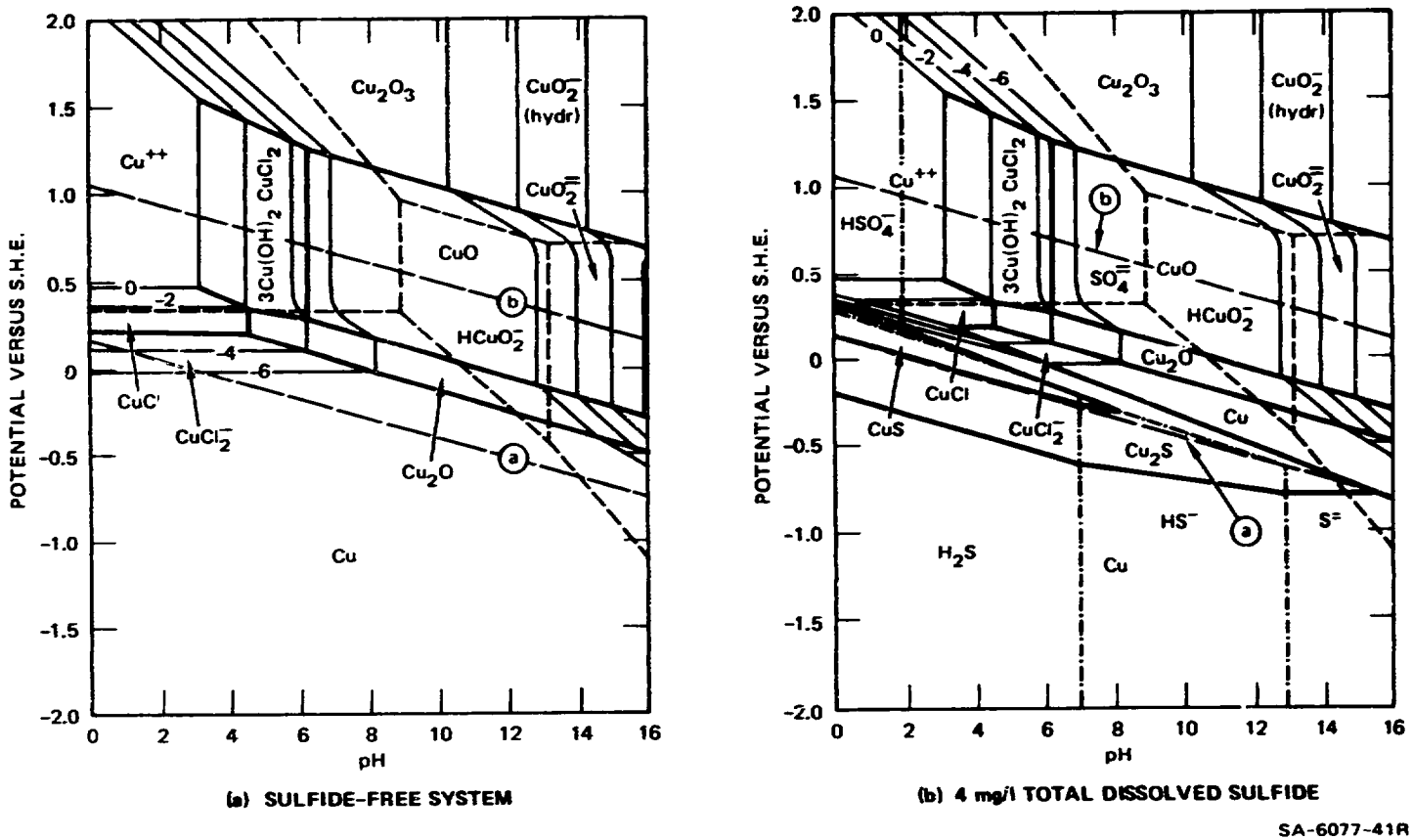

FIGURE 27 POTENTIAL — pH DIAGRAMS[26] FOR COPPER IN SEAWATER AT 25°C

The equilibrium lines for hydrogen evolution (line (a)) and oxygen evolution (line (b)) have been drawn for gas partial pressures of 10^{-5} atm.

EFFECT OF FLOW ON CORROSION OF COPPER-NICKEL ALLOYS IN AERATED SEAWATER AND IN SULFIDE-POLLUTED SEAWATER

by

Barry C. Syrett and Sharon S. Wing

Submitted for publication in Corrosion (1979)

ABSTRACT

The corrosion of 90:10 Cu:Ni and 70:30 Cu:Ni alloys in aerated seawater and deaerated seawater containing ~ 0.2 mg/dm^3 sulfide has been studied using a recirculating flow loop. Tubular specimens of each alloy were tested under well-characterized hydrodynamic and mass transfer conditions. At seawater velocities up to 5 m/s (Reynolds numbers up to 74,000), the corrosion rates in the sulfide-polluted seawater were lower than in the aerated seawater. Thus, even under comparatively adverse flow conditions, the mere presence of sulfide does not cause accelerated attack of copper-nickel alloys. Under most of the experimental conditions examined, corrosion occurred fairly uniformly across the exposed surfaces of the specimens. However, in aerated seawater, the high nickel alloy suffered localized corrosion at 3 m/s and higher velocities. The rate of localized corrosion was high and became more intese as the velocity was increased form 3 m/s to 5 m/s. This breakaway phenomenon was associated with a breakaway potential, E_B, which is defined as the potential at which a sudden increase in anodic current occurs when the potential is swept in the active to noble direction. When the corrosion potential (E_{corr}) was more active than E_B, corrosion was uniform and corrosion rates were low; but when $E_{corr} > E_B$, corrosion of the 70:30 Cu:Ni occurred. These results were interpreted in terms of the electrochemical (not mechanical) stability of the surface film.

KEY WORDS

Copper alloys, copper-nickel alloys, seawater, erosion-corrosion, velocity, localized corrosion, pitting, pollution, sulfide corrosion, corrosion mechanism.

EFFECT OF FLOW ON CORROSION OF COPPER-NICKEL ALLOYS IN AERATED SEAWATER AND IN SULFIDE-POLLUTED SEAWATER

by

Barry C. Syrett and Sharon S. Wing

Sulfide pollution of the seawater is thought to have been responsible for the accelerated corrosion and premature failure of copper-nickel alloy seawater piping in naval ships being outfitted in a polluted estuary.[1] Certainly, the adverse effects of dissolved sulfide on the corrosion of copper and its alloys in aqueous systems is well documented.[2-12] However, because the precise mechanism of the accelerated attack is unknown, a program was initiated recently at SRI International to improve our understanding of corrosion of two copper-nickel alloys, 90:10 Cu:Ni and 70:30 Cu:Ni, in polluted seawater.

In a recent report,[2] Macdonald, Syrett, and Wing demonstrated that the presence of sulfide in deaerated seawater flowing at 1.62 m/s through tubular 90:10 Cu:Ni and 70:30 Cu:Ni alloy specimens induces a loss in the passivity of the alloy surfaces. Compared with corrosion rates in sulfide-free deaerated seawater, those in sulfide-polluted (≥ 0.85 mg [S]/dm^3) deaerated seawater were about an order of magnitude higher. However, when compared with unpolluted but aerated seawater, the polluted water was not particularly aggressive to these copper-nickel alloys. Thus, it appears that the mere presence of dissolved sulfide is not a sufficient condition for accelerated attack of copper-nickel alloys.

Syrett, Macdonald, and Wing[12] later investigated the possibility that sulfide was homogeneously oxidized by dissolved oxygen to species that were considerably more corrosive towards copper-nickel alloys than sulfide itself. They performed rotating cylinder experiments in seawater containing oxygen, sulfide, sulfur, and polysulfide, either singly or in combination. Polarization resistance measurements made over a one-day

period indicated that all these species, whether they were present singly or in combination, stimulated corrosion of 90:10 Cu:Ni and 70:30 Cu:Ni alloys. Again, however, the data suggested that none of the species was sufficiently aggressive to cause the premature failure of seawater piping.

It is possible that Syrett et al.[12] did not investigate the most aggressive combination of species or, as the authors suggested, that the deleterious effects of the sulfur species may not be apparent in short-term exposures but could become important after longer exposures. However, it is also possible that the precise environmental composition and exposure time are not as important as the flow conditions. Under flow conditions that are somewhat more adverse than those used by Macdonald et al.[2] and Syrett et al.,[12] it is conceivable that the loosely adherent corrosion product formed in polluted seawater[2,12] will break down in a few areas and result in localized corrosion. A pitting type of attack (erosion-corrosion) that is exacerbated by galvanic currents flowing between the anodic exposed areas and the cathodic surface film[13] could develop.

It is generally recognized that flow conditions become more "adverse" (i.e., corrosion rates increase) as the seawater velocity increases, so one of the objectives of the present study was to determine the effect of seawater velocity on the corrosion of 90:10 Cu:Ni and 70:30 Cu:Ni alloys in sulfide-polluted seawater.

In a recent review of the literature on seawater corrosion of copper-nickel alloys, Syrett noted that corrosion rates and corrosion mechanisms were dependent not only on seawater velocity but also on flow geometry.[13] Thus, for a given nominal velocity, corrosion rates determined in a rotating disc apparatus could be significantly different from those determined in jet impingement or rotating spindle apparatus. Leumer et al.[14] and Schack et al.[15] also emphasize the importance of "flow structure" and the intensity of local turbulence. These parameters are dependent on fluid velocity in a given flow geometry but vary considerably from one flow geometry to another. As a result, some effort has been made to relate corrosion rate to more fundamental mass transfer and hydrodynamic parameters. For instance, corrosion rate has been correlated with Schmidt

(Sc), Sherwood (Sh), Stanton (St), and Reynolds (Re) numbers[16-21] in systems that lend themselves to relatively easy analysis. However, as discussed in detail by Leumer et al.,[14] even these parameters do not fully characterize the fluid and the flow. For instance, Re describes flow in various geometries and includes one property of the fluid (the viscosity), but does not include the turbulence intensity, a parameter that depends on surface roughness, bends, holes, protrusions, and the like, and that undoubtedly affects corrosion rate. Although turbulence intensity effects can be taken into account by using modified Reynolds or Schmidt numbers,[14] the important variables included in the modified numbers are not readily determined either by experiment or from theoretical considerations. Thus, from a practical standpoint, relationships between corrosion rate and hydrodynamic parameters currently have only limited applicability.

In the absence of a universally applicable relationship, it is reasonable to perform corrosion studies in an apparatus that allows a maximum of flow characterization. One approach is to pump the corrodent (seawater) through a tubular flow channel fitted with an approach section that allows hydrodynamic and mass transfer boundary layers to fully develop before the seawater reaches the tubular test specimens. If the specimens are of the same internal diameter and lie on the same axis as the approach section and if there are no protrusions in the flow field, the fluid flow is reasonably well characterized by the Reynolds number defined as $Re = LV/\nu$, where L is the internal diameter of the tube, V is the velocity of the seawater, and ν is the kinematic viscosity of the seawater.

In the present work and in related previous work,[2,22,23] we have used this type of test system. A tubular flow geometry is particularly appropriate in the present study because it facilitates correlation of the experimental results with the corrosion behavior of the geometrically similar seawater piping of interest.

In this paper, we describe how the corrosion of two copper-nickel alloys (CA 706 and CA 715) is influenced by the flow of the seawater environment. Baseline data obtained in unpolluted aerated seawater are compared with data obtained in sulfide-polluted deaerated seawater.

EXPERIMENTAL PROCEDURES

Flow Loop and Test Channels

The recirculating flow loop used in this work is shown schematically in Figure 1. It is similar in design to one described in detail elsewhere,[22] but the larger diameter feed piping (schedule 80) and the higher capacity pump used in the present system allowed us to achieve much higher seawater velocities. It was necessary to incorporate a titanium heat exchanger to remove the unwanted heat introduced by the larger pump, but periodic chemical analysis of the seawater indicated that soluble titanium species accumulated, if at all, in amounts below the detection limit (10 mg/dm^3). Similarly, one of the rotameters was fitted with a stainless steel float, but periodic chemical analysis of the seawater indicated that soluble iron species were present, if at all, in amounts below the detection limit (0.1 mg/dm^3). Except for the copper-nickel test channels, all other components of the system were either plastic or glass.

The seawater velocity in the test channel was maintained at 0.5, 2, 3, 4, or 5 m/s by adjusting the valve in the velocity-control bypass loop, shown in Figure 1. In the present system, these velocities are equivalent to Re values of about 7,400, 30,000, 44,000, 59,000, and 74,000 respectively.

Details of the test channel are shown in Figure 2. The specimens consisted of 2.54-cm lengths of annealed condenser tubing (1.35 cm ID, 1.71 cm OD) separated by Delrin spacers, and clamped tightly together with four bolts. Chemical compositions and physical properties of the two alloys are given in Table 1. A metallographic examination of the alloys revealed equiaxed grain structures and grain sizes in the range 15 to 20 μm.

Before an experiment, the five specimens of each alloy were descaled in HCl/H_2SO_4 (ASTM Recommended Practice G1-72 for copper alloys) rinsed with distilled water, and dried in warm air. During an experiment, the fifth (downstream) specimen was used solely for cyclic voltammetry, the second specimen was used solely for linear polarization measurements,

and the third specimen was used for ac impedance and potential step measurements. These electrochemical techniques are described later. The first (upstream) and fourth specimens were reserved for weight-loss and corrosion potential measurements. Other features of the flow loop and test channel are discussed in Reference 22.

Environment

Fresh, filtered, Pacific Ocean water was obtained for these experiments from the Steinhart Aquarium, San Francisco. This seawater had an initial pH of ∿8.2 and a salinity of ∿ 29 parts per thousand. The pH of the seawater was monitored at regular intervals during each experiment and, if necessary, small additions of NaOH or HCl were made to maintain the pH at ∿ 8.2. Occasionally, the pH dropped to as low as 8.04 or reached as high as 8.30 (see Table 2), but even these excursions are within the normal range for fresh seawater. The temperature of the seawater was generally 23.2 ± 1.3°C throughout an experiment, but there were occasional transient temperature changes to as high as 28.4°C and to as low as 20.0°C (see Table 2).

The seawater was sparged continuously with moist air during storage and during five of the seven experiments. In these five experiments, periodic analysis of the air-saturated seawater by Winkler titration indicated that the dissolved oxygen concentration was constant at 6.60 mg/dm^3. In the other two experiments, the seawater was first deaerated by sparging with nitrogen and then polluted with ∿ 0.2 mg/dm^3 sulfide by sparging continuously with a suitable nitrogen/hydrogen sulfide gas mixture. This sulfide level was chosen because it is representative of levels found adjacent to the affected naval ships.[1] The concentration of dissolved sulfide (primarily as HS^-) was determined intermittently using a $Pb(ClO_4)_2$ titration technique.[12] At very short exposure times, the copper-nickel alloy specimens and the approach section were sufficiently active to sharply reduce the sulfide levels below the equilibrium level of ∿ 0.2 mg/dm^3. This decrease in dissolved sulfide was counteracted by increasing the input level of H_2S in the gas mixture for a brief period until the original level was reestablished.

Electrochemical Measurements

Corrosion potentials were monitored with respect to a saturated calomel electrode (SCE) throughout each test period. Instantaneous corrosion rates were measured at regular intervals, using linear polarization, potential step, and ac impedance techniques.[2,22,23]

The linear polarization measurements were performed under potentiodynamic control by imposing a 6-mV peak-to-peak triangular voltage excitation across the interface, using a potentiostat and function generator. The apparent polarization resistance (R_{app}) was determined at several potential sweep rates in the range 0.01 to 1.0 mV/s, and the true polarization resistance (R_p) was determined by plotting $1/R_{app}$ versus potential sweep rate and extrapolating to zero sweep rate.[24]

The R_p value was also monitored by the potential step technique in which a small amplitude potential step (ΔE = 2 mV) is potentiostatically imposed across the interface and the current is recorded for 5 minutes or until an apparently constant value (ΔI) was obtained. The value of $\Delta E/\Delta I$ was determined for both an anodic and a cathodic potential step and the average taken as the R_p value.

Finally, polarization resistance was determined from ac impedance data in the complex plane. These data were obtained from an analysis of the dimensions of Lissajous figures,[2,22,25] which were generated by imposing the sinusoidal excitation voltage (11 mV peak-to-peak) and the sinusoidal current response simultaneously across the X and Y axes of an XY recorder (0.005 to 0.5 Hz) or oscilloscope (~ 0.5Hz). The low-frequency real axis intercept of the ac impedance spectrum was taken as the R_p value.

The general electrochemical behavior of the two copper-nickel alloys was determined by large amplitude cyclic voltammetry. The potential of the specimen was swept at a rate of 20 mV/s in a triangular manner between about -1.6 and +0.5 volt (SCE).

RESULTS

The dependence of corrosion rates and corrosion mechanisms on flow of the environment has been reported by most investigators in terms of the relative velocity between the metal and the environment.[13] Thus, we have also reported our data as a function of average seawater velocity. However, it should be reemphasized that, at least in our flow system, it is probably more appropriate to relate the corrosion data to Reynolds number. The relationship between velocity and Reynolds number was given in the Experimental Procedures section.

Corrosion Potentials

In Figure 3, the corrosion potentials of the two copper-nickel alloys are plotted as functions of seawater velocity and time of exposure to aerated seawater. The equivalent potential-time curves for the alloys exposed to sulfide-polluted seawater are shown in Figure 4. There appears to be no clear-cut relationship between corrosion potential and velocity, but, as expected,[2] potentials in aerated seawater were several hundred millivolts more noble than those in the sulfide-polluted seawater. In aerated seawater, the two alloys had similar corrosion potentials but, in the polluted environment, the 70:30 Cu:Ni alloy exhibited corrosion potentials that were about 200 mV more noble than those of the 90:10 Cu:Ni alloy. There is some evidence (Figure 4) that the corrosion potential of at least the high nickel alloy shifts to more noble values as the velocity of the polluted seawater increases.

Corrosion Rate Data

The reciprocal of the polarization resistance ($1/R_p$) is proportional to the instantaneous corrosion rate, as shown in Equations 1 and 2:[23]

For 90:10 Cu:Ni, $$dW/dt = 2.563 \times 10^{-4} \, B/R_p \quad (1)$$

For 70:30 Cu:Ni, $$dW/dt = 2.120 \times 10^{-4} \, B/R_p \quad (2)$$

where dW/dt is the rate of metal oxidation in g/sec, the proportionality constant B has units of volts, and R_p has units of ohms. The $1/R_p$ values for the two copper-nickel alloys in aerated seawater flowing at various velocities have been plotted as a function of time in Figures 5 through 9. The $1/R_p$ data obtained in sulfide-polluted seawater and the time dependence of the dissolved sulfide content are shown in Figure 10.

Although $1/R_p$ values are proportional to the instantaneous rate of metal oxidation averaged over the entire specimen surface, the actual corrosion rates are obtained by normalizing with respect to the area of metal being corroded (A_c). When the specimen corrodes uniformly, this area is equal to the total exposed area (10.74 cm^2 for 90:10 Cu:Ni and 10.84 cm^2 for 70:30 Cu:Ni). However, in some of the tests in aerated seawater, the high nickel alloy experienced localized corrosion, and A_c was substantially less than 10.84 cm^2. The extent of localized corrosion can be estimated for each alloy and test condition by studying Figures 11 through 17. These figures show the posttest surfaces of typical specimens after removal of corrosion products.

Although the 90:10 Cu:Ni alloy shows a slight tendency towards localized corrosion (for example, see Figure 13), corrosion is generally fairly uniform and $A_c \approx 10.74$ cm^2 in all experiments. The 70:30 Cu:Ni alloy alloy corrodes uniformly in the sulfide-polluted seawater (Figures 16 and 17) and fairly uniformly at the lower velocities in aerated seawater (Figures 11 and 12). However, in aerated seawater flowing at 3 m/s or faster (Figures 13 to 15), the high nickel alloy clearly suffered localized corrosion. The values of A_c listed in Tables 3 and 4 are based on the posttest examination of specimens (see Figures 11 through 17). Although A_c did not vary appreciably from one specimen to the next, it is conceivable that, in some instances, A_c varied during the test.

Since penetration and failure of copper-nickel piping is dependent more on the localized corrosion rate than on the average corrosion rate, the $1/R_p$ data given in Figures 5 to 10 must be interpreted with care.

Furthermore, the corrosion rates calculated using Equations 1 and 2 are dependent on the value of B, which is a function of the anodic and

cathodic Tafel coefficients. Because the Tafel coefficients are not easily determined with accuracy and may depend on flow conditions, the value of B was determined indirectly for each test by determining the total weight loss (ΔW) and the area (A_t) under the curve for $1/R_p$ versus time, and by substituting these values in Equations 3 and 4.

For 90:10 Cu:Ni, $$B = \Delta W/2.563 \times 10^{-4} A_t \quad (3)$$

For 70:30 Cu:Ni, $$B = \Delta W/2.120 \times 10^{-4} A_t \quad (4)$$

Values of ΔW, A_t, and B are listed for each experiment in Tables 3 and 4. The values of B range from 0.026 to 0.107 volt depending on the experimental conditions, but all these values are within the range reported by other workers for copper alloys in seawater.[26]

Because the values of B and A_c may vary from one alloy to the other and from one velocity to the next, the $1/R_p$ values given in Figures 5 to 10 are not necessarily directly comparable. Nevertheless, a few general observations can be made. The corrosion rates were not predictable during the first few days, increasing initially in some tests and decreasing in others. After 9 or 10 days, however, corrosion rates were invariably either relatively constant or decreasing slowly. The $1/R_p$ values measured after 230 hours (nearly 10 days) in aerated seawater are given in Table 3 for each copper-nickel alloy as a function of seawater velocity. These values were used to calculate the overall rate of corrosion, dW/dt, after 230 hours and the area-normalized corrosion rate, $(dW/dt)(1/A_c)$. Similarly, values of $1/R_p$, dW/dt, and $(dW/dt)(1/A_c)$ are listed in Table 4 for the sulfide-polluted environments.

It can be seen that the 230-hour corrosion rate of 90:10 Cu:Ni in aerated seawater increases with seawater velocity whether values of dW/dt or $(dW/dt)\ (1/A_c)$ are compared. In contrast, the overall corrosion rate for the 70:30 Cu:Ni alloy appears to be fairly insensitive to seawater velocity except at 4 m/s where dW/dt was much higher. However, if consideration is given to the area actually corroding, the corrosion rate $(dW/dt)(1/A_c)$ of the high nickel alloy increases slightly as the velocity increases from 0.5 m/s to 2 m/s, then increases dramatically at higher velocities. The area-normalized data for both alloys are shown in Figure 18 as a function of seawater velocity (or Reynolds number).

The corrosion rates given in Figure 18 are probably significantly higher than those that would have been experienced after a few months or years of service. Nevertheless, it is clear that after 230 hours in aerated seawater, the instantaneous corrosion rates for 90:10 Cu:Ni and 70:30 Cu:Ni are similar at seawater velocities up to 3 m/s, but that at 4 m/s and 5 m/s the localized corrosion rates for 70:30 Cu:Ni are very much higher than those for the low nickel alloy. The rapid increase in corrosion rate as the seawater velocity is increased above 3 m/s was also noted by Godfrey, Angell, and Taylor[27] in their study of 70:30 Cu:Ni tubes in flowing seawater.

The data in Figure 18 and Table 4 indicate that, in the sulfide-polluted environment, corrosion is uniform in both alloys and corrosion rates are significantly below those obtained in aerated seawater. Although only two velocities (3 m/s and 5 m/s) were considered, it is clear that corrosion rates are relatively independent of velocity in the 70:30 Cu:Ni alloy but that they increase significantly with velocity in the 90:10 Cu:Ni alloy. This insensitivity of the 70:30 Cu:Ni alloy to velocity in the range 3-5 m/s sharply contrasts the great sensitivity of the alloy in the aerated seawater at the same velocities.

Cyclic Voltammetry

The cyclic voltammograms obtained in this work were similar in character to those reported previously for 90:10 Cu:Ni and 70:30 Cu:Ni,[2,22] so they will not be discussed here in detail. However, it is of interest to compare the values of the corrosion potential (E_{corr}) and the potential (E_B) at which the current suddenly increases upon sweeping the potential in the noble direction. In a previous study[22] in which the effects of the dissolved oxygen content of the seawater were investigated, we demonstrated that when E_B was more active (negative) than E_{corr}, the corrosion rate of 70:30 Cu:Ni increased dramatically. This loss of corrosion resistance was thought to be related to a change in the nature of the surface corrosion film. Because the characteristics of this phenomenon were analogous to those of the breakaway velocity phenomenon reported for 70:30 Cu:Ni alloy,[13] E_B was termed the breakaway potential.

Values of E_B and E_{corr} are given in Table 5 for aerated seawater and in Table 6 for sulfide-polluted seawater as functions of velocity and exposure time. For consistency, all E_B values were taken at an anodic current density of 25 mA ($\sim$ 2.3 mA/cm^2). In the sulfide-polluted seawater, the corrosion potentials of both alloys were always several hundred millivolts more active than the breakaway potentials. In the aerated seawater, on the other hand, E_{corr} was often more noble than E_B. At 0.5 m/s, E_B for 90:10 Cu:Ni was more noble than E_{corr} at short exposure times and was equal to E_{corr} towards the end of the 10-day test. However, at velocities of 2 m/s and above, E_B was more active than E_{corr}, at least at long exposure times. At velocities up to 3 m/s, E_B for 70:30 Cu:Ni in aerated seawater was more noble than E_{corr} at all exposure times, but at velocities of 4 m/s and 5 m/s, E_B was always more active than E_{corr}.

DISCUSSION

The data presented above clearly demonstrate that, for seawater velocities up to 5 m/s (Re values up to 74,000), the mere presence of sulfide is not sufficient to cause accelerated attack of copper-nickel seawater piping. On the contrary, corrosion rates in sulfide-polluted deaerated seawater were substantially less than those in aerated seawater, particularly for 70:30 Cu:Ni in seawater flowing at 5 m/s. This finding is consistent with results obtained in preliminary rotating cylinder tests using the same materials.[12] The flow geometry was quite different in the rotating cylinder system, but at a peripheral velocity of 0.716 m/s (Re ≈ 10,200 using the tube OD as the characteristic length), $1/R_p$ values for both alloys were generally higher in aerated seawater (6.60 mg [O]/dm^3) than in sulfide-polluted deaerated seawater (6.67 mg [S]/dm^3).

The overall anodic reaction changes from Cu_2O and $Cu_2(OH)_3Cl$ formation in aerated seawater (see below) to Cu_2S and substoichiometric $Cu_{1.8}S$ formation in sulfide-polluted seawater.[2,12] Furthermore, the primary cathodic reaction in aerated seawater is oxygen reduction, whereas H^+ ion reduction occurs primarily in the polluted seawater. The kinetics of either the anodic or the cathodic reaction (or of both reactions) may be strongly influenced by the change in environment, but because only limited data are available, it is not possible to determine which half reaction is affected most; therefore, we cannot determine why the corrosion rate is lower in the sulfide-polluted seawater. However, previous scanning electron microscopic studies[2,12] suggest that the surface film formed in sulfide-polluted seawater is much more porous than the film formed in aerated seawater. Thus, it seems unlikely that a more protective surface film is formed in the polluted environment.

Whatever the mechanism, we have demonstrated that even relatively adverse flow conditions cannot induce accelerated attack of 90:10 Cu:Ni and 70:30 Cu:Ni piping exposed to sulfide-polluted deaerated seawater.

The possibility that other sulfur species, such as polysulfide, can cause accelerated attack under adverse flow conditions will be the subject of further research.

It is interesting that the observed response of the 70:30 Cu:Ni alloy to seawater velocity at a constant oxygen content (6.6 mg/dm^3) parallels the response to dissolved oxygen content at a constant velocity (1.62 m/s). The corrosion rate of 70:30 Cu:Ni after 200 hours exposure is relatively insensitive to oxygen concentration in the range 0.045-6.60 mg/dm^3, but if the oxygen concentration is increased to 26.3 mg/dm^3, the corrosion rate increases by more than an order of magnitude.[22] Similarly, the corrosion rate after 230 hours in air-saturated water is fairly insensitive to velocity in the range 0.5-2 m/s, but above 3 m/s, the corrosion rate of 70:30 Cu:Ni increases dramatically with increasing velocity (Figure 18). Furthermore, in each set of experiments, the sudden corrosion rate increase was accompanied by a transition from a condition in which $E_{corr} < E_B$ to a condition in which $E_{corr} > E_B$.

These observations can be explained by assuming that the relatively high corrosion currents at potentials above E_B are associated more with the oxidation of copper to soluble species, such as Cu^+, $CuCl_2^-$, and $CuCl_3^{2-}$, and porous nonprotective solids, such as atacamite [$Cu_2(OH)_3Cl$] and malachite [$CuCO_3 \cdot Cu(OH)_2$], than with the formation of a protective Cu_2O surface film. Supporting evidence for this hypotehsis is now discussed.

Popplewell[28] has pointed out that the incorporation of Ni^{2+} into the Cu_2O film decreases the electronic and ionic conductivities. Thus, the high nickel alloy possesses a surface film that inhibits mass (Cu^+) transfer and so inhibits corrosion if the oxide is not breached. Indeed, with one exception, the corrosion rate of 70:30 Cu:Ni in aerated seawater was shown in this and previous work[22] to be lower than that of 90:10 Cu:Ni as long as E_{corr} for the high nickel alloy does not exceed E_B. The exception occurred in this work for a seawater velocity of 0.5 m/s (see Table 3 and Figures 5 and 18). However, we believe the polarization resistance values for 70:30 Cu:Ni were underestimated in this test and that the true values were greater than those for the 90:10 Cu:Ni alloy.

Certainly, the weight loss measurements (Table 3) support this hypothesis. Thus, most of the evidence indicates that at seawater velocities of 2 m/s or less, the corrosion rate of 70:30 Cu:Ni is less than that of 90:10 Cu:Ni. It is important to note that the low corrosion rates in 70:30 Cu:Ni are accompanied by corrosion potentials that are more active than the E_B values (Table 5).

Except at very low oxygen contents[22] and very low seawater velocities, E_{corr} for 90:10 Cu:Ni exceeds E_B and corrosion rates are relatively high. It has been shown that 90:10 Cu:Ni corrodes entirely as soluble species after an initial period in which the oxide grows,[28] but the rate at which this corrosion occurs will undoubtedly depend on the perfection of the oxide film. We observed cupric compounds, such as atacamite,[29,30] on both copper-nickel alloys as small patches on top of the oxide film. It is possible that "islands" of porous, nonprotective atacamite are incorporated within the oxide layer on 90:10 Cu:Ni and enhance the metal transfer through the already defective film. We suggest that the atacamite islands on the 70:30 Cu:Ni alloy, however, do not penetrate the oxide film except under certain adverse flow conditions (see below).

Increasing the oxygen content of the seawater may have at least two effects. First, it may improve the perfection of the Cu_2O film and lead to somewhat reduced corrosion rates, as observed for the 90:10 Cu:Ni alloy.[22] Second, it may result in a more noble corrosion potential and more rapid oxidation of Cu_2O to atacamite.[29]

$$Cu_2O + 1/2\ O_2 + Cl^- + 2H_2O \rightarrow Cu_2(OH)_3Cl + OH^-$$

In the 90:10 Cu:Ni alloy, the benefits of improved film perfection outweigh the detrimental effects of increased atacamite formation. We propose that the 70:30 Cu:Ni also benefits from an increased oxygen content initially, for reasons just mentioned, but when the oxygen content reaches 26.3 mg/dm^3, islands of atacamite grow at a sufficient rate that they eventually penetrate the passive oxide layer and lead to locally increased transfer of cuprous species into solution. The corollary is that increasing the oxygen content causes E_{corr} to shift in the noble direction until it exceed E_B.

An increase in the seawater velocity will increase mass transfer to and from the electrode surface, although as Figures 3 and 4 indicate, a velocity increase does not have a large effect on the corrosion potential. The more quickly cathodically produced OH^- ions are transported from the surface and the more quickly Cl^- ions are transported to the surface, the more likely the Cu_2O will dissolve:

$$Cu_2O + H_2O + 4Cl^- \rightarrow 2CuCl^- + 2OH^-$$

At any given velocity, there will be a steady-state oxide thickness for which the rate of oxide formation is equal to the rate of dissolution. This steady-state thickness will decrease with increasing velocity and, in the limit, the alloy surface will be film-free. Thus, as the velocity increases, mass transfer across the film increases and, therefore, the corrosion rate increases, as observed for the 90:10 Cu:Ni alloy.

Similarly, the corrosion rate of 70:30 Cu:Ni is expected to increase with increasing velocity. However, the response of the high Ni alloy to velocity will differ from that of the 90:10 Cu:Ni because of the different natures of the surface films. The low nickel alloy initially has a more defective surface film, probably with atacamite islands completely penetrating the oxide in some places, so a decrease in film thickness causes a relatively predictable increase in corrosion rate. In the high nickel alloy, on the other hand, the film is initially more protective and atacamite does not penetrate the oxide. However, as the oxide film decreases in thickness, the likelihood of penetration by atacamite islands increases. At some critical velocity (or film thickness), the oxide will finally be breached, and accelerated localized attack will ensue. The bulk of the oxide will remain intact and, while offering protection to much of the surface, will actually promote corrosion in the penetrated areas by providing a large cathodic area.

It should be emphasized that, although we have rationalized the various results of our research, much work still needs to be performed. For instance, a detailed study of the makeup of the surface films as a function of seawater velocity and oxygen content would help substantiate our predictions regarding the role of atacamite islands. However, the mechanisms outlined in this section are consistent with the available data.

It should also be noted that we are advocating a breakaway corrosion mechanism (in 70:30 Cu:Ni, in particular) that is electrochemical in nature, in sharp contrast to the belief of many authors that accelerated localized corrosion is caused by mechanically stripping the oxide from the surface. As Syrett[13] has indicated, average shear stresses at the pipe wall are exceedingly small. Although higher shear stresses are possible in localized regions,[14] we believe the breakaway phenomenon is associated with electrochemical breakdown of the protective surface film.

SUMMARY AND CONCLUSIONS

The corrosion rates of 90:10 Cu:Ni and 70:30 Cu:Ni have been measured as a function of velocity in aerated seawater and deaerated seawater containing ~ 0.2 mg/dm sulfide. At seawater velocities up to 5 m/s, the corrosion rates after a 230-hour exposure were lower in the sulfide-polluted seawater than in the aerated seawater. Thus, we have demonstrated that, even under comparatively adverse flow conditions, the mere presence of sulfide does not cause accelerated attack of copper-nickel alloys.

The corrosion rate of 90:10 Cu:Ni in both environments and the corrosion rate of the high nickel alloy in the sulfide-polluted environment increased gradually with increasing velocity, and corrosion occurred fairly uniformly across the entire exposed surface. However, the corrosion rate of 70:30 Cu:Ni in aerated seawater increased slightly as the seawater velocity was increased from 0.5 m/s to 2 m/s but, at 3 m/s and above, the alloy suffered localized corrosion that rapidly increased in intensity as the velocity was increased. The onset of this accelerated attack was accompanied by a transition from a condition in which $E_B > E_{corr}$ to one in which $E_{corr} < E_B$. The results were interpreted in terms of the electrochemical (not mechanical) stability of the surface oxide film.

ACKNOWLEDGMENTS

Financial support of this work by the Office of Naval Research (Contract No. N00014-77-C-0046) is gratefully acknowledged. The authors also thank D. D. Macdonald for the many helpful discussions during this work.

REFERENCES

1. R. B. Niederberger, J. P. Gudas, and G. J. Danek, "Accelerated Corrosion of Copper-Nickel Alloys in Polluted Waters," Paper No. 76 presented at NACE CORROSION/76, Houston, Texas (1976).

2. D. D. Macdonald, B. C. Syrett, and S. S. Wing, "The Corrosion of Copper-Nickel Alloys 706 and 715 in Flowing Seawater, II Effect of Sulfide." Accepted for publication Corrosion (1978).

3. P. A. Akolzin and A. F. Bogachev, Protection of Metals, Vol. 5, p. 262 (1969).

4. H. Yamada and T. Nakamura, J. Japan Foundrymen's Soc., Vol. 36, p. 470 (1964).

5. J. C. Rowlands, J. Appl. Chem., Vol. 15, p. 57 (1965).

6. E. D. Mor and A. M. Beccaria, Corrosion, Vol. 30, p. 354 (1974).

7. J. F. Bates and J. M. Popplewell, Corrosion, Vol. 31, p. 269 (1975).

8. E. D. Mor and A. M. Beccaria, Br. Corr. J., Vol. 10, p. 33 (1975).

9. J. P. Gudas and H. P. Hack, Paper No. 93 presented at NACE CORROSION/77, San Francisco, California (1977).

10. B. C. Syrett, Corrosion, Vol. 33, p. 257 (1977).

11. L. Giuliani and G. Bombara, Br. Corr. J., Vol. 8, p. 20 (1973).

12. B. C. Syrett, D. D. Macdonald, and S. S. Wing, "Corrosion of Copper-Nickel Alloys in Seawater Polluted With Sulfide and Sulfide Oxidation Products." Accepted for publication Corrosion (1979).

13. B. C. Syrett, Corrosion, Vol. 32, p. 242 (1976).

14. G. Leumer, R. P. Schack, K. J. Graham, and J. Perkins, "The Effect of Flow Structure on Corrosion: Circling-Foil Studies on 90/10 Copper-Nickel, And Hydrodynamic Modeling of the Erosion-Corrosion Process," Naval Postgraduate School Technical Report NPS-69PS-78-004, Technical Report No. 8 to the Office of Naval Research, Contract No. N000 14-78-WR-80105, NR-036-120, (May 1978).

15. R. P. Schack, G. Leumer, K. J. Graham, and J. Perkins, "The Effect of Flow Structure on Corrosion: Flow Channel Studies on 90/10 Copper Nickel," Naval Postgraduate School Technical Report NPS-69PS-78-003, Technical Report No. 7 to the Office of Naval Research, Contract No. N00014-78-WR-80105, NR-036-120, (April 1978).

16. A. Tvarusk, J. Electrochem. Soc., Vol. 123, p. 490 (1976).

17. I Cornet, E. A. Barrington, and G. U. Behrsing, J. Electrochem. Soc., Vol. 108, p. 947 (1961).

18. P. V. Shaw and T. J. Hanratty, A.I.Ch.E. J., Vol. 10, p. 475 (1964).

19. B. T. Ellison and I. Cornet, J. Electrochem. Soc., Vol. 118, p. 68 (1971).

20. W. Van Krevelen, P. J. Hoftijzer, and J. C. Van Hooren, Rec. Trav. Chim. Pays-Bas, Vol. 66, p. 513 (1947).

21. T. K. Ross and D. H. Jones, J. Appl. Chem., Vol. 12, p. 314 (1962).

22. D. D. Macdonald, B. C. Syrett, and S. S. Wing, Corrosion, Vol. 34, p. 289 (1978).

23. B. C. Syrett and D. D. Macdonald, "The Validity of Electrochemical Methods for Measuring Corrosion Rates of Copper-Nickel Alloys in Seawater." Accepted for publication in Corrosion (1978).

24. D. D. Macdonald, J. Electrochem. Soc., Vol. 125, p. 1443 (1978).

25. D. D. Macdonald, Transient Techniques in Electrochemistry, Plenum Press, New York (1977).

26. L. M. Callow, J. A. Richardson, and J. L. Dawson, Br. Corros. J., Vol. 11, p. 123 (1976).

27. D. J. Godfrey, B. Angell, and A. F. Taylor, "Present and Future Full-Scale Land-Based Corrosion/Erosion Studies of Ships' Seawater Piping Systems." Paper presented at the Inst. of Metals International Conference, Amsterdam (Sept. 1970). Proceedings ("Copper and Its Alloys") published by Institute of Metals, London (1970), p. 339.

28. J. M. Popplewell, "Marine Corrosion of Copper Alloys, An Overview," Paper No. 21 presented at NACE CORROSION/78, Houston, Texas (March 1978).

29. G. Bianchi, G. Fiori, P. Longhi, and F. Mazza, Corrosion, Vol. 34, p. 396 (1978).

30. J. M. Popplewell, R. J. Hart, and J. A. Ford, Corrosion Sci., Vol. 13, p. 295 (1973).

Table 1

CHEMICAL COMPOSITIONS AND MECHANICAL PROPERTIES OF
CA 706 (90:10 Cu:Ni) AND CA 715 (70:30 Cu:Ni)

Alloy	Composition* (wt%)								Strength (MPa)	
	Cu	Ni	Mn	Fe	P	Pb	S	Zn	Yield	Tensile
706	87.9	10.2	0.24	1.34	≤0.02	0.010	≤0.02	0.28	148	319
715	68.7	29.7	0.61	0.53	0.001	0.007	0.016	0.45	152	420

*Composition of CA 706 and CA 715 supplied respectively, by the Anaconda Co., Brass Division, Paramount, California, and Phelps Dodge Brass Co., Tube Division, Los Angeles, California.

Table 2

RANGES AND MEAN VALUES OF TEMPERATURE
AND pH FOR THE SEVEN FLOW-LOOP EXPERIMENTS

Environment	Velocity (m/s)	Temperature (°C)			pH		
		mean	min	max	mean	min	max
Air	0.5	23.6	20.8	25.0	8.18	8.04	8.24
	2	24.4	22.5	28.4	8.20	8.15	8.22
	3	24.0	20.1	27.0	8.19	8.15	8.22
	4	22.0	21.5	23.0	8.20	8.20	8.22
	5	22.6	21.5	25.0	8.20	8.19	8.21
Sulfide	3	21.9	20.0	23.4	8.29	8.27	8.30
	5	22.6	21.5	24.0	8.27	8.25	8.30

Table 3

CORROSION RATE DATA FOR 90:10 Cu:Ni AND 70:30 Cu:Ni ALLOYS IN AIR-SATURATED SEAWATER AS A FUNCTION OF VELOCITY

Alloy	Velocity (m/s)	A_t (C/V)	ΔW (mg)	B (V)	$1/R_p$ [230 h] (kilohms^{-1})	A_c (cm^2)	dW/dt [230 h] (ng/s)	(dW/dt)(1/A_c) ($\mu g/m^2 \cdot s$)
90:10	0.5	1,162	31.9 ± 1.1	0.107 ± 0.004	0.2	10.74	5.48 ± 0.21	5.10 ± 0.20
	2	3,774	54.8 ± 1.1	0.057 ± 0.001	2.2	10.74	32.1 ± 0.6	29.9 ± 0.6
	3	9,490	105.4 ± 2.9	0.043 ± 0.002	4.0	10.74	44.1 ± 2.1	41.1 ± 2.0
	4	3,887	67.7 ± 2.9	0.068 ± 0.003	3.6	10.74	62.7 ± 2.8	58.4 ± 2.6
	5	11,048	112.7 ± 22.1	0.040 ± 0.008	7.8	10.74	82.0 ± 14.0	76.3 ± 13.0
70:30	0.5	1,335	19.9 ± 3.6	0.070 ± 0.013	1.6	10.84	23.7 ± 4.4	21.9 ± 4.1
	2	2,243	38.1 ± 0.4	0.080 ± 0.001	1.5	10.84	25.4 ± 0.3	23.4 ± 0.3
	3	7,132	62.4 ± 1.9	0.041 ± 0.002	3.1	~5.4*	27.0 ± 1.4	~50.0
	4	5,887	70.8 ± 4.8	0.057 ± 0.001	8.4	~0.54*	101.5 ± 7.1	~188
	5	3,690	20.6 ± 0.4	0.026 ± 0.001	3.7	~0.54*	20.4 ± 0.8	~378

*Estimated values of A_c could be in error by as much as ± 10% at 3 m/s and 4 m/s and by as much as ± 50% at 5 m/s.

Table 4

CORROSION RATE DATA FOR 90:10 Cu:Ni and 70:30 Cu:Ni ALLOYS IN SULFIDE-POLLUTED (~ 0.2 mg [S]/dm³) DEAERATED SEAWATER AS A FUNCTION OF VELOCITY

Alloy	Velocity (m/s)	A_c (C/V)	ΔW (mg)	B (V)	$1/R_p$[230 h] (kilohms^{-1})	A_c (cm^2)	dW/dt[230 h] (ng/s)	(dW/dt) (1/Ac) (μg/m^2.s)
90:10	3	612.8	6.66 ± 0.07	0.042 ± 0.001	0.75	10.74	8.07 ± 0.20	7.51 ± 0.19
	5	1435	34.3 ± 1.3	0.093 ± 0.003	1.9	10.74	45.3 ± 1.5	42.2 ± 1.4
70:30	3	390.3	5.58 ± 0.44	0.067 ± 0.006	0.40	10.84	5.68 ± 0.51	5.24 ± 0.47
	5	318.0	6.85 ± 0.85	0.102 ± 0.013	0.25	10.84	5.41 ± 0.69	4.99 ± 0.64

Table 5

COMPARISON OF THE CORROSION POTENTIAL (E_{corr}) AND THE BREAKAWAY POTENTIAL (E_B) FOR 90:10 Cu:Ni AND 70:30 Cu:Ni IN AERATED SEAWATER AS A FUNCTION OF VELOCITY AND EXPOSURE TIME

Alloy	Velocity (m/s)	Exposure Time (min)	E_{corr} (volt (SCE))	E_B (volt (SCE))	$E_B < E_{corr}$
90:10	0.5	275	-0.220	-0.100	No
	0.5	14,506	-0.050	-0.050	Borderline
	2	37	-0.235	-0.160	No
	2	16,146	-0.130	-0.140	Yes
	3	13,285	-0.081	-0.380	Yes
	4	239	-0.235	-0.180	No
	4	13,114	-0.065	-0.140	Yes
	5	156	-0.040	-0.140	Yes
	5	14,520	-0.075	-0.100	Yes
70:30	0.5	260	-0.220	-0.150	No
	0.5	14,470	-0.045	-0.025	No
	2	86	-0.045	+0.025	No
	2	16,224	-0.155	-0.020	No
	3	12,981	-0.155	-0.080	No
	4	111	-0.070	-0.090	Yes
	4	13,144	-0.075	-0.125	Yes
	5	137	-0.045	-0.150	Yes
	5	14,635	-0.060	-0.070	Yes

Table 6

COMPARISON OF THE CORROSION POTENTIAL (E_{corr}) AND THE BREAKAWAY POTENTIAL (E_B) FOR 90:10 Cu:Ni AND 70:30 Cu:Ni IN SULFIDE-POLLUTED DEAERATED SEAWATER AS A FUNCTION OF VELOCITY AND EXPOSURE TIME

Alloy	Velocity (m/s)	Exposure Time (min)	E_{corr} volt (SCE)	E_B volt (SCE)	$E_B < E_{corr}$
90:10	3	215	-0.710	-0.230	No
	5	367	-0.708	-0.520	No
	5	11,535	-0.720	-0.220	No
70:30	3	240	-0.530	-0.170	No
	5	350	-0.475	-0.200	No
	5	11,608	-0.480	-0.175	No

LIST OF FIGURES

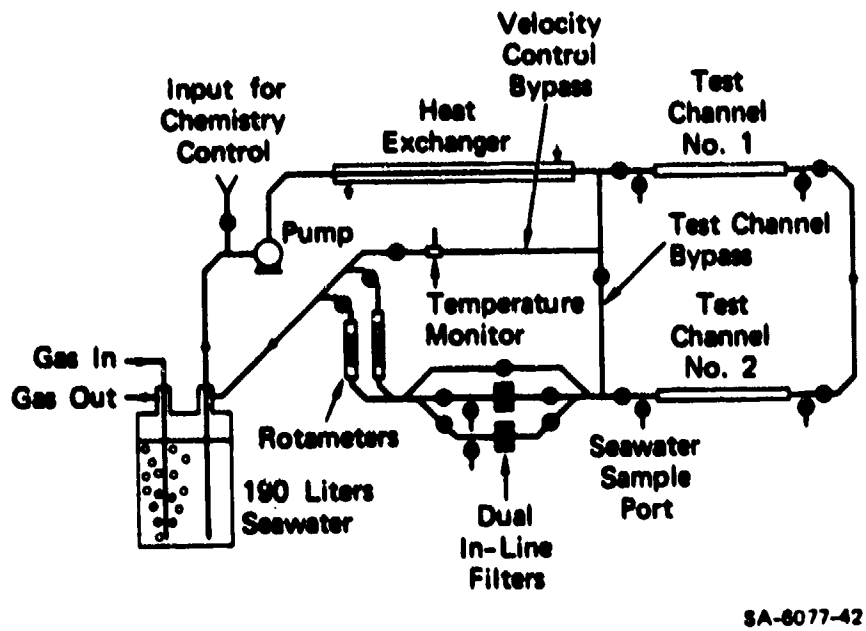

FIGURE 1 SCHEMATIC DIAGRAM OF THE FLOW LOOP

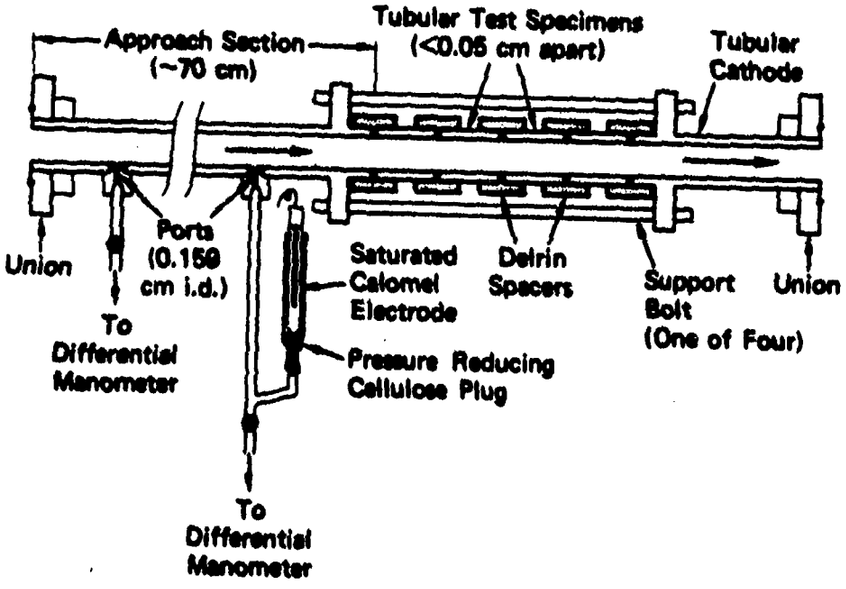

FIGURE 2 DESIGN OF TEST CHANNEL

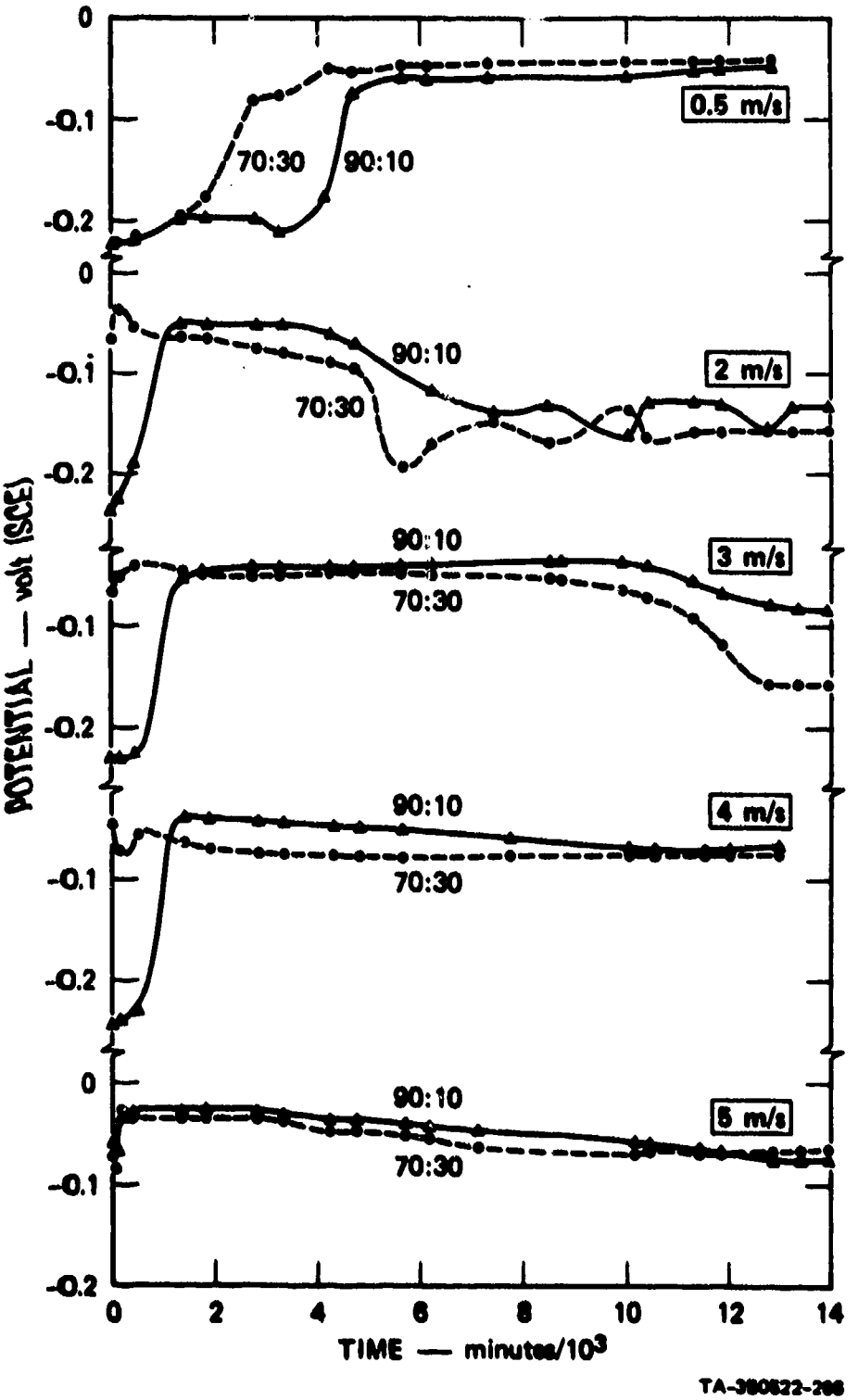

FIGURE 3 POTENTIAL-TIME CURVES FOR 90:10 Cu:Ni AND 70:30 Cu:Ni IN AERATED SEAWATER FLOWING AT VARIOUS VELOCITIES

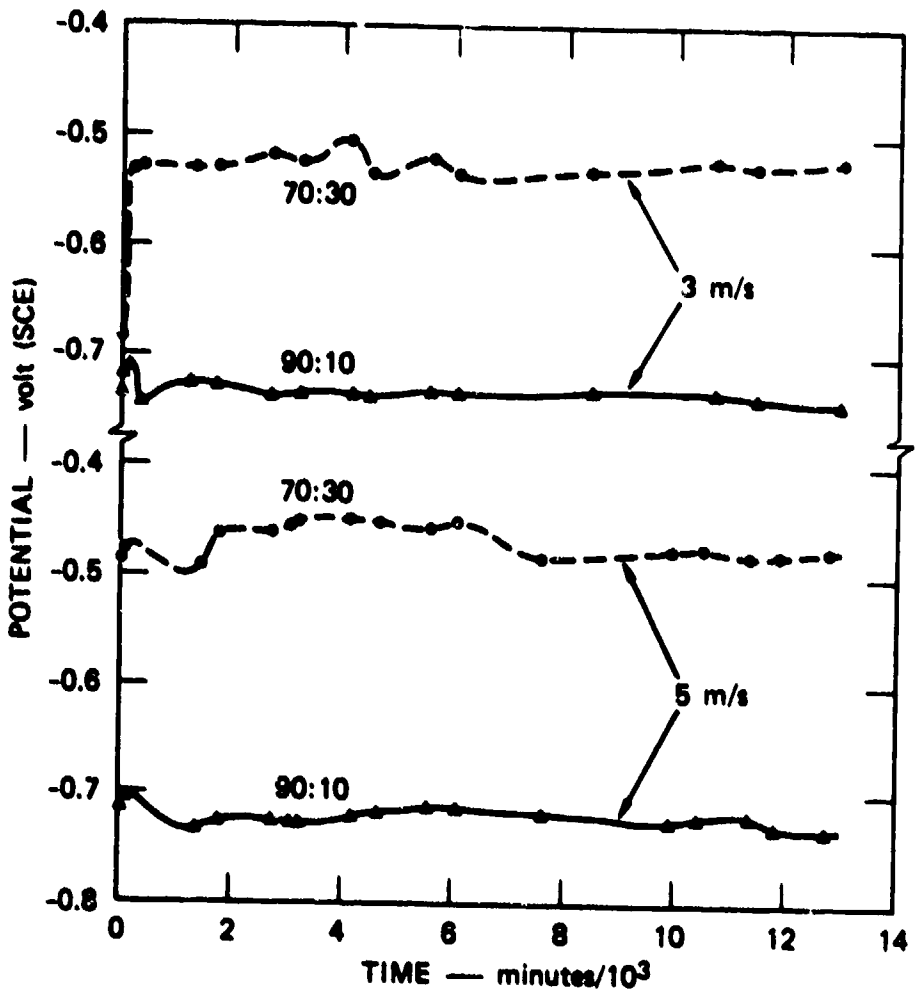

FIGURE 4 POTENTIAL-TIME CURVES FOR 90:10 Cu:Ni AND 70:30 Cu:Ni IN DEAERATED SEAWATER CONTAINING ~ 0.2 mg/dm³ SULFIDE AND FLOWING AT 3 m/s OR 5 m/s

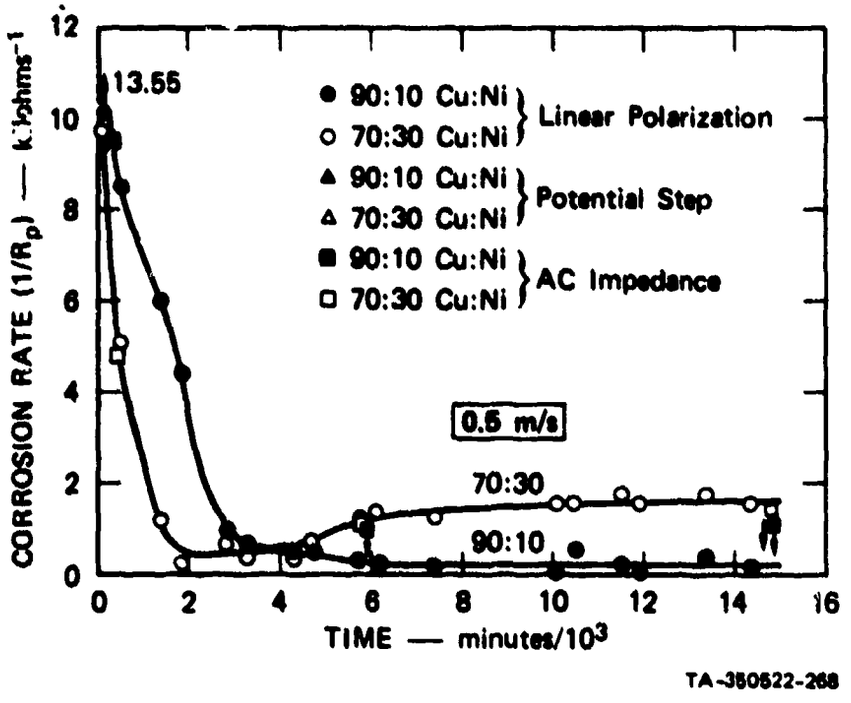

FIGURE 5 AVERAGE CORROSION RATE ($1/R_p$) OF 90:10 Cu:Ni AND 70:30 Cu:Ni ALLOYS AS A FUNCTION OF TIME IN AERATED SEAWATER FLOWING AT 0.5 m/s

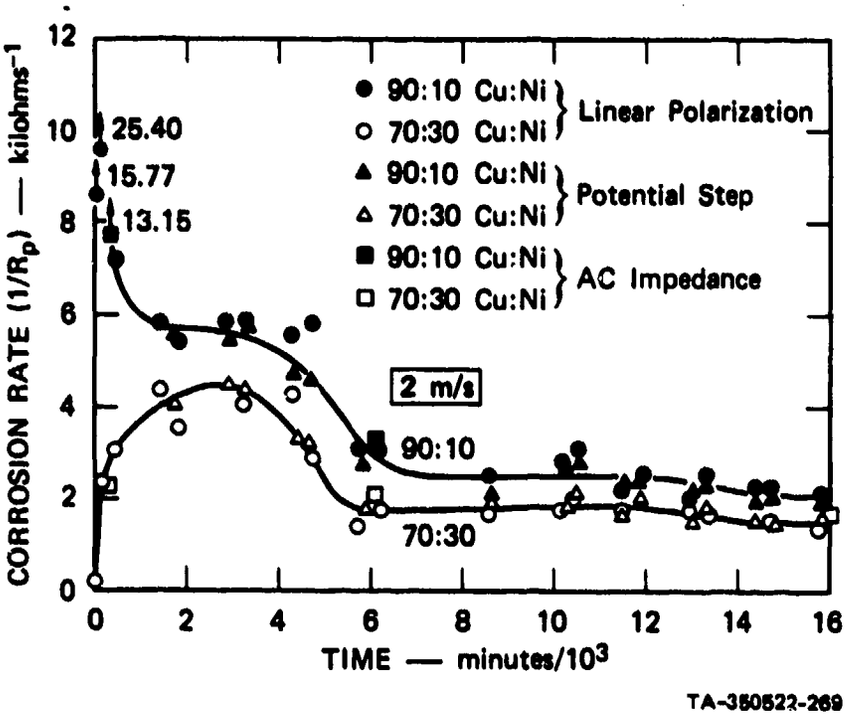

FIGURE 6 AVERAGE CORROSION RATE ($1/R_p$) OF 90:10 Cu:Ni AND 70:30 Cu:Ni ALLOYS AS A FUNCTION OF TIME IN AERATED SEAWATER FLOWING AT 2 m/s

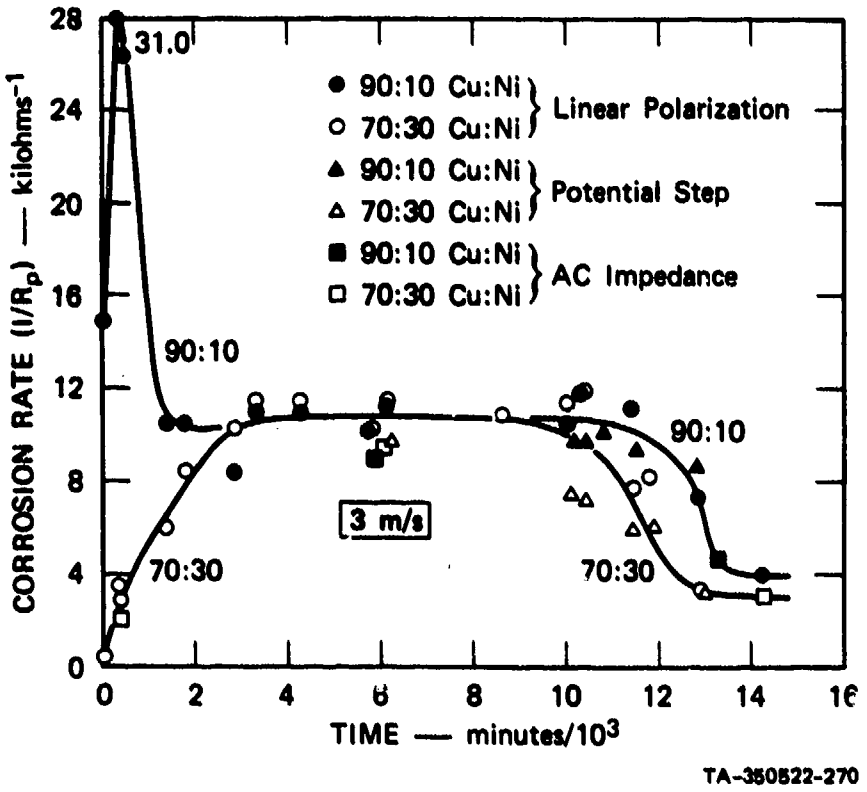

FIGURE 7 AVERAGE CORROSION RATE ($1/R_p$) OF 90:10 Cu:Ni AND 70:30 Cu:Ni ALLOYS AS A FUNCTION OF TIME IN AERATED SEAWATER FLOWING AT 3 m/s

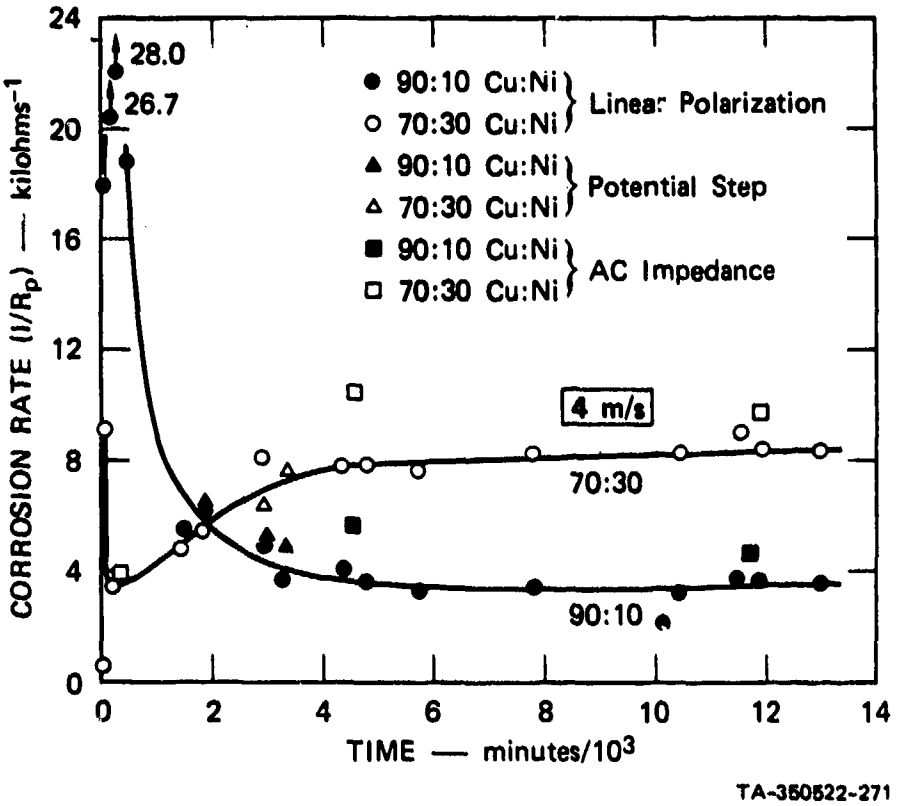

FIGURE 8 AVERAGE CORROSION RATE ($1/R_p$) OF 90:10 Cu:Ni AND 70:30 Cu:Ni ALLOYS AS A FUNCTION OF TIME IN AERATED SEAWATER FLOWING AT 4 m/s

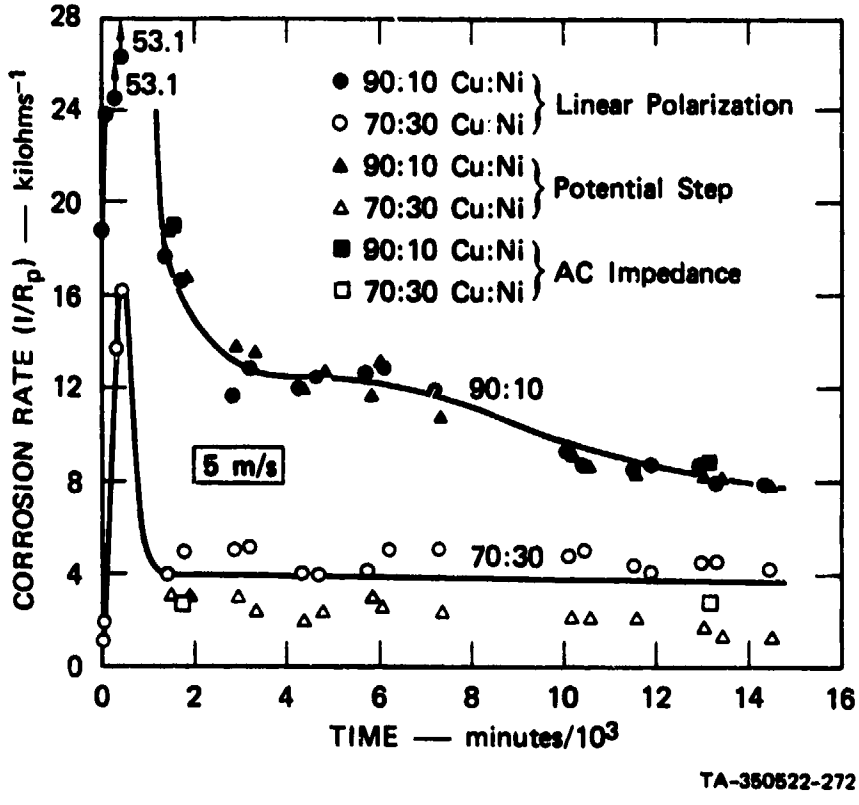

FIGURE 9 AVERAGE CORROSION RATE ($1/R_p$) OF 90:10 Cu:Ni AND 70:30 Cu:Ni ALLOYS AS A FUNCTION OF TIME IN AERATED SEAWATER FLOWING AT 5 m/s

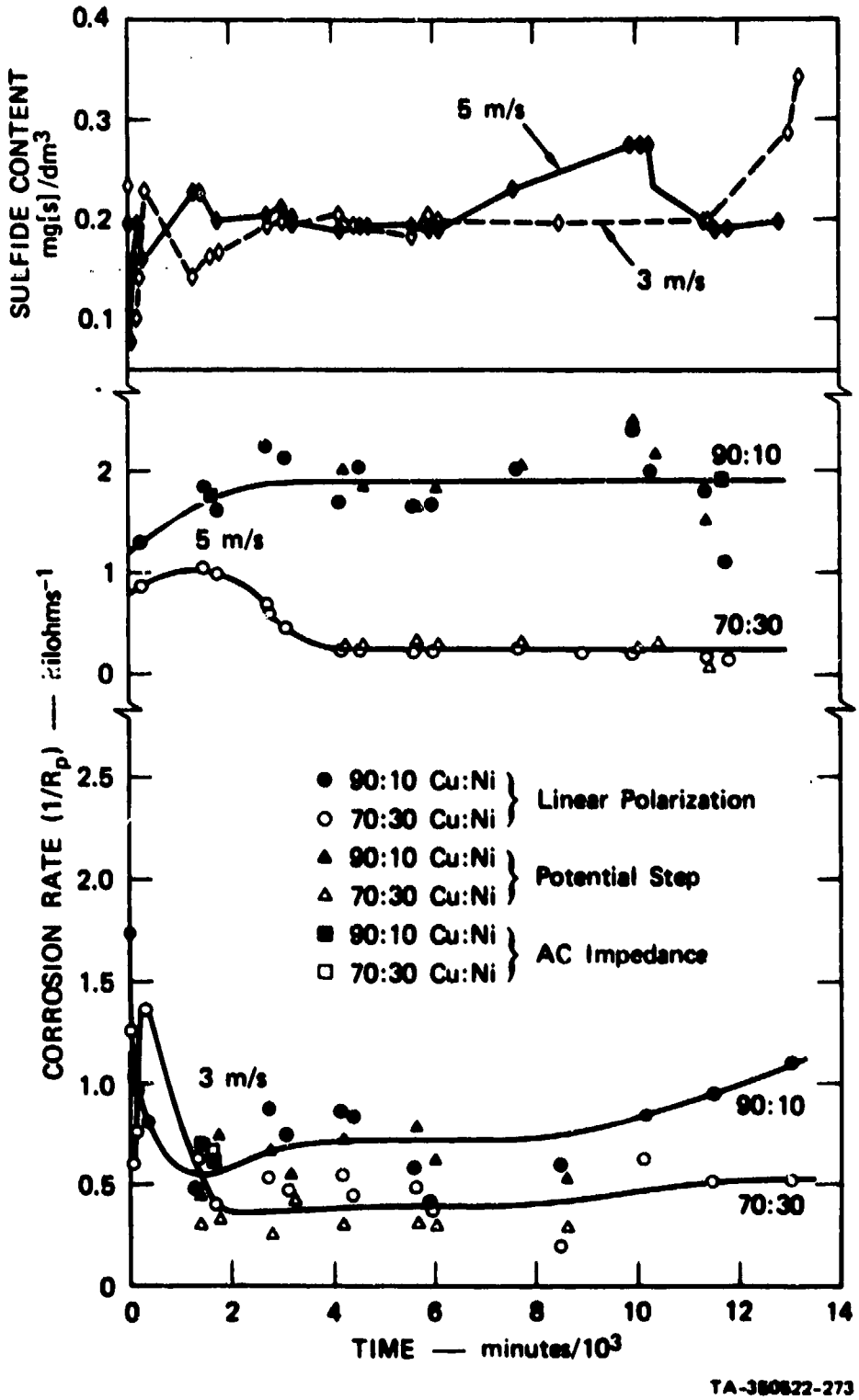

FIGURE 10 AVERAGE CORROSION RATE ($1/R_p$) OF 90:10 Cu:Ni AND 70:30 Cu:Ni ALLOYS AS A FUNCTION OF TIME IN DEAERATED, SULFIDE-POLLUTED SEAWATER FLOWING AT 3m/s OR 5 m/s. THE TIME DEPENDENCE OF THE DISSOLVED SULFIDE CONTENT IS ALSO GIVEN.

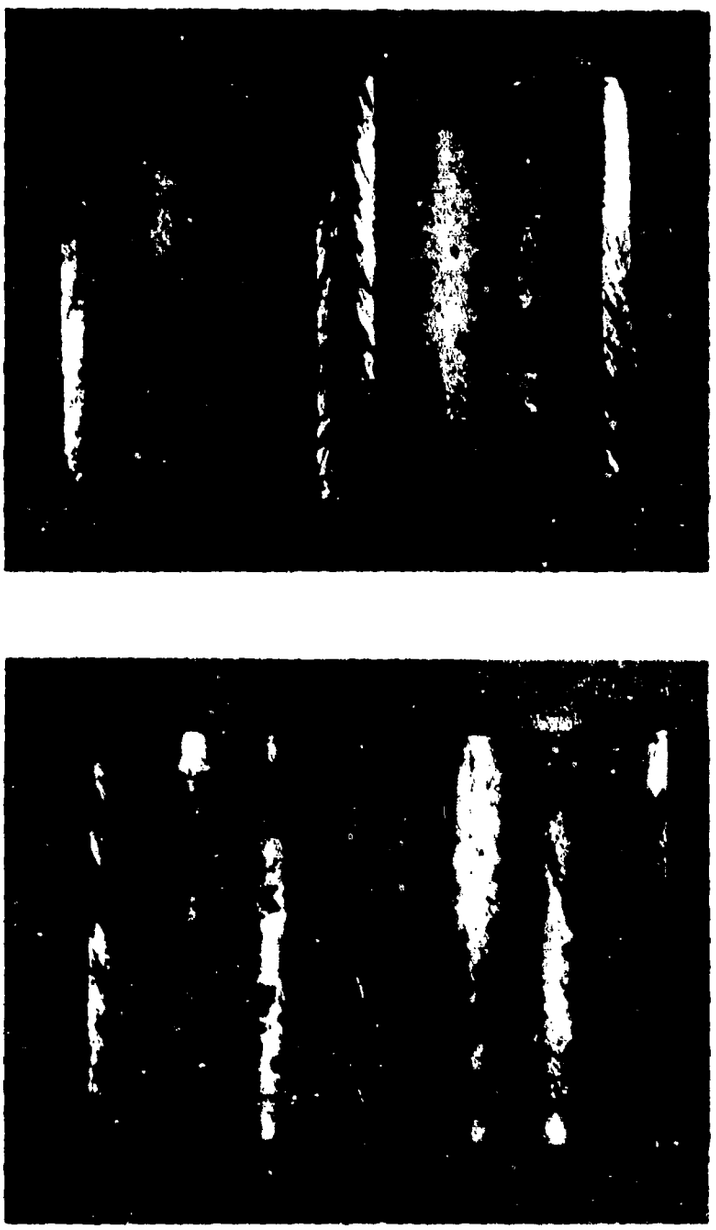

TA-350622-274

FIGURE 11 CLEANED INTERNAL SURFACES OF 90:10 Cu:Ni AND 70:30 Cu:Ni SPECIMENS EXPOSED TO AERATED SEAWATER FLOWING AT 0.5 m/s

[Note: Tarnish was not completely removed from 70:30 Cu:Ni specimen.]

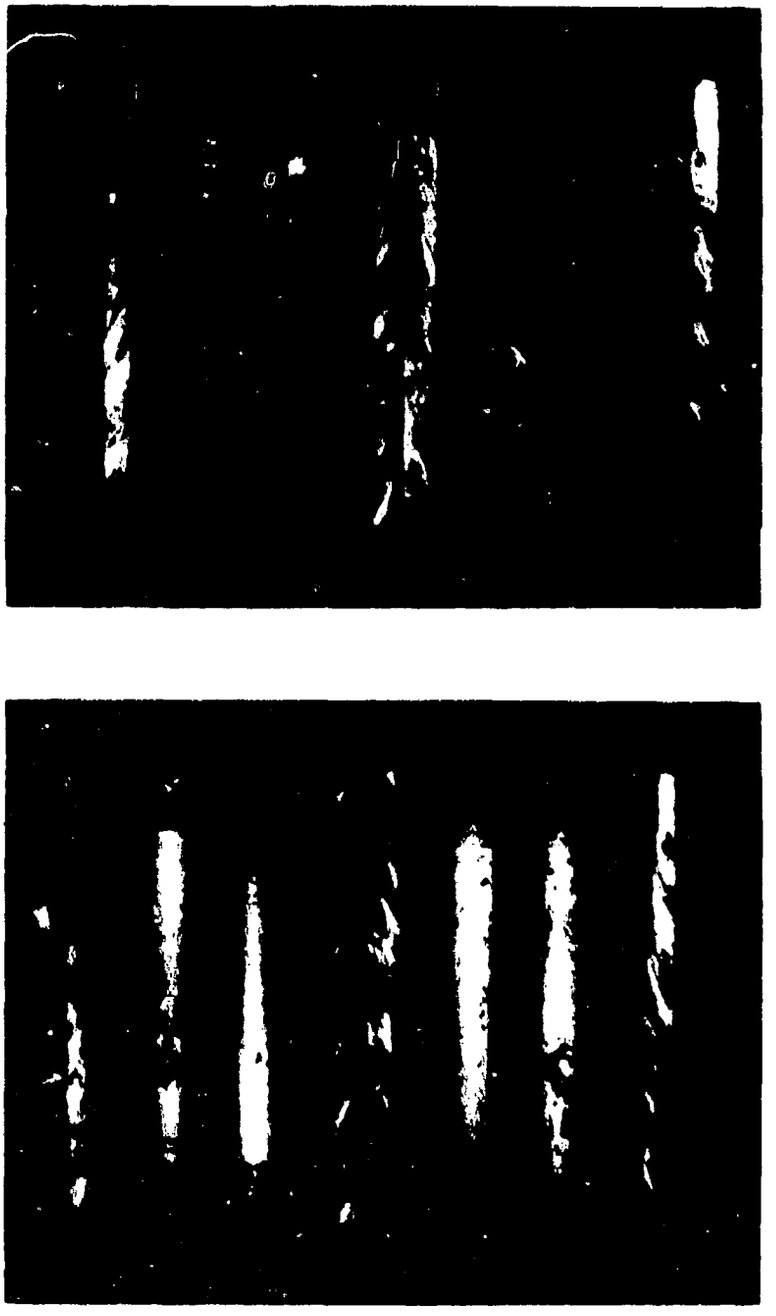

TA 850522 275

FIGURE 12 CLEANED INTERNAL SURFACES OF 90 10 Cu Ni AND 70:30 Cu:Ni SPECIMENS EXPOSED TO AERATED SEAWATER FLOWING AT 2.0 m s

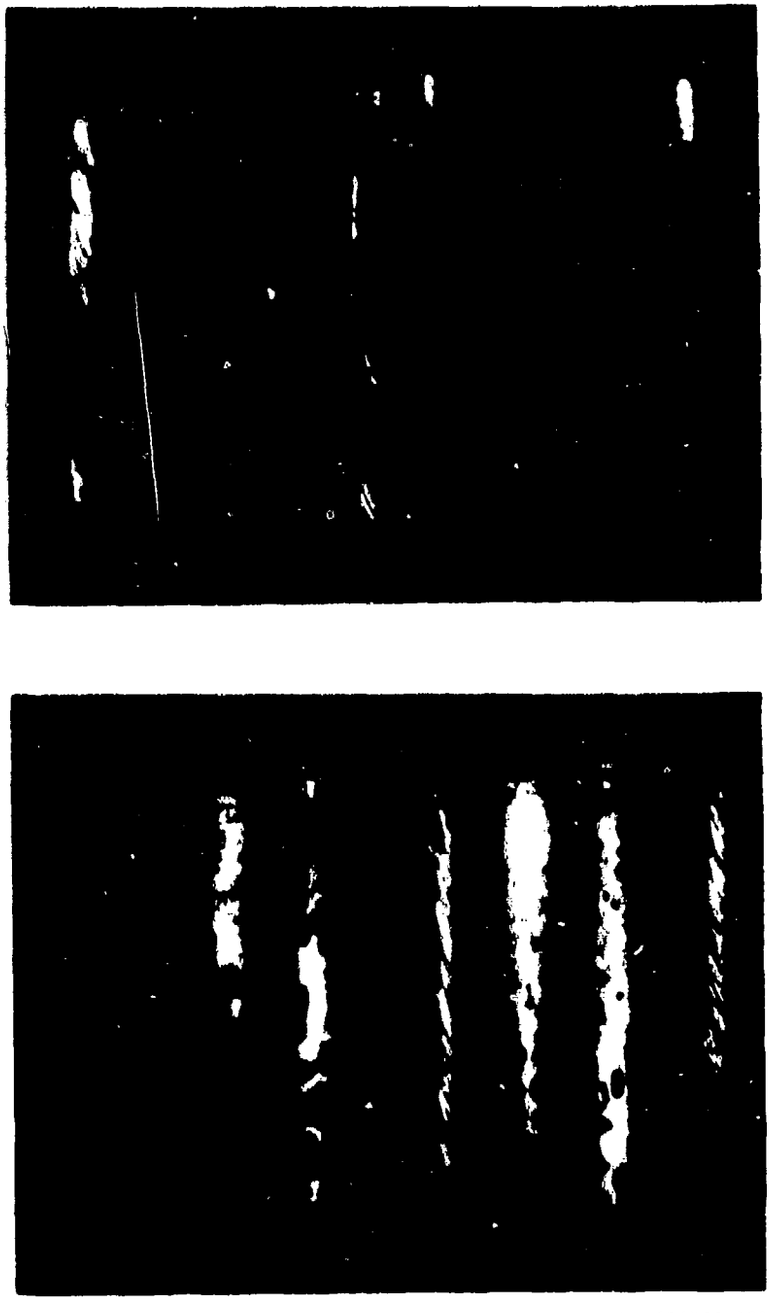

TA-350522-276

FIGURE 13 CLEANED INTERNAL SURFACES OF 90:10 Cu:Ni AND 70:30 Cu:Ni SPECIMENS EXPOSED TO AERATED SEAWATER FLOWING AT 3.0 m s

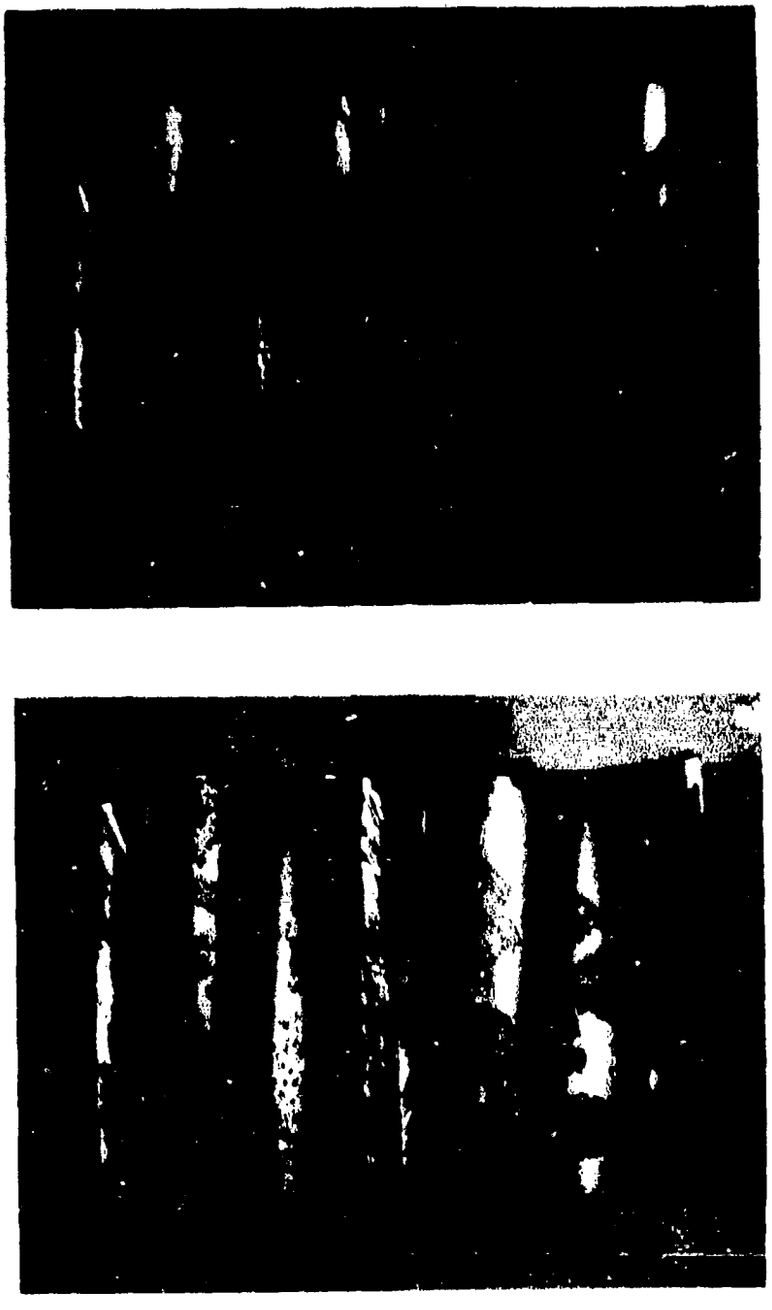

TA-350622-277

FIGURE 14 CLEANED INTERNAL SURFACES OF 90:10 Cu:Ni AND 70:30 Cu:Ni SPECIMENS EXPOSED TO AERATED SEAWATER FLOWING AT 4.0 m/s

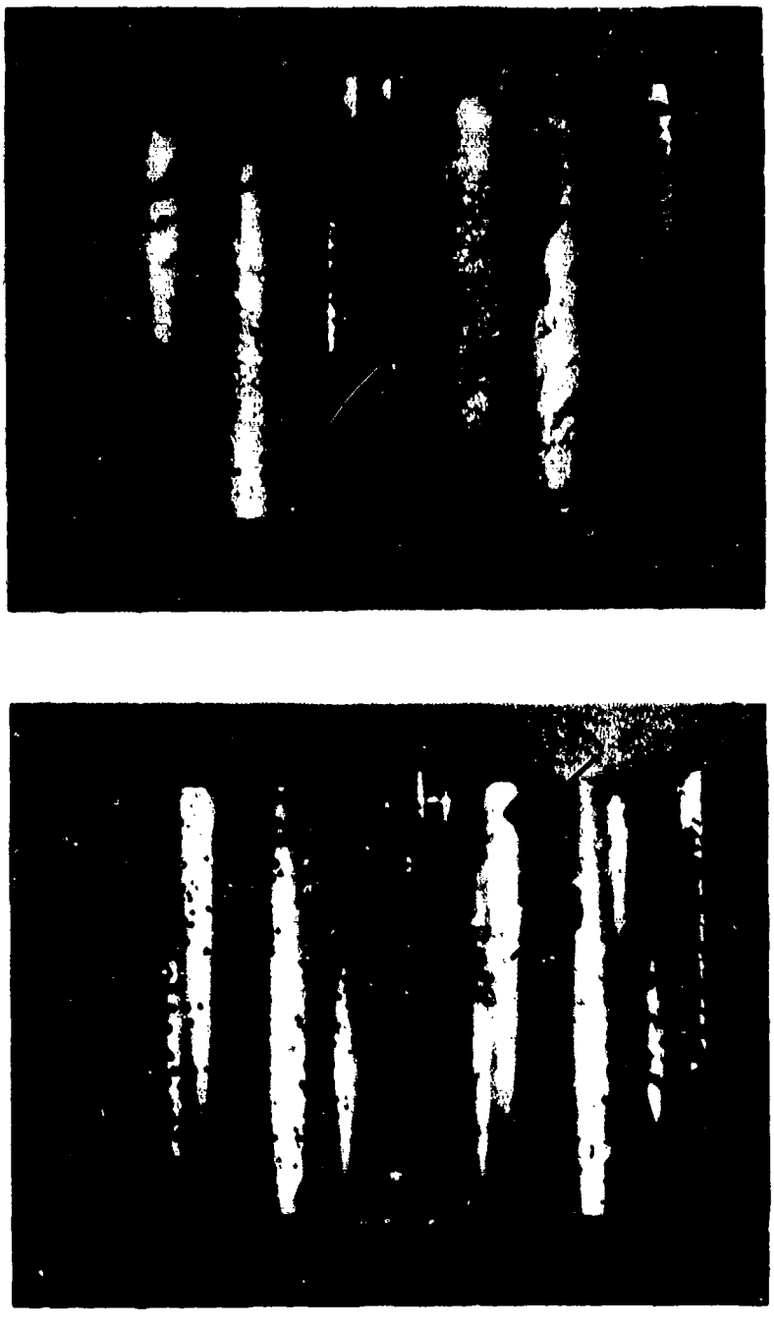

TA-380522-278

FIGURE 15 CLEANED INTERNAL SURFACES OF 90:10 Cu:Ni AND 70:30 Cu:Ni SPECIMENS EXPOSED TO AERATED SEAWATER FLOWING AT 5.0 m/s

Arrows mark the locations of two particularly deep pits on the 70:30 Cu:Ni specimen.

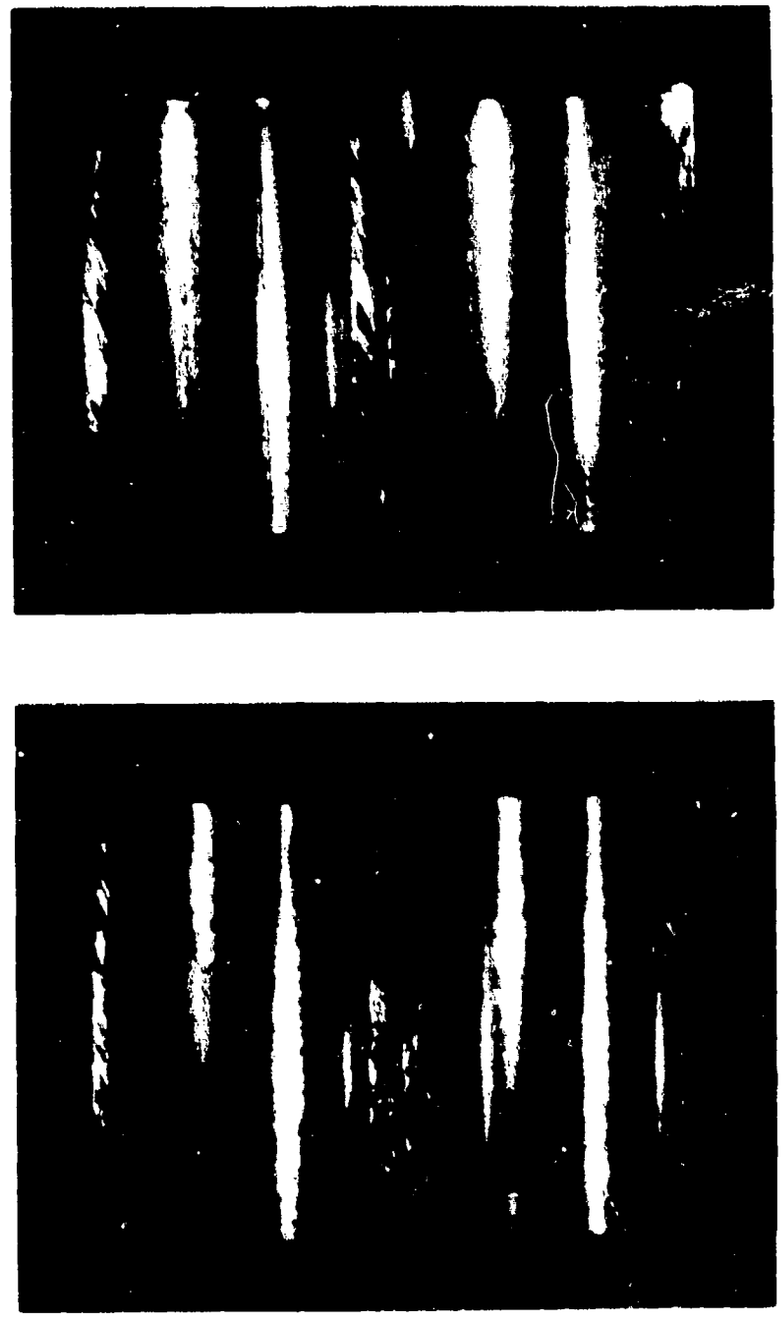

TA-350522-279

FIGURE 16 CLEANED INTERNAL SURFACES OF 90:10 Cu:Ni AND 70:30 Cu:Ni SPECIMENS EXPOSED TO DEAERATED SULFIDE-POLLUTED SEAWATER FLOWING AT 3.0 m/s

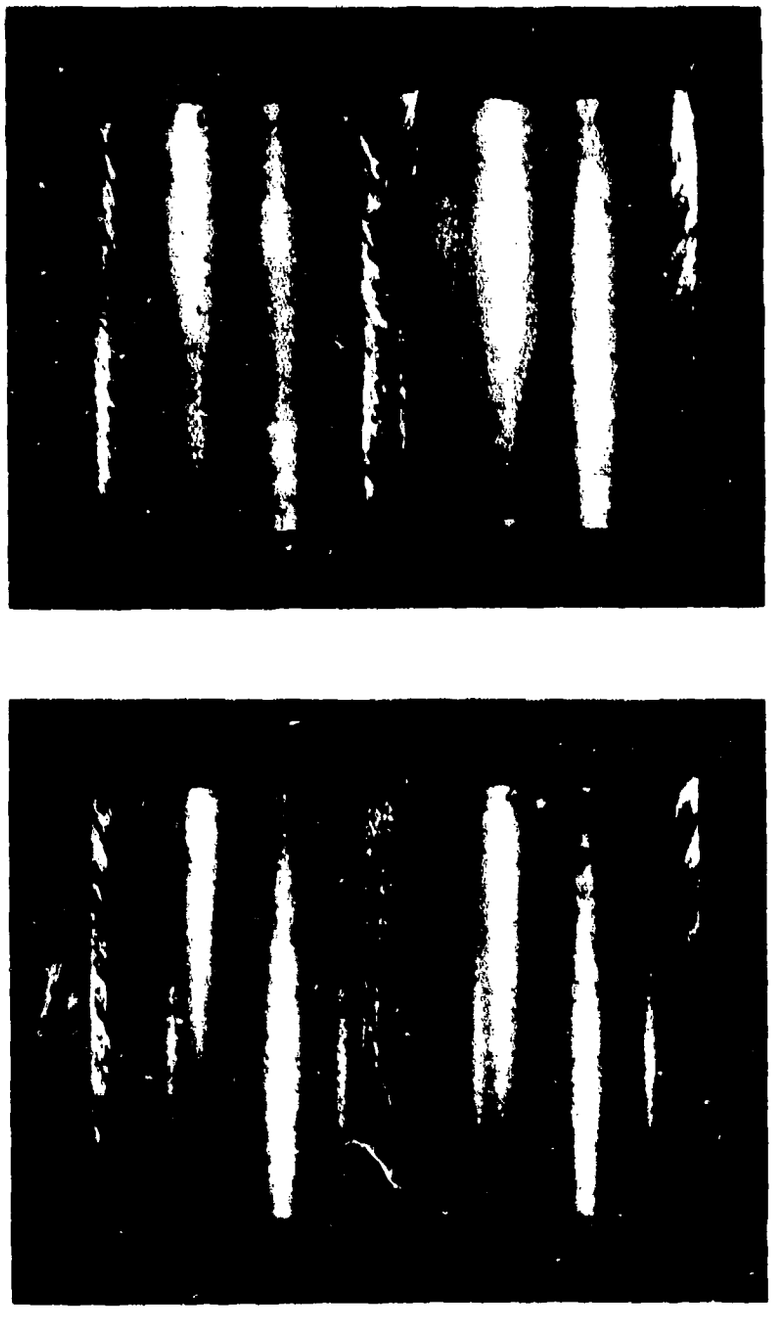

TA-370522-280

FIGURE 17 CLEANED INTERNAL SURFACES OF 90:10 Cu:Ni AND 70:30 Cu:Ni SPECIMENS EXPOSED TO DEAERATED SULFIDE-POLLUTED SEAWATER FLOWING AT 5.0 m/s

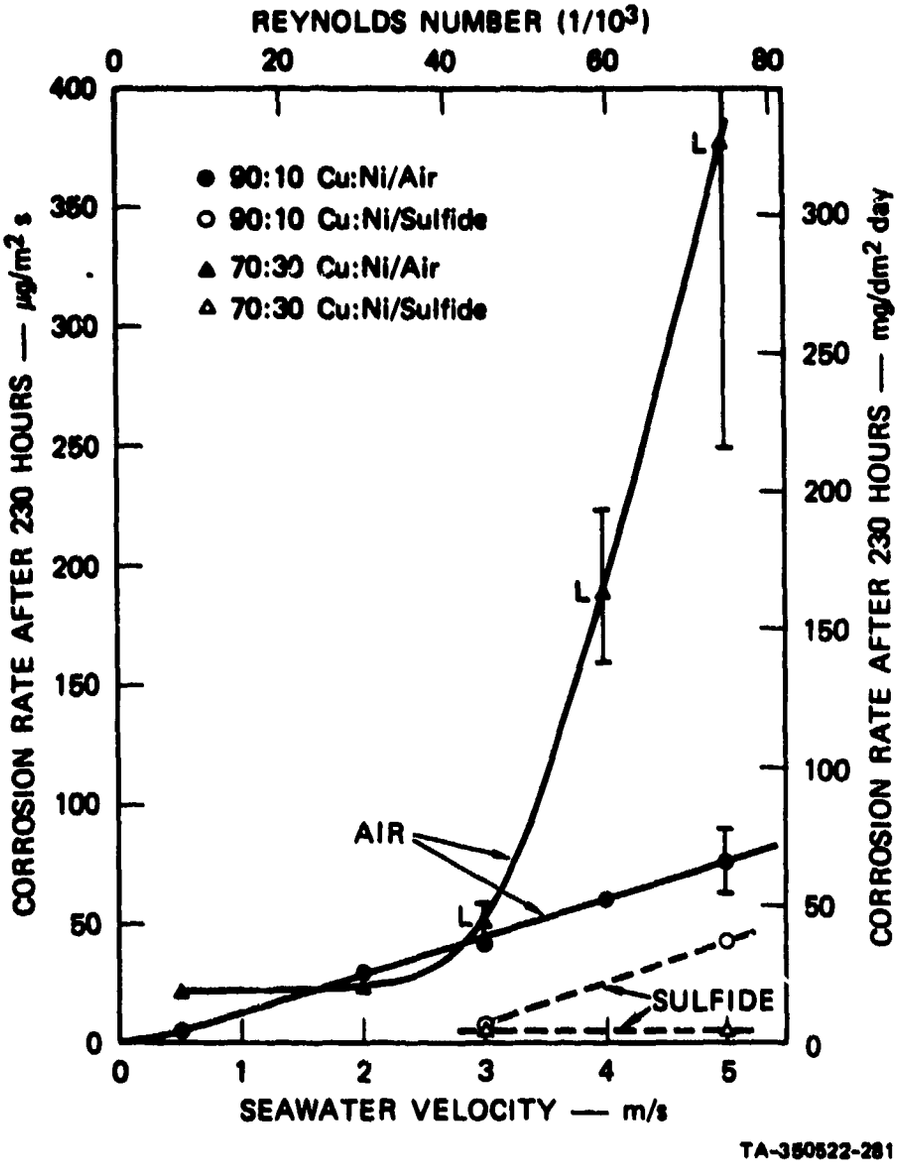

FIGURE 18 CORROSION RATES OF 90:10 Cu:Ni AND 70:30 Cu:Ni ALLOYS AFTER 230 HOURS EXPOSURE TO AERATED SEAWATER AND TO DEAERATED, SULFIDE-POLLUTED SEAWATER, AS A FUNCTION OF VELOCITY (OR REYNOLDS NUMBER)

[Data points labeled L are localized corrosion rates (see text)]